

THE DEVELOPMENT OF SOME ELECTROCHEMICAL  
DETECTION SYSTEMS BASED ON  
MICROELECTRODES AND MODIFIED ELECTRODES

BY

THOMAS JOSEPH O'SHEA

A Thesis Submitted for the Degree

of

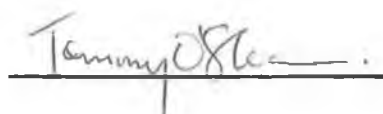
Doctor of Philosophy

Dublin City University

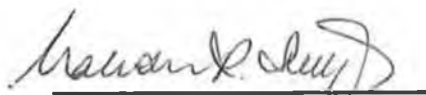
January 1992

Declaration

*I hereby declare that the contents of this thesis, except where otherwise stated, are based entirely on my own work, which was carried out in the School of Chemical Sciences, Dublin City University, Dublin, and in the Department of Physical and Analytical Chemistry, University of Oviedo, Asturias, Spain, and in the Department of Chemistry, University of Kansas, Lawrence, U.S.A.*

A handwritten signature in dark ink, appearing to read 'Tommy O'Shea', is written over a horizontal line.

*Thomas J. O'Shea*

A handwritten signature in dark ink, appearing to read 'Malcolm R. Smyth', is written over a horizontal line.

*Malcolm R. Smyth*  
*(Supervisor)*

*To my Parents, Kevin and Carmel*

## ACKNOWLEDGEMENTS

*Firstly, I would like to thank the postgraduates and staff of Dublin City University, the University of Oviedo, and the University of Kansas who assisted me during my research.*

*I would like to acknowledge the University of Oviedo, and the University of Kansas for giving me the opportunity of working in their research laboratories.*

*I am also thankful to Dr. Susan Lunte and Dr. Craig Lunte for the hospitality and help they extended to me during my stay in Lawrence.*

*Special thanks to my supervisor, Dr. Malcolm Smyth for his support and direction of my research, and for organising my research exchanges to Spain and the U.S.*

*Finally, I am indebted to my family for their support and encouragement during my years of study.*

## CONTENTS

	Page No.
Title page	1
Declaration	ii
Dedication	iii
Acknowledgements	iv
Table of Contents	v
Abstract	xi
<u>CHAPTER 1:</u>	
<u>Development of Detection Systems Based</u>	
<u>On Microelectrodes and Modified Electrodes</u>	1
1.1	2
INTRODUCTION	
1.2	3
CARBON FIBRE MICROELECTRODES	
1.2.1	4
Preparation of Carbon Fibres	
1.2.2	6
Structure of Carbon Fibres	
1.2.3	7
Construction of Carbon Fibre	
Microelectrodes	
1.2.4	8
Analytical Applications of	
Microelectrodes	
1.2.4.1	8
Theory of Voltammetry at	
Microelectrodes	
1.2.4.2	13
<u>In Vivo</u> Voltammetry	
1.2.4.3	14
Voltammetry in Flowing Streams	
1.2.4.4	16
Stripping Voltammetry	
1.2.4.5	17
Potentiometry	
1.2.4.6	19
Coulometry	
1.2.4.7	20
Other Electrochemical Applications	
1.3	21
MODIFIED ELECTRODES	
1.3.1	22
Electrochemical Biosensors	
1.3.2	26
Permselective CME's	

1.3.3	Preconcentration CME's	29
1.4	CONCLUSION	34
1.5	REFERENCES	35
CHAPTER 2:	<u>Determination of Nitrite Based on its Mediated Oxidation at a Chemically Modified Electrode</u>	40
2.1	INTRODUCTION	41
2.1.1	Mechanism of Operation	42
2.1.2	Analytical Applications	43
2.2	DETERMINATION OF NITRITE AT A RUTHENIUM POLYMER-MODIFIED CARBON PASTE ELECTRODE	52
2.2.1	EXPERIMENTAL	53
2.2.1.1	Reagents	53
2.2.1.2	Apparatus	53
2.2.1.3	Procedures	55
2.2.2	RESULTS AND DISCUSSION	56
2.2.2.1	Cyclic Voltammetry	56
2.2.2.2	Batch Amperometry in Stirred Solution	58
2.2.2.3	Flow Injection Analysis	62
2.2.2.4	Determination of Nitrite in Saliva	65
2.3	CONCLUSION	65
2.4	REFERENCES	66
CHAPTER 3:	<u>The Electrochemical Pretreatment of Carbon Fibre Microelectrodes</u>	69
3.1	INTRODUCTION	70
3.1.2	Pretreatment Methods for Solid Electrodes	71

3.2	A STUDY ON THE ELECTROCHEMICAL PRETREATMENT OF CARBON FIBRE MICROELECTRODES FOR THE DETERMINATION OF FOLIC ACID	82
3.2.1	EXPERIMENTAL	83
3.2.1.1	Reagents	83
3.2.1.2	Apparatus	83
3.2.1.3	Procedures	84
3.2.1.3.1	Construction of Microelectrodes	84
3.2.1.3.2	Microelectrode Pretreatment	84
3.2.2	RESULTS AND DISCUSSION	86
3.2.2.1	Polishing Pretreatment	86
3.2.2.2	Electrochemical Pretreatment	87
3.2.2.3	Determination of Folic Acid	97
3.3	CONCLUSION	97
3.4	REFERENCES	99

<u>CHAPTER 4:</u>	<u>The Design and Evaluation of Some Detection Techniques for Capillary Electrophoresis</u>	101
4.1	INTRODUCTION	102
4.1.1	Modes of Capillary Electrophoresis	103
4.1.1.1	Capillary Zone Electrophoresis	103
4.1.1.2	Micellar Electrokinetic Capillary Chromatography	107
4.1.1.3	Capillary Gel Electrophoresis	109
4.1.2	Detection Methods	109
4.1.2.1	Optical Detection	110
4.1.2.2	Conductivity Detection	111
4.1.2.3	Amperometric Detection	112

4.2	THE DETERMINATION OF AMINO ACID NEUROTRANSMITTERS IN RAT BRAIN HOMOGENATE BY CAPILLARY ELECTROPHORESIS WITH UV DETECTION	113
4.2.1	EXPERIMENTAL	115
4.2.1.1	Reagents	115
4.2.1.2	Apparatus	115
4.2.1.3	Procedures	116
4.2.1.3.1	Sample Derivatisation	116
4.2.1.3.2	Brain Homogenate Preparation	116
4.2.1.3.3	Determination of Electrophoretic Mobility	117
4.2.2	RESULTS AND DISCUSSION	119
4.2.2.1	Analysis of Amine Standards	119
4.2.2.2	Quantitation of Amino Acids in Rat Brain	125
4.2.3	CONCLUSION	127
4.3	THE DESIGN AND EVALUATION OF AN AMPEROMETRIC DETECTOR FOR CAPILLARY ELECTROPHORESIS	129
4.3.1	EXPERIMENTAL	130
4.3.1.1	Reagents	130
4.3.1.2	Apparatus	130
4.3.1.2.1	Construction of the Joint Assembly	130
4.3.1.2.2	CE System	131
4.3.1.2.3	Electrochemical Detection System	133
4.3.1.3	Procedures	135
4.3.2	RESULTS AND DISCUSSION	135
4.3.2.1	Linearity and Detection Limit for Hydroquinone	136
4.3.2.2	Analysis of Apple Juice	140
4.3.3	CONCLUSION	143
4.4	REFERENCES	144



CHAPTER 5:	<u>Capillary Electrophoresis with Electrochemical Detection of Microdialysis Samples for In Vivo Studies</u>	147
5.1	INTRODUCTION	148
5.1.1	Neurochemical Applications	152
5.1.2	Pharmacokinetics and Drug Metabolism	153
5.2	PHARMACOKINETIC STUDY OF L-DOPA BY MICRODIALYSIS SAMPLING COUPLED TO CAPILLARY ELECTROPHORESIS WITH ELECTROCHEMICAL DETECTION	155
5.2.1	EXPERIMENTAL	156
5.2.1.1	Reagents	156
5.2.1.2	Apparatus	156
5.2.1.2.1	CE System	156
5.2.1.2.2	Cyclic Voltammetry	156
5.2.1.2.3	Microdialysis System	156
5.2.1.3	Procedures	158
5.2.1.3.1	Microdialysis Probe Characterisation	158
5.2.1.3.2	<u>In Vivo</u> Pharmacokinetic Experiments	158
5.2.1.3.3	Electrochemical Pretreatment	159
5.2.2	RESULTS AND DISCUSSION	160
5.2.2.1	Electrochemical Pretreatment	160
5.2.2.2	Linearity and Detection Limit	162
5.2.2.3	Electrophoretic Analysis of Dialysis Samples	162
5.2.2.4	Voltammetric Characterisation	164
5.2.2.5	Pharmacokinetic Experiments	166
5.3	NEUROCHEMICAL APPLICATION OF MICRODIALYSIS COUPLED TO CAPILLARY ELECTROPHORESIS WITH ELECTROCHEMICAL DETECTION	170

5.3.1	EXPERIMENTAL	170
5.3.1.1	Reagents	170
5.3.1.2	Apparatus	171
5.3.1.2.1	CE System	171
5.3.1.2.2	Cyclic Voltammetry	171
5.3.1.2.3	Microdialysis System	171
5.3.1.3	Procedures	171
5.3.1.3.1	Microdialysis Probe Characterisation	171
5.3.1.3.2	<u>In Vivo</u> Experiments	172
5.3.1.3.3	Derivatisation Procedure	173
5.3.1.3.4	Electrochemical Pretreatment	173
5.3.2	RESULTS AND DISCUSSION	173
5.3.2.1	Electrochemical Pretreatment and Behaviour	173
5.3.2.2	Detection Limit	176
5.3.2.3	Voltammetric Characterisation	178
5.3.2.4	Potassium-Evoked Amino acid Overflow Analysis	180
5.4	CONCLUSION	182
5.5	REFERENCES	184
<u>CHAPTER 6:</u>	<u>CONCLUSIONS</u>	186
<u>APPENDIX I:</u>	<u>PUBLICATIONS</u>	A1

## *Abstract*

### *THE DEVELOPMENT OF SOME ELECTROCHEMICAL DETECTION SYSTEMS BASED ON MICROELECTRODES AND MODIFIED ELECTRODES*

*Thomas J. O'Shea*

*The thesis begins with a description of recent advances in the development of microelectrodes and chemically modified electrodes and reviews some of the more important and interesting examples of their analytical applications.*

*The second chapter describes the development of a chemically modified electrode for the amperometric detection of nitrite. The sensor is based on the immobilisation of a ruthenium polymer in a carbon paste matrix which serves to lower the overpotential for nitrite oxidation, hence permitting its determination at a lower potential.*

*An investigation into the electrochemical pretreatment of carbon fibre microelectrodes is presented in chapter 3, and a pretreatment regime was optimised for the determination of folic acid. The effects of the pretreatment on the functional characteristics of the microelectrode is also presented.*

*In chapter 4, the design and evaluation of two capillary electrophoresis systems, one employing a UV/VIS detector, and the other employing an amperometric detector based on a carbon fibre microelectrode, is described.*

*Finally, in chapter 5, and presented in two sections, is the application of microdialysis sampling coupled to capillary electrophoresis with electrochemical detection (employing the system developed in chapter 4), for *in vivo* studies. The first study involves a pharmacokinetic investigation of the drug L-dopa. The second study presented is a neurochemical analysis of amino acid neurotransmitters.*

## CHAPTER 1

DEVELOPMENT OF DETECTION SYSTEMS

BASED ON MICROELECTRODES

AND MODIFIED ELECTRODES

## 1.1 INTRODUCTION

Electroanalytical chemistry originated in the early 1920's with Heyrovsky's pioneering work on the dropping mercury electrode (DME) [1]. One of the most important advantages of the DME is the continuous renewal of the electrode surface which results in a very reproducible response. Since its inception, the technique has undergone something of a renaissance thanks to the use of modern electronics, and the application of potential pulse programmes and of current sampling procedures. However, polarography, whilst extensively used, has a number of drawbacks; in particular it is not a technique that readily lends itself to flow applications, and it is almost exclusively limited to electrochemical reduction reactions.

Since about 1950, electrochemistry at solid electrodes has become increasingly popular as evidenced by the number of publications in this area [2]. This increased popularity can be attributed in part to the development of electrochemical techniques which employ solid or stationary electrodes, and in part to theoretical studies which have advanced the interpretation of reactions occurring at solid electrodes. Most important, is the fact that many interesting reactions can be studied which are not accessible at a mercury surface and that solid electrodes can be employed in flow systems.

Electrochemical detectors have proven themselves as highly sensitive and selective systems for the determination of many electroactive species in a variety of samples. Over the past two decades, amperometric techniques have become widely accepted for analyte detection and quantitation in flow systems. In particular, liquid chromatography/electrochemical (LCEC) detection procedures are often the method of choice for the

determination of easily oxidisable species. These electrochemical detection systems offer excellent sensitivity, a wide linear range, discrimination against non-electroactive species and low cost. However, as with most measurement tools, solid electrodes encounter specific phenomena that reduce their applicability to analytical schemes. Chief among these are fouling of the electrode by unwanted precipitation or adsorption processes, and the slow electrochemical reaction rates that require high overpotentials to induce the desired reaction to occur. Therefore, improvements in the stability, selectivity and scope of electrochemical detection systems are highly desirable, particularly in the light of new challenges posed by complex biological and environmental matrices.

Much research in this field has focused on the development of new electrode materials or detector configurations, new detection schemes, or new applications. The past decade has seen the development of electrochemical detection systems based on microelectrodes and chemically modified electrodes, both of which have assumed a dominant position in modern electrochemistry and have resulted in many interesting advances in electroanalytical techniques. This chapter describes recent advances in the development of such electrodes and reviews some of the more important and interesting examples of their analytical applications.

## 1.2 CARBON FIBRE MICROELECTRODES

Carbonaceous materials have found extensive use as voltammetric electrodes in the last 20 years. They are advantageous as working electrodes primarily because of the low residual current they exhibit over a range of approximately  $\pm 1$  V in aqueous media and an even further extended range in organic solvents. Since the late 1970's increasing interest has been

shown in the use of microelectrodes fabricated from carbon fibres of micrometre dimensions. The unusual and attractive features of microelectrodes, including their high rates of mass transport and greatly reduced ohmic and capacitance effects, permit studies under conditions not possible with conventional electrodes. Among these, are experiments involving short time scales and fast kinetics, research on new solvents or phases, in vivo monitoring, flow detection with enhanced signal-to-noise characteristics, and electrochemical imaging with micrometre resolution. Such capabilities have already had a tremendous impact on electroanalytical chemistry.

Although the advantageous properties of microelectrodes were recognised for many years, research in this area did not become active until the late 1970's. The advances made in the field of electronics, especially in the measurement of small currents, were largely responsible for providing the impetus for such research. Fleischmann and co-workers [3] initiated much of this activity with an interest in understanding electrode mechanisms under conditions of high current density. At the same time, miniature electrodes were being developed for in vivo applications [4,5]. By 1981, it was clear that many new areas that were inaccessible to conventional electrodes could be explored with microelectrodes, and an early review summarises many of these expectations [6]. The aim of the literature survey presented in this section is to discuss the preparation and structure of carbon fibres and their electroanalytical applications. The theory and analytical applications of microelectrodes has been treated in several reviews [7,8].

#### 1.2.1 Preparation of Carbon Fibres

Carbon fibres have been known for nearly a century when Thomas Edison first used them as filaments for incandescent

lamps. These early carbon fibres were prepared by the carbonisation of bamboo and rayon. Today the manufacturing process is quite complicated, with many fabrication steps, depending on the desired fibre properties. The first consideration is the nature of the source material, such as polymeric, pitch and phenolic precursors. Pitch is an important and widely used low cost material used for carbon fibre manufacture. The most commonly employed pitches are those obtained from petroleum, asphalt, coal, tar and PVC.

The suitability of pitch for the production of carbon fibres is determined by its ability to spin and be converted to a nonfusible state so that the fibres can be carbonised without melting [9]. These properties are largely dependent upon their chemical composition and their molecular weight distribution. The molecular weight of the pitch determines the temperature and the speed of spinning by controlling the viscosity of the melt and the melting range. This can be controlled by chemical additives or by distillation. The fibre is then shaped by extrusion through an aperture and spinning.

Pitches are thermoplastic in nature. Therefore, it is difficult to carbonise them without some kind of thermosetting to maintain the filament shape during carbonisation. Oxidative infusion is commonly used to stabilise the fibre by cross-linking the molecular layers through peroxide-type linkages. The cross-linking renders the filament insoluble in all solvents and infusible on further heat treatment.

The fibres are then carbonised between 500 to 1000°C and volatile components in the fibre matrix, in addition to most of the non-carbon elements, are desorbed. Depending on the temperature used, deoxygenation, denitrogenation and dehydrogenation will occur. This heat treatment also results in



the fusion of the aromatic rings in the fibre into a polycyclic structure. At this stage, the fibre consists of ribbons of carbon atoms which begin to resemble the basal planes of true graphitic structures.

Heating up to 2000°C causes the degree of perfection to increase, so that the fibre begins to become more graphitic in nature. These fibres are most frequently encountered in structural materials and in analytical applications. Further heat treatments up to 2500°C, and stretching, causes the fibres to undergo plastic deformation, giving additional strength, elastic modulus, and preferred orientation. Detailed descriptions of different manufacturing processes can be found in several publications [9,10].

#### 1.2.2 Structure of Carbon Fibres

The microfibrillar structural model of carbon fibres first proposed by Fourdeaux et al. [11] is generally the most accepted. According to this model the basic unit of the structure consists of ribbon-shaped monatomic layers of  $sp^2$ -type carbon atoms. There is no correlation between the general direction of the ribbon and the direction of the a-axis of the internal two-dimensional hexagonal structure of the ribbons. Several of these ribbons run parallel to form microfibrils which have a preferred orientation parallel to the fibre axis. Since the contours of the microfibrils do not match (i.e. they are wrinkled), the space cannot be completely filled and creates a number of needle-like voids. Typically these voids are 20 to 30 nm long and 1 to 2 nm wide. The microfibrils are generally orientated in a tree-ring structure within the carbon fibre so that the axial surface is made up graphitic basal planes with a few lateral edges, whereas the cross-section of the fibre consists of concentric rings of graphitic edges.

The surfaces of the carbon fibres have a composition consisting of appreciable amounts of oxygen and traces of hydrogen and nitrogen. This surface composition is determined partly by the nature of the precursor material and partly by the reactivity of the carbon fibre with oxygen. The oxygen in carbon fibres may be derived either from the starting material, in which case it becomes part of the chemical structure of the fibre as a result of imperfect carbonisation, or becomes chemically bonded to the surface during activation.

### 1.2.3 Construction of Carbon Fibre Microelectrodes

The small dimension and fragility of carbon fibres requires that the construction design results in a relatively rugged electrode. Most workers have chosen a method that seals the fibre into glass capillaries. Individual fibres are inserted into a capillary and the capillary is pulled to a fine taper around the fibre using a commercially available pipette puller. A tight seal is achieved using epoxy, or a non-conducting wax. However, the use of this procedure must alter the surface composition of the fibre due to the high temperatures involved. Golas and Osteryoung [12] demonstrated that carbon fibres which were flame-sealed in glass were more fragile and required more electrochemical preconditioning than similar fibres sealed with heat shrinkable plastic. To avoid this problem, other workers pull the glass capillaries to a controlled tip diameter before insertion of the fibre. Electrical contact to the fibre is generally established via carbon epoxy or mercury. The design allows the fibre to be operated in a cylindrical or disc electrode configuration.

#### 1.2.4 Analytical Applications of Microelectrodes

##### 1.2.4.1 Theory of Voltammetry at Microelectrodes

The largest number of applications of carbon microelectrodes to date has involved voltammetry. The voltammetric response at microelectrodes can differ greatly from those observed at conventional electrodes. When microelectrodes are used in a disc configuration, the diameter of the electrode is smaller than the diffusion zone for the time scale of a typical experiment. This feature results in a number of electrochemical consequences. In linear sweep voltammetry at slow scan rates, an S-shaped curve replaces the peak-shaped response typical of an electrode of conventional size. The S-shaped response profile is due to a steady-state current being obtained at the limiting current region of this curve. The steady-state current arises because the electrolysis rate is approximately equal to the rate of diffusion of molecules to the electrode surface. When the direction of the sweep is reversed, the current essentially follows that obtained with the initial scan because the products of the electrolysis have diffused away from the electrode before further electrochemical steps can occur, i.e. there is no accumulation of reduced or oxidised species at the electrode.

Several investigators have addressed the problem of describing the current at microelectrodes. The approaches have been mainly based on the fact that the limiting current at the plateau of a voltammetric curve obtained with a microelectrode, may be described by the steady state term of the appropriate chronoamperometric equation. Dayton et al. [13] have shown that a reasonable approximation is made by considering a disc-shaped microelectrode as a hemisphere. In their study, the equation for the current was obtained in quiescent solution under conditions where the potential step was of sufficient magnitude to cause

the surface concentration of electroactive species to be zero and was described by:

$$I = nFAD^{1/2}C(\pi t)^{-1/2} + arnFDC \quad (1.1)$$

where  $A$  is the electrode area,  $r$  is the electrode radius,  $a$  is a coefficient which depends on the electrode geometry, and the other terms have their usual electrochemical meanings. However, it is not always appropriate to use chronoamperometric equations for spherical or hemispherical diffusion zones to describe the currents at microelectrodes. Aoki et al. [14] have derived equations for linear scan voltammetry under cylindrical diffusion conditions when the thickness of the diffusion layer becomes greater than the radius of the electrode. In the case of a reversible electrode reaction, it was shown to be impossible to obtain a steady-state voltammogram, even if the radius tended to zero. The authors derived an approximate expression for the peak current,  $I_p$ :

$$I_p = 2\pi nFCD(0.446p + 0.335p^{0.15}) \quad (1.2)$$

where  $r$  is the radius of the electrode and  $p$  is given by  $(nFr^2v(RTD)^{-1})^{1/2}$  where  $v$  is the sweep rate and the other terms have their usual meanings.

One of the main problems associated with the use of solid electrodes is the presence of chemical reactions that precede or follow the initial electron-transfer and also contribute to the overall current. The theoretical affect of this type of reaction has been extensively studied and several of the derivations of

the current response have been compiled by Galus [15]. It has been shown by these derivations that chemical processes that follow the initial electron-transfer and are of a moderate rate, will have much less effect on the current at microvoltammetric electrodes. This is illustrated by considering a typical catalytic reaction:



At a large electrode, the regenerated O will return to the electrode surface, resulting in an increased current. However at a microelectrode, with moderate values of k, very little enhanced current is obtained. This is due to the fact that the average distance into the solution that R diffuses before reacting to form O, given by  $(Dt)^{1/2}$  where t is the half life of the reaction and D is the diffusion coefficient, is larger than the radius of a microelectrode. Thus a large part of the regenerated oxidant is removed from the vicinity of the electrode surface, and therefore a minimal catalytic contribution to the current is observed. ECE mechanisms are also less obvious at microelectrodes, as the chemical reactions tend to be masked because of the rapid diffusion of the first electrogenerated species away from the electrode. Accordingly, Edmonds and Guoliang [16] reported that the electroreduction of copper(II) ions in chloride media yields two or more peaks at a conventional electrode, but resulted in only one peak at a carbon fibre microelectrode.

At conventional electrodes the capacitance current can be a major interference since it may exceed the value of the faradaic current at short times or with low concentrations of

electroactive species. However, since the magnitude of the double-layer capacitance is proportional to the electrode area, it is much reduced at microelectrodes. Therefore, when a microelectrode is operated under conditions where the faradaic current is steady-state, a considerable improvement in the faradaic-to-capacitance current ratio ( $i_F/i_C$ ) is obtained. Pulsed voltammetric techniques have been employed at conventional electrodes to improve ( $i_F/i_C$ ) ratios under conditions of linear diffusion. Thus, pulsed voltammetric techniques should be even more successful with microelectrodes if the background is purely capacitative in nature. Ewing et al. [17] demonstrated this with the detection of micromolar levels of catecholamines using normal pulse voltammetry at carbon fibre microelectrodes. The use of alternating current (AC) voltammetry can also be used to distinguish between faradaic and charging current, and this approach has been investigated by Baranski at disc microelectrodes [18].

In addition to the reduced effects of the double-layer capacitance, the effects of solution resistance are reduced at microelectrodes. This resistance ( $R$ ) is due to the current that flows through the solution which generates a potential that opposes the applied potential. In other words, the ohmic drop (given by the product  $iR$ ) will be subtracted from the applied potential difference between the working and reference electrodes. Although charging and faradaic currents are diminished in amplitude, the solution resistance at disc-shaped microelectrodes is inversely proportional to the radius. This occurs because the resistance of a microelectrode is dominated by the resistance near the electrode surface, described by the following equation [19]:

$$R = \rho 4r^{-1} \quad (1.3)$$

where  $p$  is the specific resistance of the solution and  $r$  is the radius of the microelectrode. Because the  $iR$  drop of a working microelectrode is concentrated in its immediate vicinity, the distinction between reference and auxiliary electrode becomes unimportant, and also because the low currents generated at microelectrodes do not polarise the reference electrode significantly, a two-electrode cell configuration (reference and working electrode) can be employed which requires much less electronic hardware [20]. The substantial elimination of the  $iR$  drop also provides the possibility of analysing samples without the addition of supporting electrolyte, which is one of the main sources of impurities in trace analysis and a source of unwanted water in non-aqueous solvents. Bond and co-workers [21] presented the first measurable voltammetric waves (of ferrocene) in solvents containing no deliberately added electrolyte. The same workers recorded voltammograms of ferrocene in solid organic solvents (low temperature 'glasses') [22]. Electrochemical behaviour has even been observed in the absence of solution with a microelectrode comprised of two concentric rings [23]. In this case it was presumed that the conductive phase was the epoxy contained between the two rings. The device was demonstrated to be suitable as a gas chromatographic detector for a wide range of compounds.

Another consequence of the response of microelectrodes is the ability to utilise fast scan rates in voltammetric studies. The capacitative nature of the impedance of any electrochemical cell precludes rapid changes in potential. Thus electrochemical measurements with conventional electrodes have generally been restricted to the millisecond or longer time scale. McCreery's group was the first to demonstrate that the reduced values of resistance and capacitance at microelectrodes lowers the cell-time constant allowing the working electrode to assume the applied potential at a very short time scale [24]. Taking

advantage of this feature, Howell and Wightman [25] have obtained cyclic voltammograms with very little distortion at scan rates as fast as  $20,000 \text{ V s}^{-1}$  when using disc electrodes of radii less than  $7 \mu\text{m}$ . This ability for fast-scan voltammetric measurements has been used for the investigation of several chemical systems which are not accessible to conventional electrodes. An example of such a study with this technique is that by Wehmeyer and Wightman [26] who observed the oxidised form of ascorbic acid which has a half-life of less than a millisecond. The use of fast-scan voltammetry has also been shown to enable the measurement of heterogeneous electron transfer reactions with rate constants up to  $20 \text{ cm s}^{-1}$  [25].

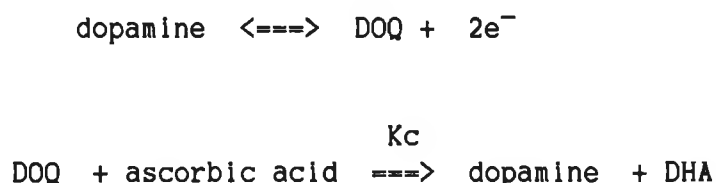
#### 1.2.4.2 In Vivo Voltammetry

A large number of voltammetric applications of carbon fibres involve the in vivo monitoring of neurotransmitters and the subject has been reviewed extensively [27]. Voltammetry is the only technique that provides instantaneous information about the functionality of a neurotransmitter system, and undoubtedly the small dimensions of microelectrodes have been a major factor in their selection for in vivo voltammetric studies. The microelectrode can be inserted into selected regions of mammalian brain tissue with high accuracy and minimal disruption. Furthermore, the electrochemical and surface characteristics of carbon fibre microelectrodes has proven advantageous for such studies. Several compounds are routinely monitored in vivo with microelectrodes, including dopamine, ascorbic acid, norepinephrine, 5-hydroxytryptamine, 3,4-dihydroxyphenylacetate acid (DOPAC) and 3,4-dihydroxyphenylalanine. Dopamine, norepinephrine and 5-hydroxytryptamine and their metabolites all oxidise in a very restricted range; ascorbic acid, uric acid and other compounds are also oxidised



in the same range. Therefore, from the beginning, electrochemical selectivity has been an overriding concern with in vivo measurements. Good progress has been made in achieving better selectivity (and sensitivity), principally through electrode pretreatments [28,29] and coating with ionomer films like Nafion to restrict access for anionic species like ascorbic acid and uric acid [30].

The unique electrochemical properties of microelectrodes have been utilised by Dayton et al. [31] for the in vivo detection of dopamine. Oxidation of dopamine at carbon electrodes in the presence of ascorbic acid, present in millimolar concentration in the mammalian brain, results in a homogeneous catalytic oxidation of ascorbic acid described in the following equations:



where DOQ and DHA represent the oxidised forms of dopamine and ascorbic acid, respectively. The regenerated dopamine returns to the electrode surface resulting in an enhanced current. However, the authors demonstrated that because of the small size of microelectrodes, only a small portion of the catalytically-generated dopamine returns to the electrode and thus these electrodes are essentially 'blind' to this interference.

#### 1.2.4.3 Voltammetry in Flowing Streams

With all common electrochemical cells which are employed in flowing streams (channel, tubular or wall jet), the magnitude of

the mass transport-controlled faradaic current arising from electrolysis of analyte or buffer is proportional to the flow rate. Fluctuations in the flow rate thus lead to a noise level that is directly proportional to the degree of fluctuation and the concentration of electroactive species [32]. The relatively small distance that the diffusion zone around a microelectrode extends into solution generally isolates the faradaic current from convection in solution. Therefore, the current at this electrode should be independent of flow rate and much less susceptible to pulsing that can arise in pumped systems. Such a system was described by Caudill et al. [33]. The electrode consisted of 100 discs, each of 5  $\mu\text{m}$  radius, positioned at least 30  $\mu\text{m}$  from its nearest neighbour to prevent diffusional cross-talk. The improved signal-to-noise ratio obtained was demonstrated compared to the response at a conventional glassy carbon electrode. Carbon fibre microelectrodes have also been used to measure the radial dispersion which occurs during laminar flow inside tubes ( $r = 0.4 \text{ mm}$ ) [34]. With the use of a microelectrode of total diameter 20  $\mu\text{m}$ , the stagnant region near the wall of the tube was clearly observed.

The small size of microelectrodes makes them ideal for use as chromatographic detectors with small capillary columns. An individual carbon fibre for electrochemical detection for open tubular LC was described by Knecht et al. [35]. The compounds detected amperometrically were ascorbic acid, catechol and 4-methylcatechol. In a later paper, White and co-workers [36] used the same system as a scanning microvoltammetric detector where the reduced double-layer capacitance permitted scan rates of up to  $1 \text{ V s}^{-1}$ . Three dimensional and topographical plots were obtained, as data in both the chromatographic and electrochemical domains could be viewed simultaneously. Therefore peaks which overlapped chromatographically, yet resolved electrochemically, could be detected separately. An

alternative procedure to positioning the microelectrode in the outlet of the chromatographic column was described by Hou et al. [37]. A two-electrode cell was constructed by fixing a carbon fibre through a PVC tube. This tube was then connected to reference electrode compartment and the other end of the tube was connected to the outlet of an LC column. A similar, but more simply constructed design, was reported by Hua et al. [38], and was demonstrated to be applicable for stripping and voltammetric analyses. More recently, carbon fibre microelectrodes have been used as detectors for capillary electrophoresis [39]. A detailed description of this application is presented in chapter 4.

#### 1.2.4.4 Stripping Voltammetry

Cushman et al. [40] were the first to utilise carbon fibres as support electrodes for mercury film formation. The performance of this electrode for the differential pulse anodic stripping voltammetry of cadmium(II) was investigated. The first advantage of using microelectrodes in stripping voltammetry is that stirring is not required during the deposition step because of the enhanced steady-state diffusion of species to the electrode. This minimises one of the sources of error in this type of experiment. Secondly, the analyte, which is accumulated in the very small volume of the liquid electrode, is completely stripped off during the scan leading to very sharp peaks. Another advantage of using microelectrodes in stripping voltammetry, demonstrated by Frenzel [41], was the ability of using small volumes. The construction of a microvoltammetric cell for the determination of lead(II) and cadmium(II) in volumes of 5  $\mu$ L in stripping analysis was described.

Potentiometric stripping analysis was first demonstrated with mercury-coated carbon fibres by Schulze and Frenzel [42]. In their study of lead(II) and copper(II), the decreased

background signal at the microelectrodes led to sharply pronounced breaks at the equivalence points in the potential vs. time curves.

Traditionally, stripping experiments have involved high concentrations of supporting electrolyte. At lower concentrations of electrolyte, apart from severe peak distortions, large  $iR$  drops can affect the 'true' plating potential in stripping experiments and hence may affect the efficiency of the preconcentration step. The ohmic-drop problem becomes extremely severe when stripping experiments in resistive media are attempted. Due to the negligible losses obtained with microelectrodes, Wang and Tuzhi [43] demonstrated the feasibility of stripping analysis in resistive solutions without the addition of supporting electrolyte using carbon fibre microelectrodes. A two-electrode configuration yielded virtually undistorted stripping voltammograms of cadmium(II), zinc(II) and lead in methanol and acetonitrile. Compared in Figure 1.1 are stripping voltammograms obtained in this study, recorded at conventional-size hanging mercury drop and mercury-coated glassy carbon electrodes, as well as the mercury-coated microelectrode. The conventional electrodes exhibited severe peak distortion (curves a and b), while in contrast, well-defined and sharp peaks with good resolution were observed at the microelectrode (curve c) despite the absence of supporting electrolyte.

#### 1.2.4.5 Potentiometry

The surface of carbon fibres is populated with oxide functions. Accordingly, carbon fibres may be considered as electrodes of the second kind, in which class are a range of pH-sensitive metal/metal oxide electrodes. The potentiometric response to pH was first reported by Jennings et al. [44]. In

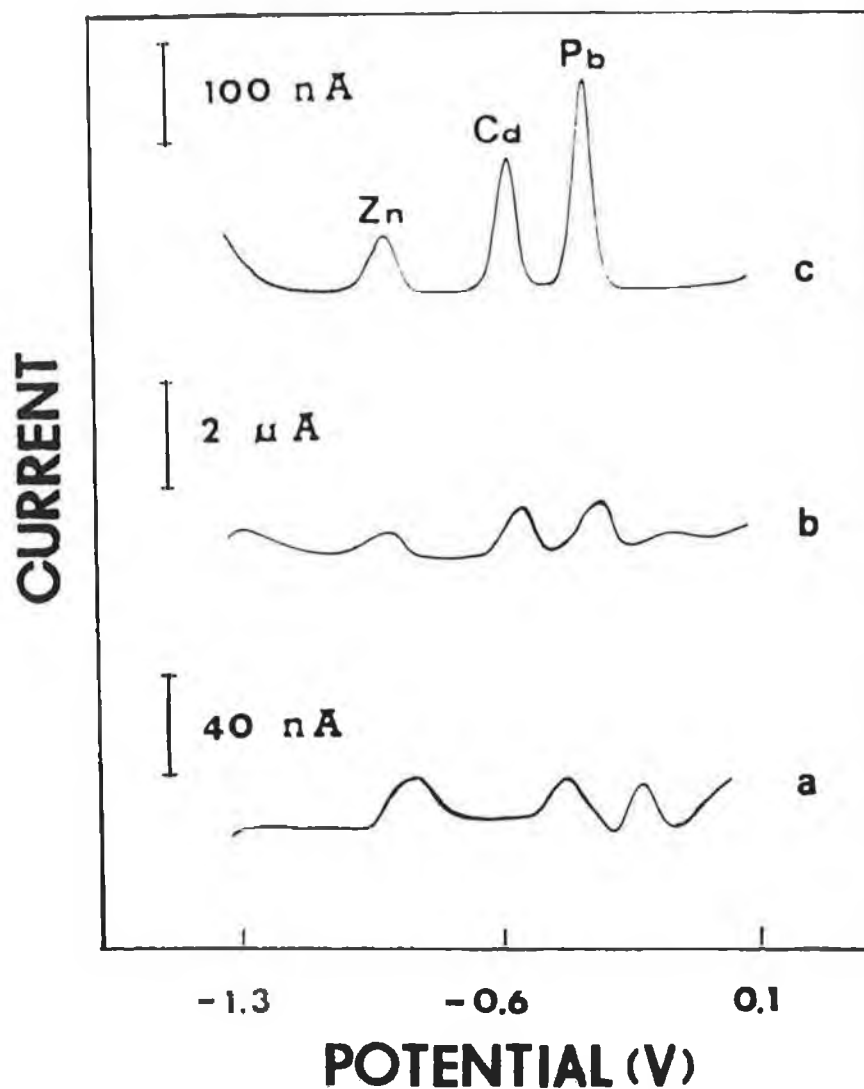


**Figure 1.1:** Differential pulse anodic stripping voltammograms of  $1 \times 10^{-6}$  M Zn(II), Cd(II) and Pb(II) recorded in methanol. (a) Hanging mercury drop, (b) mercury-coated glassy carbon electrode, and (c) mercury-coated microelectrode. Deposition time, 2 minutes; deposition potential, -1.35 V; scan rate,  $10 \text{ mV s}^{-1}$  [43].

this paper it was noted that the carbon fibre microelectrode responded to pH in the range 1 to 13. A linear relationship with slope of  $50 \text{ mV pH}^{-1}$  was obtained, and the potential was stable in a given buffer to 1 mV within minutes. Later research by the same group [45] used these electrodes for end-point detection in titrations of hydrochloric acid and orthophosphoric acid in aqueous solutions and for titrations of glycine in anhydrous acetic acid. The advantage of this pH indicator were considered to be its low impedance and its capability to analyse microvolumes. Further research by Jennings et al. [46] examined the effect of different manufacturing heat treatments on the pH response of the fibres. A fibre surface treated at low temperature was found to give the best result with an electrode slope of 80% of the Nernstian value. Edmonds et al. [47] also investigated the dependence of the surface conditions of carbon fibres on the potentiometric response to pH. It was demonstrated that the response could be dramatically improved by electrochemical pretreatment in the presence of typical buffer constituents.

#### 1.2.4.6 Coulometry

The large surface area of carbon fibres was exploited by Jennings and co-workers [48] for the coulometric generation of iodine. It was found that a carbon fibre bundle working electrode gave essentially the same results as platinum for the titration of sodium thiosulphate with coulometrically generated iodine; however, the accuracy of the titration was poorer. In a further paper, Jennings and Bailey [49] explored the use of a single fibre as a working electrode in the microcoulometric titration of hydrochloric acid and potassium hydrogen phthalate. A visual observation of the end point was not feasible due to the small volumes used ( $5 \mu\text{L}$ ); therefore a second carbon fibre microelectrode was employed as a pH indicator. A RSD of 1.4%

was reported for 5 titrations of 5  $\mu\text{L}$  of 10 mM hydrochloric acid.

#### 1.2.4.7 Other Electrochemical Applications

Laser light scattered by cylindrical carbon fibres was used to carry out adsorption spectroelectrochemistry on electrogenerated chromophores by Robinson and McCreery [24]. These workers identified several advantages of performing such studies at microelectrodes as a result of the relatively small currents generated. Lower demands are placed upon the potentiostat, a low cell constant is obtained, less error from solution resistance occurs and a better capability for applications involving fast reactions. The higher diffusional flux of reactants, and a faster re-establishment of initial conditions, renders time averaging more practicable as a higher duty cycle can be used. In addition, cylindrical diffusion dilutes the products of the charge transfer reaction rapidly, suppressing second-order reactions of electrogenerated species.

Engstrom and co-workers [50] exploited the small size of microelectrodes to investigate the diffusion layer of a conventional electrode. With the aid of a micromanipulator, the microelectrode could be moved in a direction either parallel or perpendicular to the macroelectrode surface, providing spatial resolution of concentration in three dimensions within the diffusion layer.

Another recently reported application of microelectrodes is the combination of the principles of scanning tunnelling microscopy (STM) with electrochemical measurements. In this way, spatial and electrochemical measurements can be made with sub-micrometre resolution [51]. Rather than rely on the tunnelling current flowing between the STM tip and the surface

being scanned, the tip can be backed off slightly from the 1 nm distance used for tunnelling measurements and faradaic currents can be imposed. The STM tip behaves as a microelectrode and effective mass transport to the tip results. Lin et al. [51] combined these features to electrochemically etch and read sub-micrometre patterns on the surface of an integrated circuit board.

### 1.3 MODIFIED ELECTRODES

The field of chemically modified electrodes (CME's) has been the focus of a high level of activity in recent years, and has assumed a dominant position in modern electrochemistry since its inception nearly 20 years ago. Interest in CME's has spread in various directions, including synthetic design of electrochemical reactive polymers, basic studies of electrocatalysis, photoelectrochemistry, electron transfer kinetics, membrane permeation, and electroanalysis. The electroanalytical applications of such electrodes has been the subject of recent reviews [52,53]. This short literature review will be concerned with the electroanalytical use of CME's, and will present a brief overview of the various designs of such electrodes with a representative sample of their applications.

Substantial enhancements of sensitivity, selectivity and/or stability of electroanalytical measurements has been the driving force for the development of modified electrodes. The principal modifying systems have generally involved the use of:

- (a) electrocatalytic redox modifiers that activate the electrode towards analytes that exhibit unfavourable overpotentials (this type of CME will be the subject of a later chapter);
- (b) enzyme and related biomolecular modifiers which impart

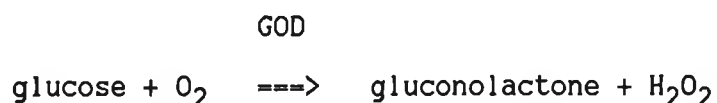


- specific biological activity to the CME;
- (c) permselective coatings that restrict access of interferences to the electrode surface; and
- (d) preconcentration of the analyte by a modified layer on the electrode surface.

### 1.3.1 Electrochemical Biosensors

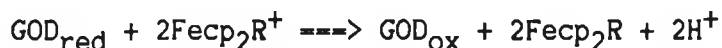
The term 'biosensor' as it is used in this section is a device which utilises biomolecules immobilised at a transducer surface to detect or respond to specific interactions with particular analytes. The transducer can take many electronic configurations, such as field-effect transistors, opto-electronic detectors, and potentiometric or amperometric electrodes. In this review, the focus will be on amperometric biosensors.

At present, biocatalytic surfaces (based on enzymatic processes) are receiving widespread attention. Such biologically modified electrodes measure the products or reactants of the mediated reaction. The high specificity of enzymes with regard to recognition of substrates enables CME's incorporating enzymes to achieve high selectivity for target species. In the case of amperometric enzyme electrodes, oxidoreductase or dehydrogenase enzymes are typically involved. Probably the most widely quoted example is the glucose oxidase (GOD) enzyme electrode for the determination of glucose which is based on the following reaction:



The reaction may be monitored either through formation of hydrogen peroxide or uptake of oxygen. One of the earlier examples of a CME utilising this reaction was reported by Wlecek and co-workers [54]. In their work, glucose oxidase was immobilised onto the surface of a flow-through reticulated carbon electrode by reaction with a water-soluble carbodiimide. In a flow system, injections of glucose samples resulted in the enzymatic production of  $H_2O_2$  at the modified surface. The oxidation current of  $H_2O_2$  so produced permitted glucose quantitation over the range  $10^{-4}$  to  $10^{-1}$  M.

One potential difficulty in the use of oxidoreductases is oxygen limitation under conditions of low oxygen tension. This can be particularly acute for in vivo applications where the concentration of unbound oxygen may be lower than that of the analyte, resulting in a stoichiometric limitation of the reaction by oxygen. To circumvent this, the most widely adopted approach is to replace oxygen with an artificial mediator of electron transfer. Cass et al. [55] employed a substituted ferricinium ion as a mediator of electron transfer between immobilised glucose oxidase and a graphite electrode. A voltammogram obtained in this study, of ferrocene-monocarboxylic acid ( $Fecp_2R$ ) in the presence of glucose alone, is shown in Figure 1.2a.. Upon addition of GOD (Figure 1.2b), a large catalytic current flows at oxidising potentials (GOD is not electroactive at these potentials). The behaviour is indicative of the regeneration of ferrocene from the ferricinium ion by the enzyme glucose oxidase in its reduced form. The latter is maintained in the reduced state by the presence of substrate. The following scheme describes the reaction sequence:



A linear current response for glucose concentration over a range commonly found in diabetic blood samples (1 to 30 mM) was reported, and results obtained with whole blood samples exhibited good agreement with a standard method of analysis.

Immobilisation of enzymes in a carbon paste matrix was introduced recently by Matuszewski et al. [56] for the production of reagentless enzyme electrodes. In this study, GOD was the enzyme utilised for the determination of glucose in a flow system. Wang and co-workers [57] investigated the simultaneous incorporation of glucose oxidase and several ferrocene-derivatives into a carbon paste electrode. The inclusion of stearic acid into the enzyme-containing paste reduced the interference due to ascorbic acid via electrostatic repulsion. In a further study, Wang et al. [58] replaced the carbon paste with a rigid graphite epoxy material which resulted in a polishable (i.e. renewable) enzyme probe. Robust glucose electrodes were constructed based on the incorporation of GOD and various ferrocene mediators into graphite-epoxy.

Another approach taken in the design of biosensors involves replacing isolated enzymes with tissue materials. The major advantage derived from the use of such materials are high stability and activity (associated with the presence of the enzyme in large quantities in its natural environment) and low cost. Early electrodes designed by Rechnitz [59] were based on the placement of the tissue slice on the top of the working electrode surface with the aid of a dialysis membrane. Using a

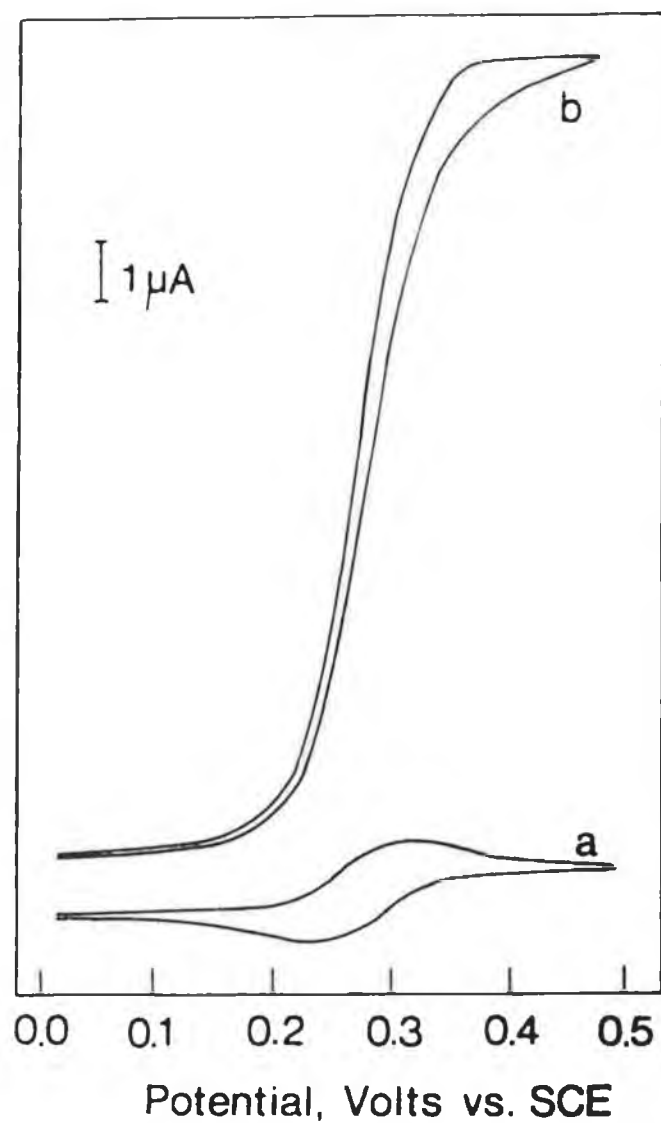


**Figure 1.2:** Cyclic voltammogram of 0.5 M ferrocene monocarboxylic acid in the presence of 50 mM D-glucose at a scan rate of  $1\ \text{mV s}^{-1}$ . (b) As for (a) but with the addition of 10.9  $\mu\text{M}$  glucose oxidase [55].

slice of kidney tissue, a dynamic linear range for glutamine of  $6.5 \times 10^{-5}$  to  $6.7 \times 10^{-3}$  M was reported with a limit of detection of  $2 \times 10^{-5}$  M. However, the electrode suffered from long reaction times, of the order of 5 to 7 minutes. A more attractive sensing design was described by Wang and Lin [60] based upon incorporating the tissue biocatalyst into a carbon paste matrix. The main advantage of this sensor was the substantial reduction of response time owing to the absence of a layer that hindered mass transport. The amperometric detection of dopamine [60], hydrogen peroxide [61] and phenols [62] using carbon paste electrodes modified with banana, horseradish root and mushroom tissue, respectively, have been reported recently. In addition to substrate detection, it has been demonstrated that tissue materials incorporated in carbon paste electrodes can offer elimination of potential interferences. In situ enzymatic digestion of proteins was accomplished by electrodes incorporating papaya tissue [63]. This protein digesting property was attributed to the presence of the enzyme papain found in papaya.

#### 1.3.2 Permselective CME's

Most detectors utilise electrodes which are subject to a gradual loss of activity. This is primarily due to adsorption of sample components or reaction products. One approach to improve the stability and selectivity is to cover the electrode with an appropriate film, a permselective membrane, which rejects certain components arriving at the electrode surface. The membranes used to date have generally consisted of polymeric films coated onto the surface of the electrode. The membrane's

design must provide rapid diffusion of the desired analyte, so films employed are generally thin. However, the optimal thickness always reflects a compromise between the efficient exclusion of interfering species and the free and rapid diffusion of the analyte. The selectivity of transport at the modified electrode can usually be related to analyte charge, polarity and molecular size or shape. A frequently used membrane is Nafion, which is a non-crosslinked perfluorinated polymer containing strongly acidic sulphonate groups, which is permeable to cationic and neutral species but excludes anions. This capability has been extensively exploited for the in vivo determination of catecholamines in the presence of high levels of ascorbate [64].

Another widely exploited film is cellulose acetate. This polymer is uncharged, and therefore shows no selectivity between anions and cations; however, it undergoes slow hydrolysis and pore formation when exposed to alkaline media. As a result, different permeabilities (molecular size cut-off) of the film can be formed by control of pH and hydrolysis time. Such manipulation of access to the electrode surface allows monitoring of a variety of analytes, representing different sizes. Sittampalam and Wilson [65] used a platinum electrode with a film of unhydrolysed cellulose acetate which permitted only small molecules to pass, such as hydrogen peroxide. Wang and Hutchins [66] subsequently demonstrated that the range of applications could be extended to larger molecules such as acetaminophen, phenol and ascorbic acid by the use of controlled hydrolysis. In both of these studies, the ability of the cellulose layer to resist fouling by macromolecules in biological samples, such as proteins, was demonstrated.

Further research by Wang and co-workers [67] reported the use of a bilayer electrode coating, a cellulose acetate film

over a Nafion layer, which offered a bifunctional capability, i.e., the prevention of electrode passivation while maintaining the permselectivity of the Nafion membrane. With this modified electrode the determination of epinephrine and dopamine in the presence of the surface active compounds, gelatin and albumin, was possible.

A CME exhibiting both size-selective and electrocatalytic response was obtained by the co-deposition of cobalt phthalocyanine with cellulose acetate onto the surface of a glassy carbon electrode [68]. The bifunctional CME retained the catalytic activity of the cobalt complex for the oxidation of hydrazine, oxalic acid and cysteine, while the permeability of the coating was determined by the extent of alkaline hydrolysis of the cellulose. In a flow system, the advantages of the modified layer were demonstrated as reduced operating potentials for detection, increased selectivity, and decreased fouling by surface active agents.

The determination of glucose at physiological levels was possible in a flow system with pulsed amperometric detection using a polymer modified gold electrode [69]. A bilayer of Nafion and collagen was used as the modifier coating. An inner Nafion layer retained  $\text{OH}^-$  at the gold surface while it excluded anions such as  $\text{Cl}^-$ , amino acids and ascorbic and uric acids. The outer layer of collagen prevented protein penetration and adsorption.

Several other polymers have also found use in permselective CME's. For example, Wang and Golden [70] coated a glassy carbon electrode with Eastman AQ55D poly(ester sulphonic acid) cation exchanger. Improvements in selectivity, as a result of excluding anionic species from the surface, was demonstrated with a variety of compounds of neurological significance. A stable

response was obtained in a flow system for acetaminophen in the presence of albumin. Poly(3-methylthiophene) coated electrodes exhibited resistance to surface fouling normally associated with oxidation of phenolic compounds [71]. In addition, the CME demonstrated enhanced sensitivity and selectivity. Another polymer film reported for permselective CME's is poly(4-vinylpyridine) (PVP) [72]. These films coated on a glassy carbon electrode, which are cationic at pH's lower than 6, demonstrated attenuated responses to catecholamines and other positively charged species but still exhibited large currents for anionic species.

Wang and co-workers [73] have recently described a sensor array of several amperometric electrodes, each covered with a different permselective film. Coatings with different transport properties, based on size (cellulose acetate), charge (Nafion, PVP, poly(ester sulphonic acid)), and polarity (phospholipid) were employed in connection with a four electrode thin layer flow detector. With equipotential operation, the response pattern provided for each analyte by the array provided a unique 'fingerprint' of the individual compounds. Multicomponent analysis was achieved by taking advantage of the partial selectivity of the individual sensors and using a statistical pattern recognition method. The merits of the array was demonstrated for the analysis of several neurologically significant compounds.

### 1.3.3 Preconcentration CME's

In the analysis of dilute samples it is often necessary to employ some type of preconcentration step prior to actual analysis, whereby the bulk of diluent is removed. Preconcentrating CME's bear formal analogy to trace analysis by the electrochemical technique of stripping voltammetry. The



sample species is partitioned from a dilute solution into the modified layer, where it is subsequently reduced or oxidised by application of an electrode potential sweep or step. These partitioning and measurement steps are analogous to the deposition and stripping procedures used in stripping voltammetry. To date, the use of the hanging mercury drop and the mercury thin film electrodes as working electrodes for the trace quantitation of electroactive compounds by stripping analysis has been most popular [74]. However, the use of a chemically tailored electrode surface has demonstrated several advantages over mercury such that the analyte can be very selectively extracted from a sample matrix on the basis of chemical functionality, stereochemistry, electrostatics or size.

Modified carbon paste electrodes prepared by the incorporation of ion-exchange resins directly into the paste matrix have found a wide range of application in the determination of ionic species. The ion-exchange process involves no electron transfer but is purely physicochemical, so no potential needs to be applied during the preconcentration step. Thus, the analytical procedures involving these CME's invariably involve accumulation of the analyte at the electrode without application of a potential, and then, after exchange of the medium, a voltammetric method is applied to determine the preconcentrated species.

Kalcher [75] used a liquid anion-exchanger, Amberlite LA2, for the voltammetric determination of Au(III) at levels as low as 100 ppb. It was demonstrated that ion exchangers in a liquid form are preferable over a resin or gel form, as the liquid phase exposes more functional groups to the solution than do particles in a matrix, resulting in a substantial increase in sensitivity. In further work, Kalcher [76] employed another exchanger, Aliquat 336, for the determination of nitrite.

Regeneration of the initial state of the surface of the modified electrode after a voltammetric analysis of nitrite was investigated, using exposure of the CME to a saturated sodium chloride solution, the anion of which should replace all other sorbed ions. This procedure, in addition to acid and alkaline treatments, failed, and only a mechanical renewal of the surface resulted in a satisfactory reproducibility. Wang et al. [77] incorporated the cation-exchange resin, Dowex CGC241 sulphonated polystyrene crosslinked to 8%, for the preconcentration of Cu(II) into the modified carbon paste electrode. DPV was used to quantify the accumulated ions. The procedure exhibited good linearity for  $6.25 \times 10^{-5}$  to  $3.0 \times 10^{-4}$  M Cu(II).

Baldwin and co-workers [78] also used a carbon paste electrode for the fabrication of a nickel selective CME. The electrode was based upon the immobilisation of dimethylglyoxime (DMG). DMG complexes Ni(II), which is subsequently quantified using DPV in a separate solution. The modified surface was regenerated by exposure to 1 M nitric acid. A linear response for Ni(II) of  $5 \times 10^{-8}$  to  $5 \times 10^{-6}$  M was reported. In further research, Baldwin et al. [79] employed the same CME in a flow system for the determination of Ni(II) in coal ash. The flow system was computerised, which facilitated the medium exchange and regeneration steps.

Recently, Ghao and co-workers [80] designed a chemically modified carbon paste electrode for the determination of cobalt(II). The electrode was based on the chemical reactivity of an immobilised modifier, i.e. 2,2'-bipyridyl (bpy), toward cobalt(II) ion to yield the corresponding cation complex,  $((bpy)_3Co)^{2+}$ . In initial experiments it was found that carbon paste electrodes containing bpy were not stable when immersed in aqueous solutions, due to the solubility of the modifier. However, this was overcome by the addition of Nafion

to the paste matrix. The cationic cobalt complex was accumulated by Nafion to form an insoluble complex which remained stable. DPV was employed in the analysis step, and for a five minute preconcentration period a linear range extending from  $7 \times 10^{-7}$  to  $1 \times 10^{-5}$  M and a detection limit of  $3 \times 10^{-7}$  M was obtained. A rapid acid removal procedure permitted the use of an individual modified electrode surface in multiple analytical quantitations, with a 4.3% relative standard deviation.

The use of polymeric films for the technique of preconcentration has also been exploited. O'Riordan and Wallace [81] designed such a modified surface by the immobilisation of poly(pyrrole-N-carbodithioate) on a glassy carbon electrode. The ability of this polymeric, ligand-containing, modified electrode for the uptake of copper(II) ions was investigated. The accumulated copper was subsequently determined voltammetrically. Under specified preconcentration conditions and using cyclic voltammetry, a detection limit of 1 ppm was estimated.

A major advance in the design of polymer films for preconcentration CME's was reported by Abruna and co-workers [82,83]. Their approach was based upon the use of polymer films that bear both an electroactive group as well as a ligand moiety. The internal redox centre serves to immobilise the polymer on the electrode surface via electroprecipitation. This is advantageous since it allows for the direct control of and determination of the coverage of the polymer on the electrode surface by controlling the deposition conditions, and by monitoring the electrochemical response of the electroactive centre after deposition, respectively. This latter point is important, as it allows an a priori determination of a saturation response. The ligand itself is chosen so as to have a high affinity and selectivity to the metal ion of interest. The

ligand can then be incorporated by being part of the polymer backbone or, alternatively, by ion-exchange to a polycationic polymer film. An example of this design, involved a ligand, sulphonated bathophenanthroline, incorporated through ion-exchange into a quaternised layer of poly(vinylpyridine)/vinyl ferrocene on the surface of a glassy carbon electrode [84]. The CME was used for the selective determination of Fe(II) in the range 1 to 40 ppm. In a more recent study, Cha and Abruna [83] investigated the utility of platinum electrodes modified with seven different ligands (incorporated by ion-exchange into a polycationic film of electropolymerised  $(\text{Ru}(4\text{-vinyl-4'-methyl-2, 2'-bpy})_3)^{2+}$ , whose formation constants for copper(II) vary over a broad range. As an initial step, the response of the seven ligand-modified electrodes toward copper(II) was investigated. Also investigated were the effects on the analytical signal of other competing ligands at varying co-ordination strengths toward copper(II). The relevance of these investigations to speciation studies was investigated.

Chastel et al. [85] recently described a modified electrode for the preferential accumulation of the anti-tumour drug, marcellomycin. A glassy carbon electrode was modified by deposition of a hydrophobic coating of the lipid, asolectin. In neutral aqueous media, this negatively charged lipid modified electrode selectively accumulates organic molecules, depending on their charge and their hydrophilic-hydrophobic balance. A linear working range of  $2 \times 10^{-6}$  to  $5 \times 10^{-5}$  M and a detection limit of  $5 \times 10^{-7}$  M for marcellomycin was reported using this electrode. Wang and Ozsoz [86] also employed a lipid coated electrode for the determination of the antihypertensive drugs, reserpine and rescinnamine. These compounds were shown to partition readily into a cast lipid (phosphatidylcholine) layer. Detection limits of  $5 \times 10^{-9}$  M were estimated for both

drugs based on a ten minute preconcentration time. The hydrophobic lipid coating was also demonstrated to reject species that would otherwise interfere at the unmodified carbon surface (e.g., ascorbic and uric acids).

#### 1.4 CONCLUSION

Analysis with CME's has been shown to benefit from their catalytic and discriminative capabilities, as well as their use as preconcentrating electrodes. As a result, substantial improvements in the selectivity, sensitivity, versatility, and reproducibility of voltammetric measurements can be achieved. By virtue of these approaches, the judicious employment of CME's has already had a significant impact on the performance and scope of electrochemical detection systems.

The development of microelectrodes has also greatly expanded the scope of electroanalytical measurements. The unusual and attractive features of these electrodes, including their high rates of mass transfer and greatly reduced ohmic and capacitance effects, permit studies under conditions not possible with conventional electrodes.

## 1.5 REFERENCES

1. J Heyrovsky, Chem. Listy, 16 (1922) 256.
2. R.N. Adams, Electrochemistry at Solid Electrodes, Marcel Dekker, New York, 1969.
3. P. Bindra, A.P. Brown, M. Fleischman and D. Pletcher, J. Electroanal. Chem., 58 (1975) 31.
4. R.N. Adams, Anal. Chem., 48 (1976) 1125A.
5. J.L. Ponchon, R. Cespuglio, F. Gonon, M. Jouvet and J.F. Pujol, Anal. Chem., 51 (1979) 1483.
6. R.M. Wightman, Anal. Chem., 53 (1981) 1125A.
7. R.M. Wightman and D.O. Wipf, Electroanalytical Chemistry, Vol. 15, A.J. Bard (Ed.), Marcel Dekker, New York, 1989, pp 267.
8. T.E. Edmonds, Anal. Chim. Acta, 175 (1985) 1.
9. J.B. Donnet and R.C. Bansal, Carbon Fibres, Marcel Dekker, New York, 1984.
10. K. Kinoshita, Carbon: Electrochemical and Physicochemical Properties, Wiley, New York, 1988.
11. A. Fourdeaux, R. Perret and W. Ruland, J. Appl. Cryst., 1 (1968) 252.
12. J. Golas and J. Osteryoung, Anal. Chim. Acta, 181 (1986) 211.
13. M.A. Dayton, J.C. Brown, K.J. Stutts and R.M. Wightman, Anal. Chem., 52 (1980) 946.
14. K. Aoki, K. Honda, K. Tokuda and H. Matsuda, J. Electroanal. Chem., 182 (1985) 267.
15. Z. Galus, Fundamentals of Electrochemical Analysis, Halsted Press, New York, 1976.
16. T.E. Edmonds and J. Guoliang, Anal. Chim. Acta, 151 (1983) 99.
17. A.G. Ewing, M.A. Dayton and R.M. Wightman, Anal. Chem., 53 (1981) 1842.

18. A.S. Baranski, J. Electrochem. Soc., 133 (1986) 93.
19. J. Newman, J. Electrochem. Soc., 113 (1966) 501.
20. A. Fitch and D.H. Evans, J. Electroanal. Chem., 202 (1986) 83.
21. A.M. Bond, M. Fleischman and J. Robinson, J. Electroanal. Chem., 168 (1984) 299.
22. A.M. Bond, M. Fleischman and J. Robinson, J. Electroanal. Chem., 180 (1984) 257.
23. J. Ghorogachian, F. Sarfarazi, T. Dibble, J. Cassidy, J.J. Smith, A. Russell, G. Dunmore, M. Fleischman and S. Pons, Anal. Chem., 58 (1986) 2278.
24. R.S. Robinson and R.L. McCreery, Anal. Chem., 53 (1981) 997.
25. J.O. Howell and R.M. Wightman, Anal. Chem., 56 (1984) 524.
26. K.R. Wehmeyer and R.M. Wightman, Anal. Chem., 57 (1985) 1989.
27. C.P. Andrieux, P. Hapiot and J.M. Saveant, Electroanalysis, 2 (1990) 183.
28. F. Gonon, C.M. Fombarlet, M.J. Buda and J.F. Pujol, Anal. Chem., 53 (1981) 1386.
29. L. Falat and H.Y. Cheng, Anal. Chem., 54 (1982) 2108.
30. P. Capella, B. Ghasemzadah, K. Mitchell and R.N. Adams, Electroanalysis, 2 (1990) 175.
31. M.A. Dayton, A.G. Ewing and R.M. Wightman, J. Electroanal. Chem., 146 (1983) 189.
32. D.G. Swartzfagar, Anal. Chem., 48 (1976) 2189.
33. W.L. Caudill, J.O. Howell and R.M. Wightman, Anal. Chem., 54 (1982) 2532.
34. E.W. Kristensen, R.L. Wilson and R.M. Wightman, Anal. Chem., 58 (1986) 986.
35. L.A. Knecht, E.J. Guthrie and J.W. Jorgenson, Anal. Chem., 56 (1984) 479.
36. J.G. White, R.L. St. Claire and J.W. Jorgenson, Anal. Chem., 58 (1986) 293.

37. W. Hou, H. Ji and E. Wang, *Anal. Chim. Acta*, 230 (1990) 207.
38. C. Hua, K.A. Sagar, K. McLaughlin, M. Jorge, M.P. Meaney and M.R. Smyth, *Analyst*, 116 (1991) 1117.
39. R.A. Wallingford and A.G. Ewing, *Anal. Chem.*, 59 (1987) 1762.
40. M.R. Cushman, B.G. Bennett and C.W. Anderson, *Anal. Chim. Acta*, 130 (1981) 323.
41. W. Frenzel, *Anal. Chim. Acta*, 196 (1987) 141.
42. G. Schulze and W. Frenzel, *Anal. Chim. Acta*, 159 (1984) 95.
43. J. Wang and P. Tuzhi, *Anal. Chim. Acta*, 197 (1987) 367.
44. V.J. Jennings and P. Pearson, *Nature*, 31 (1975) 256.
45. V.J. Jennings, *Analyst*, 106 (1981) 1344.
46. V.J. Jennings, *Electroanalysis in Hygiene, Environmental, Clinical and Pharmacological Chemistry*, W.F. Smyth (Ed.) Elsevier, Amsterdam, 1980, pp. 199.
47. T.E. Edmonds, J.R. Dean and S. Latiff, *Anal. Chim. Acta*, 212 (1988) 23.
48. V.J. Jennings, A. Dodson and R.J. Eastman, *Anal. Chim. Acta*, 76 (1975) 143.
49. V. J. Jennings and T.D. Bailey, *Anal. Chim. Acta*, 84 (1976) 61.
50. R.C. Angstrom, M. Weber, D.J. Wunder, R. Burgess and S. Winquist, *Anal. Chem.*, 58 (1986) 844.
51. C.W. Lin, F.R.F. Fan and A.J. Bard, *J. Electrochem. Soc.*, 134 (1987) 1038.
52. R.W. Murray, A.G. Ewing and R.A. Durst, *Anal. Chem.*, 59 (1987) 397A.
53. R.P. Baldwin and K.N. Thomsen, *Talanta*, 38 (1991) 1.
54. H.J. Wieck, G.H. Heider and A.M. Yacynych, *Anal. Chim. Acta*, 158 (1984) 137.



55. A.E.G. Cass, G. Davis, G.D. Francis, H.A.O. Hill, W.J. Aston, I.J. Higgins, E.V. Plotkin, L.D.L. Scott and A.P.F. Turner, *Anal. Chem.*, 56 (1984) 667.
56. W. Matuszewski and M. Trojanowicz, *Analyst*, 113 (1988) 735.
57. J. Wang, L. Wu, Z. Lu, R. Li and J. Sanchez, *Anal. Chim. Acta*, 228 (1990) 251.
58. J. Wang and K. Varughese, *Anal. Chem.*, 62 (1990) 318.
59. G.A. Rechnitz, *Science*, 214 (1981) 287.
60. J. Wang and M.S. Lin, *Anal. Chem.*, 60 (1988) 1545.
61. J. Wang and M.S. Lin, *Electroanalysis*, 1 (1989) 43.
62. M. Bonakdar, J.L. Vilchez and H.A. Mottola, *J. Electroanal. Chem.*, 266 (1989) 47.
63. J. Wang, L.H. Wu, S. Martinez and J. Sanchez, *Anal. Chem.*, 63 (1991) 398.
64. P.A. Broderick, *Electroanalysis*, 2 (1990) 241.
65. G. Sittampalam and G.S. Wilson, *Anal. Chem.*, 55 (1983) 1608.
66. J. Wang and L.D. Hutchins, *Anal. Chem.*, 57 (1985) 1536.
67. J. Wang and P. Tuzhi, *Anal. Chem.*, 58 (1986) 3257.
68. J. Wang, T. Golden and R. Li, *Anal. Chem.*, 60 (1988) 1642.
69. D.S. Bindra and G.S. Wilson, *Anal. Chem.*, 61 (1989) 2566.
70. J. Wang and T. Golden, *Anal. Chem.*, 61 (1989) 1397.
71. J. Wang and R. Li, *Anal. Chem.*, 61 (1989) 2809.
72. J. Wang, T. Golden and P. Tuzhi, *Anal. Chem.*, 59 (1987) 740.
73. J. Wang, G.D. Rayson, Z. Lu and H. Wu, *Anal. Chem.*, 62 (1990) 1924.
74. J. Wang, *Stripping Analysis: Principles, Instrumentation, and Applications*, VCH Publishers, Weinheim, 1985.
75. K. Kalcher, *Anal. Chim. Acta*, 177 (1985) 175.
76. K. Kalcher, *Talanta*, 33 (1986) 489.

77. J. Wang, B. Greene and C. Morgan, Anal. Chim. Acta, 158 (1984) 15.
78. R.P. Baldwin, J.K. Christensen and L. Kryger, Anal. Chem., 58 (1986) 1790.
79. K.N. Thomas, L. Kryger and R.P. Baldwin, Anal. Chem., 60 (1988) 151.
80. Z. Ghao, G. Wang, P.Li and Z. Zhao, Anal. Chem., 63 (1991) 953.
81. D.M.T. O'Riordan and G.G. Wallace, Anal. Chem., 58 (1986) 128.
82. L.M. Weir, A.R. Guadalupe and H.D. Abruna, Anal. Chem., 57 (1985) 2011.
83. S.K. Cha and H.D. Abruna, Anal. Chem., 62 (1990) 274.
84. A.R. Guadalupe and H.D. Abruna, Anal. Chem., 57 (1985) 142.
85. D. Chastel, J.M. Kauffmann, G.J. Patriarche and G.D. Christian, Anal. Chem., 61 (1989) 170.
86. J. Wang and M. Ozsoz, Analyst, 115 (1990) 831.

## CHAPTER 2

DETERMINATION OF NITRITE BASED  
ON ITS MEDIATED OXIDATION AT A  
CHEMICALLY MODIFIED ELECTRODE

## 2.1 INTRODUCTION

As mentioned in chapter one, one approach to the preparation of CME's involves the incorporation of electrocatalytic redox modifiers that activate the electrode toward analytes which exhibit substantial overpotentials. Many redox reactions are rate limited by the kinetics of the electron transfer processes and not by the rate of diffusion. These heterogeneous electron transfer rates can be dramatically influenced by electrocatalysts, and the modification of electrode surfaces provides an opportunity to immobilise these catalysts and thereby extend electrochemical methodology to the study of such systems. The need for mediation of this type arises whenever the rate of direct electron transfer is slow. As a consequence of this, a potential in excess of the standard (thermodynamic) potential of the analyte i.e. an overpotential, must be applied in order for the desired redox process to proceed at an appreciable rate. However, with the use of an electrocatalytic CME, the redox process is accelerated to take place at the redox potential of the mediator. A decrease in the magnitude of the applied potential is desired in many applications as it can substantially improve the analytical performance, in that reduced detection potentials result in lower detection limits and improved selectivity, as a result of lower background currents and the restricted range of electroactive compounds which interfere at lower potentials. For those compounds whose electrochemical processes normally occur beyond the decay of the supporting electrolyte, the use of electrocatalytic CME's also permits them to be determined by electrochemical methods.

The purpose of this chapter is to present an overview of the analytical applications of electrocatalytic CME's, followed by a description of the research work detailing the design of such an electrode for the detection of nitrite.

### 2.1.1 Mechanism of Operation

The basic principle involved in decreasing the overpotential of an analyte by accelerating the desired reaction using an immobilised catalyst mediator for a generalised oxidation process is illustrated in Figure 2.1A [1]. The analyte diffuses from the bulk solution to the electrode surface where it is oxidised in a purely chemical reaction with the oxidised form of the mediator. At a working electrode, the potential is maintained at a value sufficiently positive for the oxidised form to be the stable form of the mediator and its reduced form to be rapidly re-oxidised to the catalytically active form. Thus the heterogeneous electron transfer takes place between the electrode and the mediator and not directly between the mediator and the analyte. This catalysed reaction occurs near the formal potential of the mediator couple.

Redox polymer coated electrodes for the catalysis of electrochemical reactions have been the object of active investigation during the past decade. The main reason for the interest they have aroused is the expectation that they can combine the advantages of monolayer derivatised electrodes with those of homogeneous catalytic systems. With redox polymer coatings as with monolayer derivatised surfaces, high local concentrations of catalytic sites can be achieved even though the total amount of catalyst remains small. The two systems also share the advantage of a good separation of the reaction products from the catalyst. On the other hand, redox polymer coatings, as homogeneous catalytic systems, offer a three-dimensional dispersion of the reacting centers as opposed to the two-dimensional arrangement prevailing at monolayer derivatised surfaces. Kinetic models have been developed for steady-state regimes that permit the identification of the rate-controlling factors, to describe their interplay, to

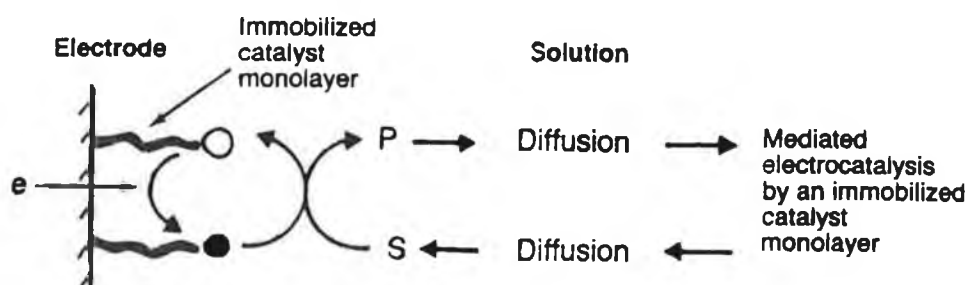
extract the pertinent kinetic constants from the experimental data, and to optimise the catalytic efficiency for the polymer coating. These models are based on the fact that, besides the transport of the substrate from the bulk of the solution to the solution-polymer interface, the current is governed by three rate-limiting phenomena in the polymer film: the catalytic reaction itself, the diffusion-like charge propagation, and the substrate diffusion across the coating [2,3]. These processes are illustrated in Figure 2.1B.

### 2.1.2 Analytical Applications

The analytical application of electrocatalytic CME's has been the subject of a number of recent reviews [4,5]. The solution-phase electrocatalysis of many analytes has been investigated and an extensive range of chemical information relevant to the selection of catalytic mediators as electrode modifiers is available. Electrocatalytic CME's employed in studies in quiescent media have successfully utilised mediators of both organic and inorganic origin [4].

An interesting example of employing electrocatalysis to improve the voltammetric behaviour of analytes can be seen by considering the physiologically important analyte, dihydronicotinamide adenine dinucleotide (NADH). The direct oxidation of NADH at carbon electrodes is slow, and its oxidation reaction involves radical intermediates which cause electrode fouling. Kuwana and co-workers [5,6] used a systematic approach to the design of an electrode surface for the electrocatalysis of NADH oxidation. First they examined the homogeneous solution kinetics using several quinones and identified o-quinone as the most potent catalytic mediator. In the preparation of the CME they chemically immobilised a monolayer of an o-quinone polymer, on a glassy carbon

**A**



**B**

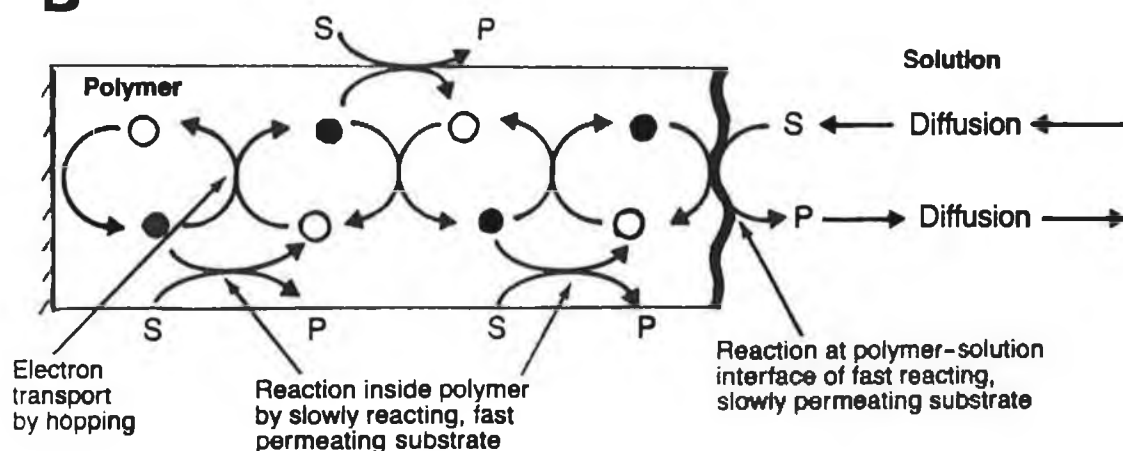


**Figure 2.1:** Schematic illustrations of mediated electrocatalysis by (A) an immobilised catalyst monolayer, and (B) a redox polymer film, where  $\circ$  is the reduced form, and  $\bullet$  is the oxidised form of the mediator catalyst [1].

electrode and as predicted from homogeneous solution data, the electrooxidation of the o-quinone polymer led to a mediated oxidation of NADH at a significantly reduced potential than that at a bare carbon electrode. In addition to the electrocatalysis of NADH, a reduced overpotential was observed at the CME for the oxidation of ascorbic acid. Subsequently Lau and Miller [7] incorporated the same o-quinone moiety into a polymer film electrode. Using this modified electrode the oxidation of NADH was reported at a potential 250 mV less positive than that at the bare carbon surface.

In another study involving NADH, Yon and Lowe [8] developed a CME by the electrodeposition of the hexacyanoferrate(II/III) couple on nickel by anodisation of porous nickel electrodes in electrolytes containing hexacyanoferrate(II) ions. This redox mediator was used to catalyse the oxidation of NADH. Cyclic voltammograms recorded in this study are shown in Figure 2.2. The CME was demonstrated to be capable of reoxidising enzymatically-generated NADH, and to possess many of the features desirable for use as an amperometric sensor for oxidoreductase substrates. Kulesza et al. [9] used the same redox mediator, hexacyanoferrate(II/III), electrodeposited on a glassy carbon electrode for the reduction of Fe(III), a process which is generally irreversible and irreproducible at bare glassy carbon. Because detection was operated at +0.2 V, there was no interference from dissolved oxygen. The catalytic current was used to determine Fe(III) concentration over the range  $2 \times 10^{-7}$  to  $9 \times 10^{-4}$  M.

Electrocatalytic CME's incorporating metal redox-active sites into polymer coated electrodes has recieved considerable attention [10], especially those containing ruthenium. Oyama and Anson [11] coordinately attached Ru(II)-edta to pyridine groups in a poly(4-vinylpyridine) (PVP) film on the surface of a



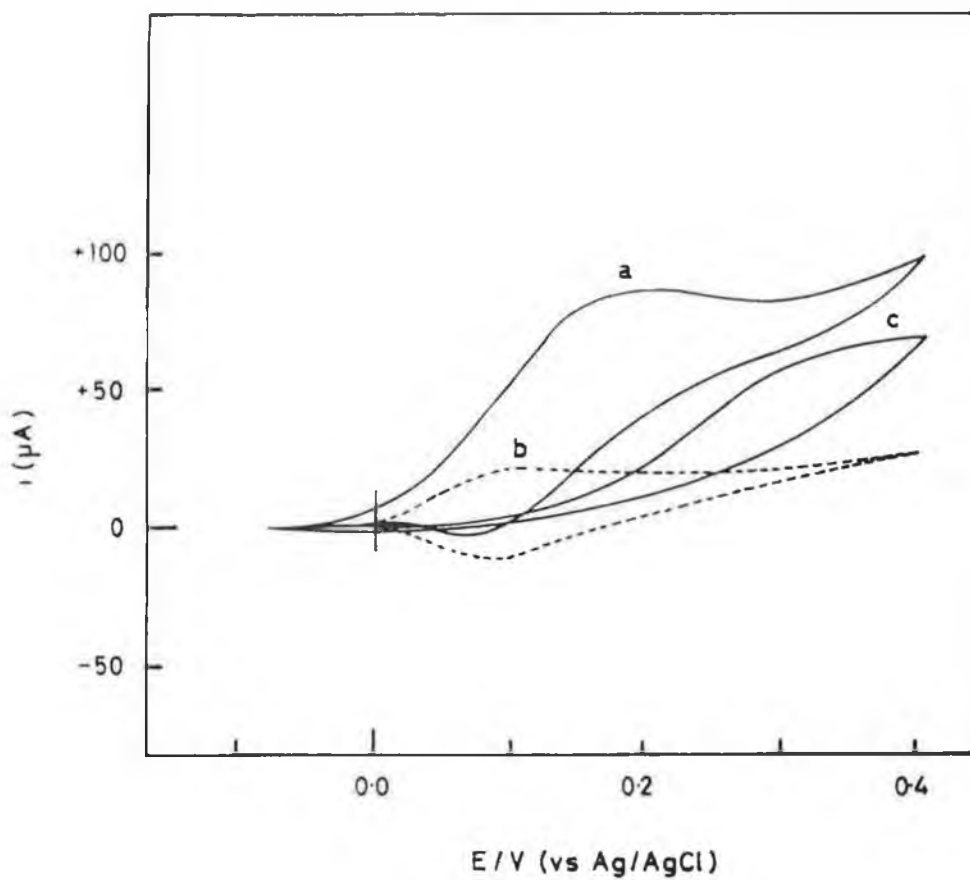


**Figure 2.2:** Cyclic voltammogram of the catalytic oxidation of 5 mM NADH at hexacyanoferrate-modified electrode (curve a). Curve b shows the behaviour of the modified electrode without NADH. Curve c shows the oxidation of NADH at the unmodified electrode. Scan rate,  $1 \text{ mV s}^{-1}$  [8].

carbon electrode. The complex was used to mediate the electroreduction of  $[\text{Fe}(\text{CN})_6]^{3-}$ . Other methods of introducing ruthenium onto an electrode surface have been reported, including incorporation of ruthenium dioxide in electrodeposited polypyrrole [12], formation of a bilayer electrode such as platinum-ruthenium-polypyrrole [13], and attachment of ruthenium(II) to amino functional groups on graphite electrodes [14]. Geraty et al. [15] used the metallopolymer  $[\text{Ru}(\text{bipy})_2(\text{PVP})\text{Cl}]\text{Cl}$ , where bipy is 2-2'-bipyridyl, chemisorbed to the surface of a glassy carbon electrode for the determination of Fe(II). A linear range of  $5 \times 10^{-6}$  to  $5 \times 10^{-5}$  M using rotating disk techniques was reported. Employing the same polymer coated electrode as a working electrode in a flow system, Barisci et al. [16] demonstrated the enhanced sensitivity obtained for various dithiocarbamate metal complexes and nitrite ions. The modified surface was also reported as being less prone to product adsorption problems. However, the practical application of this metallopolymer in flowing systems was limited due to the slow removal of the polymer from the electrode surface as a result of solvent abrasion. This instability was alleviated to some extent by treatment with UV light or by coating with other polymer films [17].

Another metallopolymer CME, described by Cox and Kulesza [18], involved electrostatically binding hexachloroiridate within a film of quaternised PVP on the surface of a glassy carbon electrode. The electrocatalytic oxidation of nitrite was demonstrated, in addition to the elimination of surface passivation problems. In a further work, the same CME was employed in a flow system [19]. A working linear range of  $1 \times 10^{-5}$  to  $1 \times 10^{-3}$  M nitrite and a detection limit of 0.07 ppm was reported. Gunasingham and co-workers [20] described a modified electrode involving a metallopolymer which was prepared by electrodeposition of platinum particles into a Nafion-coated

glassy carbon electrode. This was accomplished by first coating the electrode surface with a film of Nafion and then electrodepositing platinum particles by potential cycling in a solution of  $K_2PtCl_6$ . The CME exhibited good stability and was used for the determination of hydrogen peroxide in a flow system. The mediation of ascorbic acid over a wide pH range was reported by Lu and Dong [21] using a polyvinylferrocene modified electrode. A linear range of  $6 \times 10^{-6}$  to  $6 \times 10^{-2}$  M was observed.

In addition to the immobilisation of catalysts in polymer films, the integration of a catalyst in carbon paste electrodes has also proved successful. A notable example is cobalt phthalocyanine, which has been widely investigated for use in CME's by Baldwin's group [22-26]. The response of this CME is initiated by the electrooxidation of Co(II) to Co(III). The catalysed electrooxidation of several thiols, including cysteine, N-acetylcysteine and glutathione at a carbon paste electrode containing cobalt phthalocyanine, was demonstrated by Halbert and Baldwin [22]. Used in conjunction with reversed-phase chromatography, the CME exhibited a linear response for cysteine from 2.7 to 270 pmole. Individual surfaces were sufficiently stable for a full day of continuous use, and surfaces could be reproduced with a RSD of 7%. LCEC assay procedures using the CME were developed for cysteine and glutathione in whole blood and plasma. In a later work [23], the same CME catalysed the oxidation of oxalic acid and alpha-keto-acids over the range +0.75 to +0.90 V, which represents nearly a 0.5 V decrease in overpotential compared with the response at an unmodified electrode. At 0.75 V, the response for oxalic acid was linear from  $1 \times 10^{-7}$  to  $2 \times 10^{-5}$  M and gave a detection limit of 0.3 ppm. The detection limits for the keto-acids varied from 0.15 to 1 nmole. Assay procedures using the CME as a detector in reversed-phase

chromatography were developed for oxalic and pyruvic acids in plasma and urine samples. Other compounds determined with this modified electrode have included carbohydrates [24], ribonucleosides [25] and thiopurines [26].

Baldwin and co-workers [27] also designed another CME utilising a carbon paste matrix. PVP was immobilised in a carbon paste electrode which was immersed in a solution of ferrocyanide which was subsequently bound electrostatically. this CME was used for the electrocatalytic oxidation of ascorbic acid. Wang's group [28] have also exploited the carbon paste matrix in the construction of electrocatalytic modified electrodes. Carbon paste electrodes, containing ruthenium dioxide, were demonstrated to provide an electrocatalytic response toward carbohydrates at a low potential (0.4 V). The detection limits reported for several carbohydrates were at the picomole level.

One distinct disadvantage of carbon paste CME's used in flow systems is that the applicable mobile phases are restricted to predominately aqueous systems. This is a well known limitation for all carbon paste electrodes, modified or not, because the organic liquids used to form the the paste mixture have appreciable solubilities in most non-aqueous solvents. Recently, Baldwin and co-workers [29] have described glassy carbon electrodes modified with a cobalt phthalocyanine-containing polymer, an electrocatalyst previously only incorporated in carbon paste modified electrodes. The electrodes were formed by the electropolymerisation of Co-4,4',4'',4''',tetraamino-phthalocyanine, and exhibited electrocatalytic properties similar to those reported earlier for carbon paste electrodes containing a cobalt phthalocyanine monomer. However, these CME's offered increased stability and compatibility with organic solvents. Determination of picomole quantities of various thiols was reported following reversed-phase chromatographic separation

in mobile phases composed of 50% methanol or acetonitrile. Wring et al. [30] have also designed a CME using cobalt phthalocyanine which had superior chemical and mechanical stability over a carbon paste electrode. The construction of a polishable, and hence re-usable, surface using an epoxy resin-graphite composite containing cobalt phthalocyanine was described. The modified electrode was incorporated in a thin-layer flow cell in a LC system. The CME was found to substantially reduce the overpotential necessary for the oxidation of reduced glutathione, and exhibited a linear response over the range  $1 \times 10^{-7}$  to  $5.5 \times 10^{-3}$  M with a limit of detection of  $10 \text{ ng mL}^{-1}$ . The composite electrode was stable and could be used over a period of at least ten hours with no significant loss of activity.

A wide variety of other inorganic catalysts for the modification of electrode surfaces have found extensive use in the design of CME's. A mixed valence ruthenium(II/III) cyanide film electrodeposited on a glassy carbon electrode catalysed the oxidation of hydrazine [31]. The response was linear for concentrations from  $5$  to  $50 \times 10^{-6}$  M and gave a detection limit of  $2 \times 10^{-6}$  M. When polyaniline was co-deposited with the ruthenium cyanide as a single film, the resulting modified layer exhibited size-selective in addition to electrocatalytic properties. Another CME developed for the catalytic oxidation of various hydrazines and hydrogen peroxide was reported by Taha and Wang [32]. A glassy carbon electrode covered with a thin film of an oxymanganese species was employed for the electrocatalytic amperometric detection of these compounds in a flow system. A glassy carbon electrode coated with a mixed valence ruthenium oxide/cyanide film was demonstrated to catalyse the oxidation of cysteine and glutathione between  $0.9$  and  $1.0$  V [33]. In a flow system, detection limits for both of these compounds were below  $10^{-6}$  M and the response was linear

over three orders of magnitude. The modified electrode showed long term stability, with no deterioration in sensitivity over a two week period. The use of a ruthenium cyanide CME was also utilised for the electrocatalysis of thiocyanate [34]. The film was reported to prevent fouling of the electrode surface by oxidation products and sample constituents. The response for thiocyanate was linear from  $0.2$  to  $4.0 \times 10^{-6}$  M, and the CME was stable for over 3 months. In the same paper another modified electrode was described for the determination of thiocyanate which exhibited a broader linear range of  $5 \times 10^{-6}$  to  $1 \times 10^{-4}$  M. The CME was prepared by the adsorption of  $I^-$  on the surface of a platinum electrode which was then coated with a film of cellulose acetate. However, unlike the ruthenium cyanide CME, the modified surface was stable for several days only. An iodide-coated platinum electrode was also used for the detection of nitrite [18]. The catalytic currents observed were linear over the range  $8 \times 10^{-6}$  to  $4 \times 10^{-3}$  M.

Wang and Freiha [35] reported on the use of alumina modified electrodes for the improvement of detection performance in LCEC. The modified electrode was prepared by polishing the surface with 1  $\mu$ m alumina particles. The electrode was rinsed with deionised water and was then used for LC detection. The catalytic effect of alumina permitted the lowering of the detector operating potential for the determination of epinephrine, oxalic acid and ascorbic acid. Detection limits for all three compounds were of the nanogram level. The stability data presented in the paper indicated that most of the alumina particles remain at the surface and maintain their catalytic activity over long periods of time, despite the vigorous hydrodynamic conditions that prevail at the thin-film electrode. The CME was demonstrated for the analysis of urine samples, where its lower operating potential was shown to be advantageous.

CME's produced by the deposition of a copper(II) layer onto the surface of a glassy carbon electrode were reported for the electrocatalytic oxidation of numerous polyhydroxyl compounds, including carbohydrates, amino sugars and alditols [36,37]. In cyclic voltammetry, the electrocatalysis appeared as an irreversible anodic wave at 0.5 V and only occurred at hydroxide concentrations of  $10^{-3}$  M. Used in a LCEC system, the CME was shown to provide detection limits of the order of 1 to 5 picomoles for most mono- and disaccharides.

## 2.2 DETERMINATION OF NITRITE AT A RUTHENIUM POLYMER-MODIFIED CARBON PASTE ELECTRODE

In recent years there has been growing concern about the role of the nitrite ion as an important precursor in the formation of N-nitrosamines, many of which have been shown to be carcinogens in animal experiments [38]. The occurrence of nitrite salts in the environment, and their use as food preservatives, is widespread; therefore it is important that sensitive and accurate methods be available for the determination of the nitrite ion.

A large number of analytical methods have been developed for the determination of this ion based principally on spectrophotometric methods [39-41] but these have limited sensitivity and dynamic range, frequently depend on unstable colour formation, and involve long reaction times. Cox and Kulesza [18] reported a voltammetric procedure using a platinum electrode modified with iodine, but this method was limited by poor sensitivity. A more sensitive CME for the detection of nitrite was described by Kalcher [42] using a carbon paste

electrode modified with an anion exchanger, but this electrode suffered from long analysis times. More recently, several sensitive polarographic methods have been reported in the literature [43,44] for the detection of nM levels of nitrite. Methods based on solid electrodes are more desirable, however, for sensing and flow applications.

The purpose of the present study was to investigate the application of carbon paste electrodes modified by the incorporation of the redox-active ruthenium(II/III) for the determination of nitrite. Previous studies employing this polymer, chemisorbed to a glassy carbon electrode, suffered from limited stability in a flow system, as a result of solvent abrasion [16]. An aim of this study was to examine if the carbon paste matrix could provide a more stable environment for the immobilisation of the polymer, for use in a flow system.

#### 2.1.1 EXPERIMENTAL

##### 2.2.1.1 Reagents

Throughout this work analytical grade chemicals and deionised water (obtained by passing distilled water through a Millipore water purification system) were used. Standard solutions of sodium nitrite were prepared daily in 0.1 M  $\text{NaNO}_3$  electrolyte and carrier solution. The preparation of  $[\text{Ru}(\text{bpy})_2(\text{PVP})_{10}\text{Cl}]\text{Cl}$  has been reported elsewhere [45]. The chemical structure of this polymer is shown in Figure 2.3.

##### 2.2.1.2 Apparatus

Cyclic voltammetry was performed using an EG & G Model 362 scanning potentiostat in conjunction with a Linsels LY17100 X-Y plotter to record the voltammograms. A 10 mL homemade



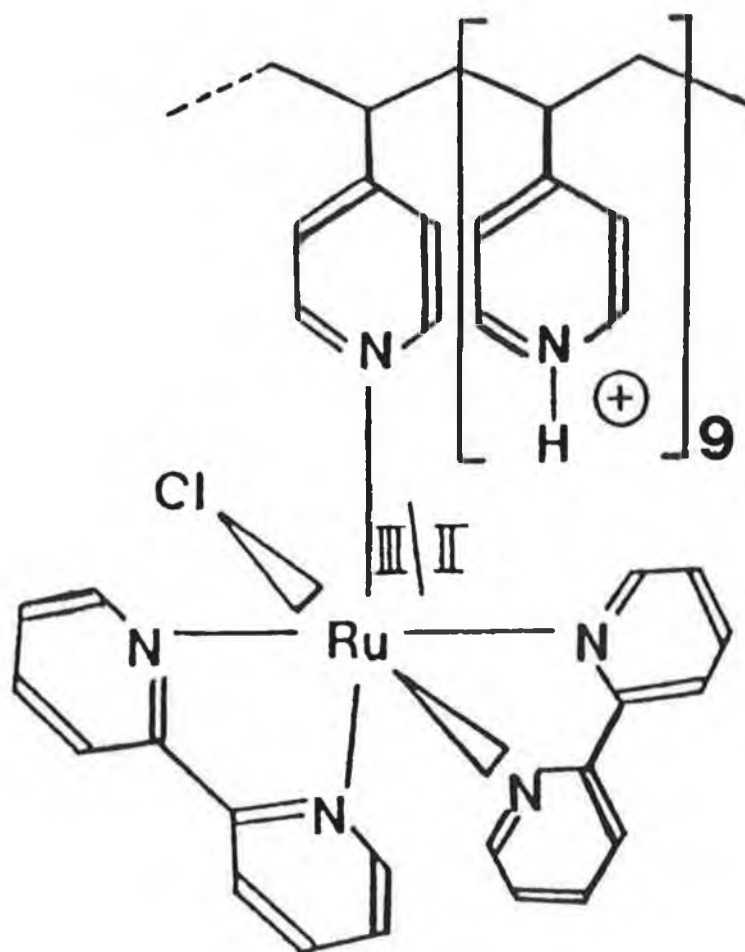


**Figure 2.3:** Chemical structure of the ruthenium polymer.

three-electrode cell was employed incorporating the modified electrode in addition to a Ag/AgCl reference electrode and a platinum wire auxiliary electrode. For batch amperometry, the detection system used was a Metrohm 641 VA detector. To achieve mass transfer, a 1 cm stirring bar was placed in the cell and rotated using an IKAMAG RET-G magnetic stirrer. A stirring rate of 600 rpm was used for all studies.

Flow injection analysis was performed using a Waters 501 HPLC pump with an EG&G Model 400 electrochemical detector equipped with a homemade thin layer carbon paste cell (3mm diameter), a Ag/AgCl reference electrode and a stainless steel auxiliary electrode. Sample injections were made through a Rheodyne injection valve (20  $\mu$ L loop).

#### 2.2.1.3 Procedures

The modified carbon paste (usually Nujol: graphite powder: Ru-polymer in a 40:55:5 ratio) was prepared by thoroughly mixing the required amounts for at least 30 minutes. Portions of the resulting mixture were then packed into either a glass tube (4 mm i.d.) or into the flow injection cell base. The surface was smoothed using filter paper. Electrical contact in the glass tube electrodes was established via a copper wire which was inserted into the back of the carbon paste mixture.

Saliva was collected by expectoration into small vials. At least 1 mL samples were collected from each subject. No sample pretreatment was carried out on the samples which were diluted with 0.1 M NaNO<sub>3</sub> supporting electrolyte.

## 2.2.2 RESULTS AND DISCUSSION

### 2.2.2.1 Cyclic Voltammetry

The formal potential for the redox reaction given by,



is 590 mV vs. SCE [46]. However, despite this formal potential, the irreversible oxidation at carbon electrodes has been reported at high overpotentials [47]. Preliminary experiments to investigate the nature of the Ru-polymer in the carbon paste matrix, and to confirm the retention of its electrocatalytic activity toward nitrite oxidation, were performed by cyclic voltammetry. Well defined oxidation and reduction responses associated with the surface-bound Ru(II/III) couple were observed in 0.1 M NaNO<sub>3</sub> (Figure 2.4, curve A). This supporting electrolyte was used as it had been found to be optimum in a previously reported study with this polymer [16]. A linear dependence of the cathodic and anodic peak currents on scan rate was obtained up to 40 mV s<sup>-1</sup>, characteristic of a surface redox reaction [48].

The addition of nitrite to the solution resulted in an electrocatalytic oxidation at the same potential as that observed for the Ru(II/III) system (Figure 2.4, curve B). Using an unmodified carbon paste electrode, the oxidation of nitrite results in a broad response at 1.05 V (Figure 2.4, curve C). The corresponding response at the modified electrode occurred at 0.78 V, indicating a significant reduction in the overpotential of the nitrite oxidation.

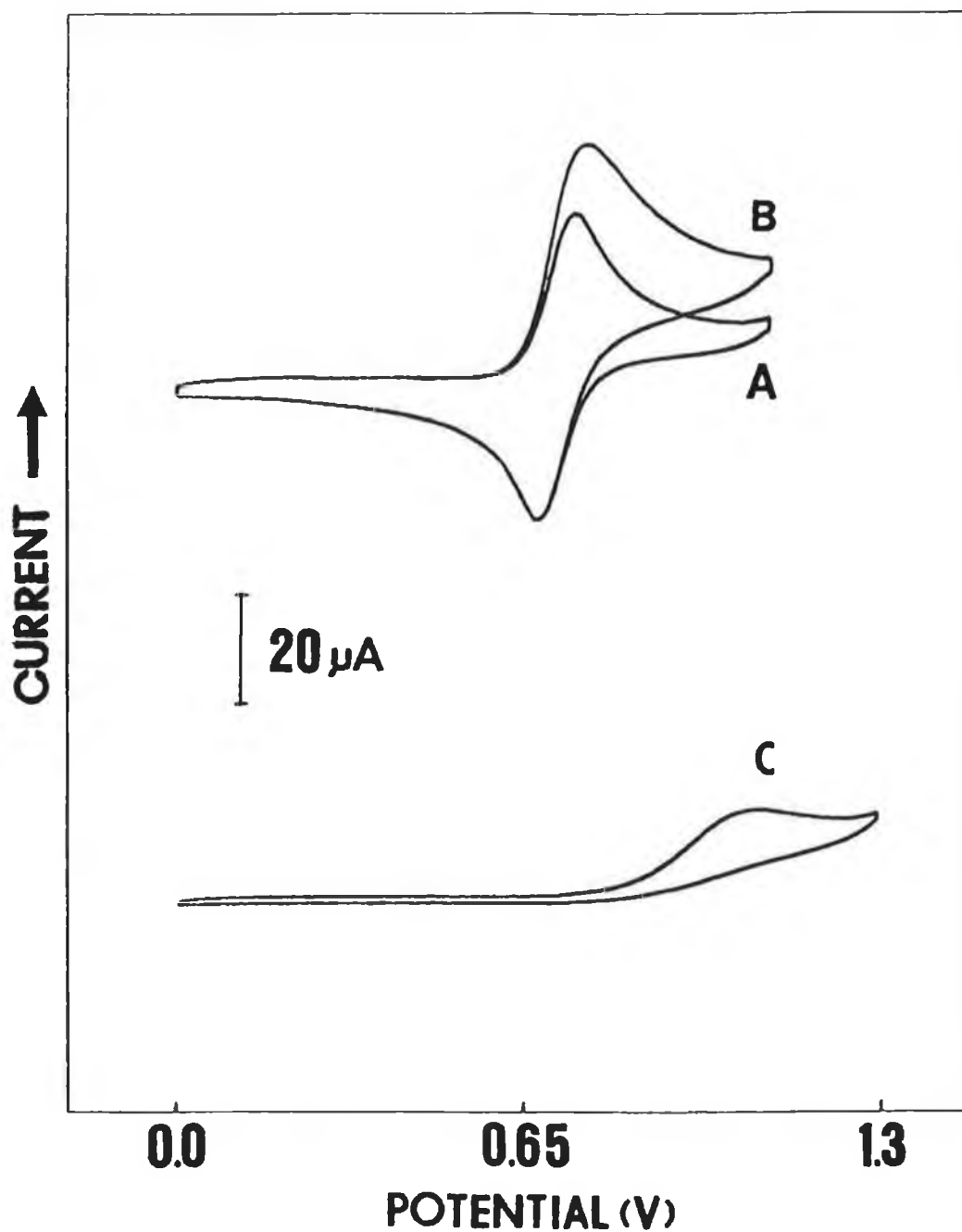


**Figure 2.4:** Cyclic voltammograms for (A) 5% (w/w) Ru-polymer CME; (B) same as (A) with the addition of  $2 \times 10^{-4}$  M nitrite. Curve (C) is the response at an unmodified electrode for  $2 \times 10^{-4}$  nitrite. Scan rate,  $100 \text{ mV s}^{-1}$ ; electrolyte,  $0.1 \text{ M NaNO}_3$ .

As the Ru(II/III) couple is always present, the analytical signal for nitrite must be recorded on top of a substantial background current. Detection using conventional voltammetric techniques are therefore not recommended. Optimisation of the analytical parameters for the mediated reaction were therefore performed using either constant potential batch amperometry or flow-injection analysis.

#### 2.2.2.2 Batch Amperometry in Stirred Solution

The effect of Ru-polymer loading in the carbon paste was investigated by constant potential batch additions (at 0.8 V) to determine the optimum composition. Calibration curves were constructed in the range  $5 \times 10^{-6}$  M to  $5 \times 10^{-4}$  M nitrite. Slopes of 0.2, 0.3, 0.3 and  $0.25 \mu\text{A } \mu\text{M}^{-1}$  and correlation coefficients ( $n = 6$ ) of 0.9995, 0.9996, 0.9997 and 0.9991 were obtained for loadings of 2.5, 5, 10 and 20% (w/w) modified electrodes respectively. A loading of 5% (w/w) Ru-polymer was chosen as increased loadings did not result in an increased response. The decrease in sensitivity at the 20% loaded electrode may be attributed to a decrease in the conductivity of the electrode matrix caused by the high loading of the polymer.

Hydrodynamic voltammetry was then attempted using a 5 % (w/w) loaded modified electrode for batch additions of  $1 \times 10^{-4}$  M nitrite. The potential of the electrode was increased in 50 mV steps and a two-plateau shaped response was observed (Figure 2.5, curve A). The first wave is a result of the mediated current for the oxidation of nitrite at the Ru-polymer at the surface of the modified electrode. The second wave presumably arises due to the response of nitrite at the bare sections of carbon paste at the surface of the modified electrode (the  $E_p$  of this second wave was 940 mV which compared to that value obtained for the oxidation of nitrite at

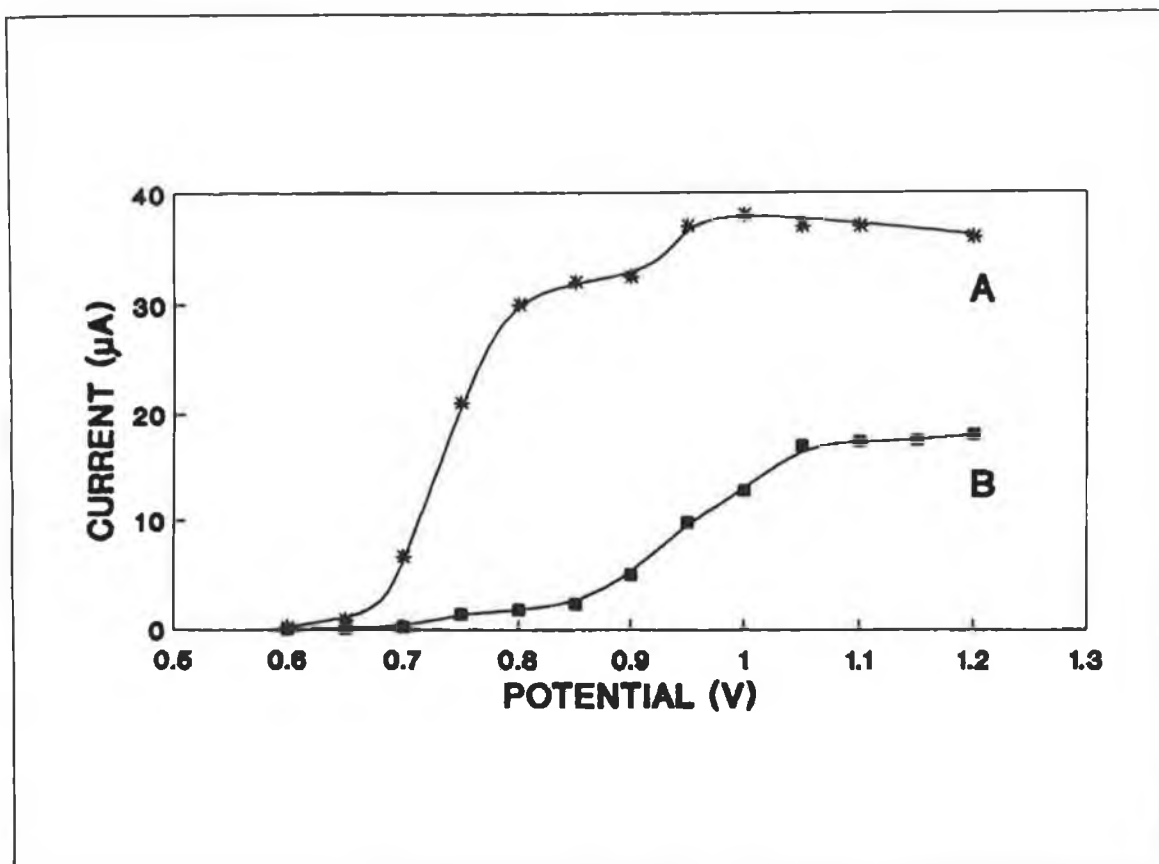


**Figure 2.5:** Hydrodynamic voltammograms obtained at (A) modified, and (B) unmodified electrode for  $1 \times 10^{-4}$  M nitrite. Electrolyte, 0.1 M  $\text{NaNO}_3$ ; stirring rate, 600 rpm.

the unmodified carbon paste electrode of 950 mV). This wave is therefore lower in current due to the reduced surface area of carbon particles in the modified versus the unmodified electrode (Figure 2.5, curve B). A potential of 0.8 V was selected for subsequent investigations in order to maximise the analytical response and minimise interferences obtained at higher potentials.

The responses of the modified and unmodified electrodes to batch additions of  $5 \times 10^{-6}$  M nitrite are shown in Figure 2.6. From this one can see the fast response time recorded for the modified electrode. In addition, one can see the large increases in signal obtained for the modified electrode in comparison to the unmodified electrode at the monitoring potential of 0.8 V. The increase in sensitivity of the modified over the unmodified electrode was nearly 20 fold. A calibration curve constructed in the range  $5 \times 10^{-8}$  M to  $5 \times 10^{-4}$  M nitrite displayed excellent linearity with a slope of  $0.3 \mu\text{A } \mu\text{M}^{-1}$  and a correlation coefficient of 0.9999 ( $n = 12$ ). The signal-to-noise characteristics ( $S/N = 3$ ) resulted in a detection limit of  $3 \times 10^{-8}$  M nitrite. To determine the surface to surface precision, 10 independently prepared electrodes were constructed and yielded calibration curves with slopes of approximately  $0.30 \mu\text{A } \mu\text{M}^{-1}$  with a standard deviation of 11.4%. The long-term stability of the modified electrode to the oxidation of nitrite was investigated over a 5 day period.

The electrode exhibited a current diminution of only 8 % during this period, in contrast to that reported by Barisci et al. [16] who reported a 50% response reduction after only 8 hours for the same polymer chemisorbed on the surface of a glassy carbon electrode. Obviously the carbon paste matrix provides a more stable fixture for the polymer.

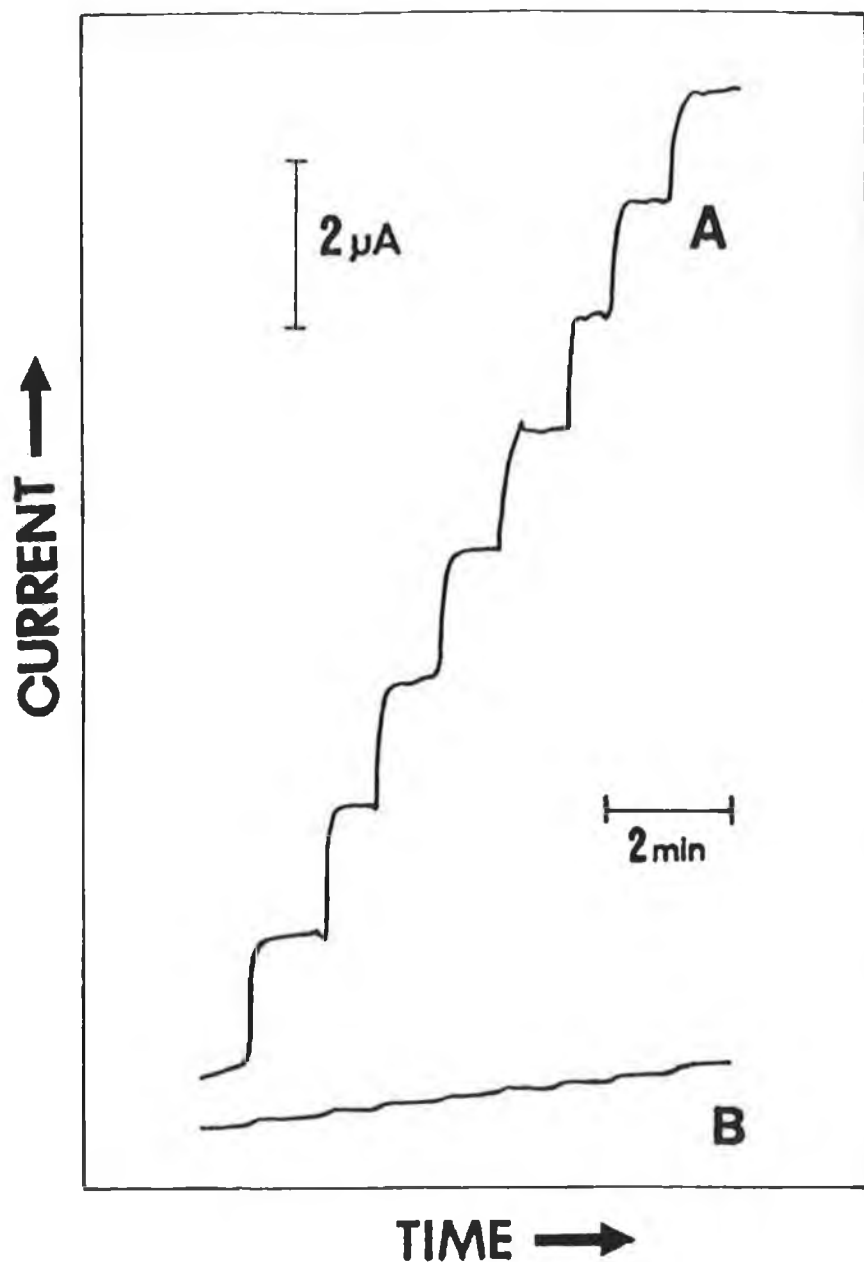


**Figure 2.6:** Batch additions of  $5 \times 10^{-6}$  M nitrite (final cell concentration) at (A) modified, and (B) unmodified electrode with constant potential detection at +800 mV vs. Ag/AgCl. Other conditions as outlined in Figure 2.5.



### 2.2.2.3 Flow Injection Analysis

When these Ru-polymer modified electrodes are used in a stationary cell with complex samples, their practical application is hampered by responses for easily oxidised species at the monitoring potential of 0.8 V. Consequently, this approach suffers from a lack of selectivity. This drawback can be alleviated by using the modified electrode in a flowing system with a view to employing ion chromatographic separation with electrochemical detection.

For flow studies, 0.1 M  $\text{NaNO}_3$  was again used as the supporting electrolyte. The effect of flow rate on the magnitude of response was investigated over the range 0.3 to 1.5  $\text{mL min}^{-1}$ . At values greater than 1  $\text{mL min}^{-1}$ , peak heights varied minimally, exhibiting only slight reductions in peak height with further increases in flow rate. Appreciable peak broadening was observed at low flow rates; i.e. peak widths of 22 and 6 s were obtained at 0.3 and 1.5  $\text{mL min}^{-1}$  respectively to injections of  $1 \times 10^{-5}$  M nitrite. A flow rate of 1  $\text{mL min}^{-1}$  was therefore selected as a compromise between sensitivity and sample throughput. Typical flow injection responses for nitrite at both the modified and unmodified surfaces are shown in Figure 2.7. The linear range was found to be  $2 \times 10^{-7}$  to  $1 \times 10^{-3}$  M nitrite. Calibration curves constructed yielded a slope of  $0.032 \mu\text{A } \mu\text{M}^{-1}$  with a correlation coefficient of 0.9998 ( $n = 12$ ). A detection limit ( $S/N = 3$ ) of  $8 \times 10^{-8}$  M nitrite was calculated. These results indicate an attractive detection system for ion chromatographic determination of nitrite.

The short-term stability was ascertained by monitoring the current response for a series of 100 replicate injections of  $2 \times 10^{-4}$  M nitrite over a 90 minute period (Figure 2.8). The RSD of

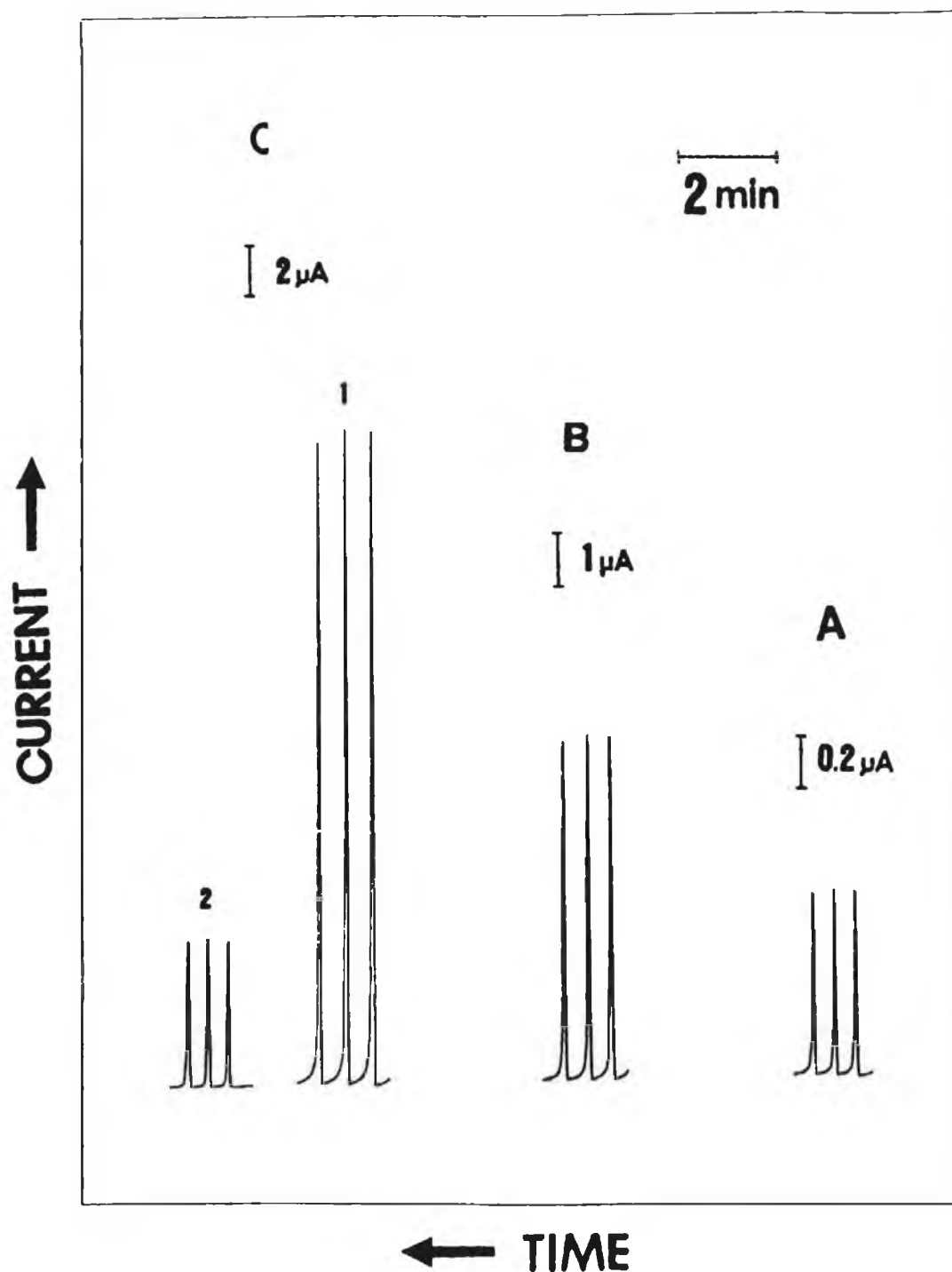


**Figure 2.7:** Flow-injection response at the Ru-polymer modified electrode of (A)  $3 \times 10^{-5}$  M, and (B)  $2 \times 10^{-4}$  M nitrite. (C) is the response for  $8 \times 10^{-4}$  M at (1) modified, and (2) unmodified electrode. Constant potential operation at +800 mV vs. Ag/AgCl; electrolyte, 0.1 M  $\text{NaNO}_3$ ; flow rate,  $1 \text{ mL min}^{-1}$ .

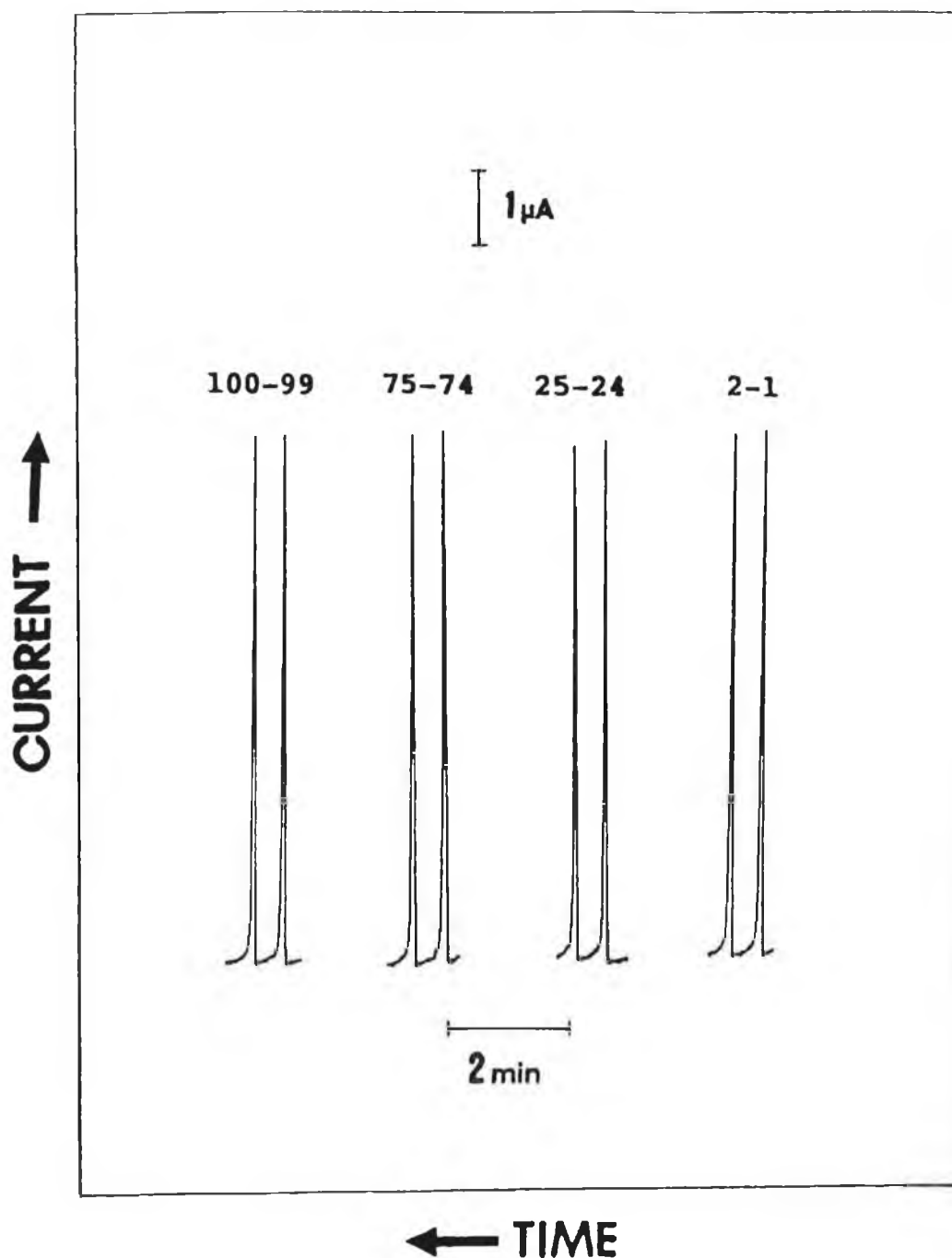


Figure 2.8: Time dependence of electrode sensitivity over a 90 minute period to repeated injections (100 in total) of  $2 \times 10^{-4}$  M nitrite. Other conditions as outlined in Figure 2.5.

these 100 injections was 2.9%, demonstrating the short term stability of the modified electrode in flowing streams.

#### 2.2.2.4 Determination of Nitrite in Saliva

The application of the Ru-polymer CME to the determination of nitrite in saliva was then investigated. Using flow injection analysis, levels in samples taken from two volunteers were determined to be  $2.05 \times 10^{-5}$  M (0.94 ppm) and  $4.45 \times 10^{-5}$  M (2.05 ppm) nitrite. For both samples, known amounts of nitrite were added to check recovery, which was estimated as  $98\% \pm 3\%$ . The nitrite levels found in each sample were within the range previously reported for human saliva [49].

#### 2.3 CONCLUSION

In conclusion, the Ru-polymer modified carbon paste electrodes have been demonstrated to be an attractive detection system for nitrite. The modified surface yields a fast and sensitive response and exhibits a substantial decrease in over-potential for nitrite oxidation. In addition, the stability and reproducibility of the electrode response should prove a useful detector coupled to LC separation. The detection limit and dynamic linear range are only bettered by polarographic methods [46,47]. As previously mentioned, however, techniques based on mercury are generally undesirable for many practical applications, including flow analysis.

## 2.4 REFERENCES

1. R.W. Murray, A.G. Ewing and R.A. Durst, *Anal. Chem.*, 59 (1987) 379A.
2. J. Leddy, A.J. Bard, J.T. Molloy and J.M. Saveant, *J. Electroanal. Chem.*, 187 (1985) 205.
3. C.P. Andrieux and J.M. Saveant, *J. Electroanal. Chem.*, 142 (1982) 1.
4. R.P. Baldwin and K.N. Thompson, *Talanta*, 38 (1991) 1.
5. D.C.S. Tse and T. Kuwana, *Anal. Chem.*, 50 (1978) 1315.
6. C. Udea, D.C.S. Tse and T. Kuwana, *Anal. Chem.*, 54 (1982) 850.
7. A.N.K. Lau and L.L. Miller, *J. Amer. Chem. Soc.*, 105 (1983) 5271.
8. B.F. Yon and C.R. Lowe, *Anal. Chem.*, 59 (1987) 2111.
9. P.J. Kulesza, K. Bratjer and E.D. Zlotorzynska, *Anal. Chem.*, 59 (1987) 2776.
10. A.J. Bard, *J. Chem. Educ.*, 60 (1983) 302.
11. N. Oyama and F.C. Anson, *Anal. Chem.*, 52 (1980) 1192.
12. R. Noufi, *J. Electrochem. Soc.*, 130 (1983) 2126.
13. K. Murao and K. Suziki, *Polym. Pre., Am. Chem. Soc. Div. Polym. Chem.*, 25 (1984) 260.
14. N. Oyama, A.P. Brown and F.C. Anson, *J. Electroanal. Chem.*, 87 (1978) 435.
15. S.M. Geraty, D.W. Arrigan and J.G. Vos in *Electrochemistry, Sensors and Analysis*, M.R. Smyth and J.G. Vos (eds.), Elsevier, Amsterdam, 1986, pp 303.
16. J.N. Barisci, G.G. Wallace, E.A. Wilke, M. Meaney, M.R. Smyth and J.G. Vos, *Electroanalysis*, 1 (1989) 245.
17. M. Meaney, M.R. Smyth, J.G. Vos and G.G. Wallace, *Electroanalysis*, 1 (1989) 357.
18. J.A. Cox and P.J. Kulesza, *J. Electroanal. Chem.*, 175 (1984) 105.

19. J.A. Cox and P.J. Kulesza, *Analyst*, 111 (1986) 1219.
20. B.T. Tay, K.P. Ang and H. Gunasingham, *Analyst*, 113 (1988) 617.
21. Z. Lu and S. Dong, *Acta Chim. Sin.*, 44 (1986) 32.
22. M.K. Halbert and R.P. Baldwin, *Anal. Chem.*, 57 (1985) 591.
23. L.M. Santos and R.P. Baldwin, *Anal. Chem.*, 58 (1986) 848.
24. L.M. Santos and R.P. Baldwin, *Anal. Chim. Acta*, 206 (1988) 85.
25. A.M. Tolbert, R.P. Baldwin and L.M Santos, *Anal. Lett.*, 22 (1989) 683.
26. M.K. Halbert and R.P. Baldwin, *Anal. Chim. Acta*, 187 (1986) 89.
27. P.W. Geno, K. Ravichandran and R.P. Baldwin, *J. Electroanal. Chem.*, 183 (1985) 155.
28. J. Wang and Z. Taha, *Anal. Chem.*, 62 (1990) 1413.
29. X. Qi, R.P. Baldwin, H. Li and T.F. Guarr, *Electroanalysis* 3 (1991) 119.
30. S.A. Wring, J.P. Hart and J. Birch, *Analyst*, 114 (1989) 1563.
31. J. Wang and Z. Lu, *Electroanalysis*, 1 (1989) 517.
32. Z. Taha and J. Wang, *Electroanalysis*, 3 (1991) 215.
33. J.A. Cox and K.R. Kulkarni, *Electroanalysis*, 2 (1990) 107.
34. J.A. Cox, T. Gray and K.R. Kulkarni, *Anal. Chem.*, 60 (1988) 1710.
35. J. Wang and B. Frelha, *Anal. Chem.*, 56 (1984) 2266.
36. S.V. Prabhu and R.P. Baldwin, *Anal. Chem.*, 61 (1989) 852.
37. S.V. Prabhu and R.P. Baldwin, *Anal. Chem.*, 61 (1989) 2258.
38. W. Lijinsky and S.S. Epstein, *Nature*, 223 (1970) 21.
39. E. Szekely, *Talanta*, 15 (1968) 795.
40. A. Chaube, A.K. Baveja and V.K. Gupta, *Talanta*, 31 (1984) 391.

41. S. Flamerez and W.A. Bashir, *Analyst*, 110 (1985) 1513.
42. K. Kalcher, *Talanta*, 33 (1986) 489.
43. C.M.G. van den Berg and H. Li, *Anal. Chim. Acta*, 212 (1988) 31.
44. Z. Gao, G. Wang and Z. Zhao, *Anal. Chim. Acta*, 230 (1990) 1.
45. J.M. Clear, J.M. Kelly, C.M. O'Connell and J.G. Vos, *J. Chem. Res.*, 3 (1981) 3039.
46. G. Milazzo and S. Caroli, *Tables of Standard Electrode Potentials*, Wiley, New York, 1978, p.191.
47. A.Y. Chamsi and A.G. Fogg, *Analyst*, 113 (1988) 1723.
48. E. Laviron and L. Roullier, *J. Electroanal. Chem.*, 115 (1980) 65.
49. S.R. Tannenbaum, A.J. Sinskey, M. Weisman and W. Bishop, *J. Natl. Cancer Inst.*, 53 (1974) 79.

## CHAPTER 3

THE ELECTROCHEMICAL PRETREATMENT

OF CARBON FIBRE

MICROELECTRODES



### 3.1 INTRODUCTION

Electroanalytical chemistry originated with the development of the dropping mercury electrode (DME). As a result of its renewable surface, a reproducible electrochemical response devoid of any electrode 'history' effects was obtained. Solid electrodes have, however, been used extensively in recent times, because they can provide a wider potential range than mercury (especially for oxidation reactions), have better mechanical properties, and can act in a catalytic role for reactions of importance to energy conversion, electrosynthesis and electroanalysis. However, whether used for analysis or for studying electrode processes, the surface of a solid electrode changes with time due to adsorption of species from solution or chemical changes to the surface itself. It has long been recognised that the behaviour of solid electrodes, unlike that of the DME, is highly dependent on history effects and that performance may be drastically altered by pretreatment procedures or processes occurring in the solution of interest [1]. These alterations take the form of changes in rates of heterogeneous electron transfer, increases in capacitance currents, variations in sensitivity, and in extreme cases, complete deactivation of the electrode. They often result in unstable and irreproducible analytical performance.

In essence, quantitative results obtained for certain redox couples depends intimately on the method of preparing the electrode surface, as well as on the electrode's prior history. For these reasons, there has been an extensive and continuing interest in developing procedures for pretreating the surface of solid electrodes. The goal of such pretreatment is to obtain reproducible and well-defined electrochemical behaviour for particular analytes. A variety of methods has been devised for

pretreating electrodes, including polishing, chemical and electrochemical pretreatment, ion-etching, and laser and vacuum heat pretreatments. All these treatments have been shown to improve heterogeneous electron transfer rates for selected redox couples at solid electrodes.

The first section of this chapter will present a discussion of the various pretreatments reported in the literature, and their effect on the electrochemistry at solid electrodes. This will be followed by a description of the work undertaken involving the electrochemical pretreatment and characterisation of carbon fibre microelectrodes for the determination of folic acid.

### 3.1.2 Pretreatment Methods for Solid Electrodes

There have been several previous indications that careful attention to electrode polishing and cleaning can yield an electrode of very good activity [2,3]. Most investigators polish the surface to a mirror-like surface using a fine grade of alumina. A highly polished surface has been found to exhibit a low residual current, resulting in a more usable electrode for analytical applications. It is also one of the most certain procedures for removing adsorbed impurities from the electrode surface. However, surface analysis has shown that the polishing material may be embedded in the surface and this may affect the electrochemical results [4]. For example, glassy carbon electrodes prepared by polishing with 1  $\mu\text{m}$  alumina resulted in a shift in the oxidation wave for ascorbate to the potential observed on mercury [5]. X-ray photoelectron spectroscopic and electron microscopic examination of the surface revealed that this treatment embeds the alumina on the surface. This alumina-coated surface is highly efficient for adsorbing organic species, which leads to the observed increase in reversibility

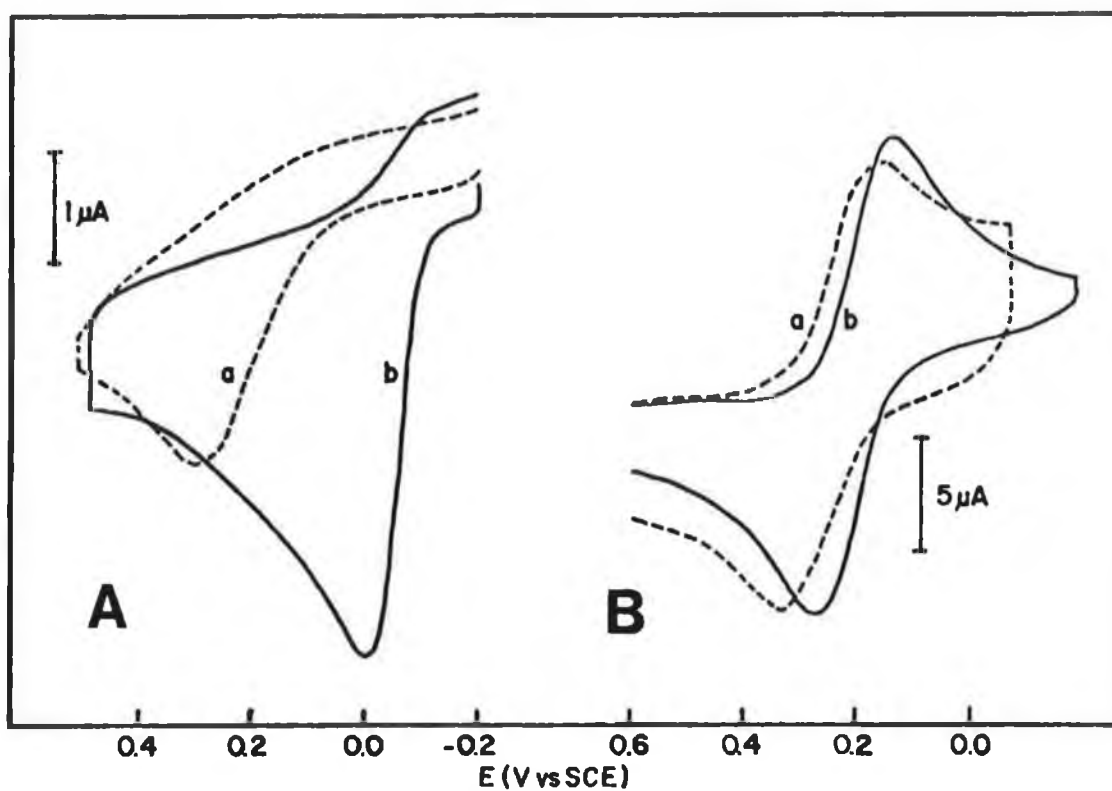


**Figure 3.1:** Cyclic voltammetry of (A) 0.02 M ascorbic acid, and (B) 1 mM ferricyanide at a glassy carbon electrode. Curve (a) control. Curve (b) after polishing with 1  $\mu\text{m}$  diamond paste and extracting in toluene. Scan rate, 100  $\text{mV s}^{-1}$  [2].

of oxidation for such substances. This effect of polishing procedures can be minimised if the electrode surface is cleaned before use. The use of ultrasonic cleaning and extraction using a soxhlet apparatus has been demonstrated to be effective.

Wightman et al. [2] demonstrated the increased charge transfer rates obtainable at glassy carbon surfaces that had been polished with diamond paste and subsequently extracted with toluene in a soxhlet apparatus. The reversibility of both ferricyanide and ascorbate was improved over that observed at a control electrode (polished with 0.05  $\mu\text{m}$  alumina). Cyclic voltammograms obtained in this study are shown in Figure 3.1. A large shift in  $E_p$  was observed for ascorbate, while the effect for ferricyanide was less pronounced. The surface exhibited reproducible behaviour for repeated scans, and adsorption was not evident for the compounds tested.

One of the more impressive examples of a polishing treatment is that described by Kamau and co-workers [3], which involves high-speed metallographic polishing with successively smaller particle size silicon carbide, diamond paste, and finally alumina. This was followed by ultrasonic cleaning. The polished electrode yielded reproducible activation for anodic oxidations of ferrocyanide, ferrocene, ascorbate, quinones and catharanthine. Electron spectroscopy revealed that the highly polished electrodes had a higher oxygen content in the outer 20 to 30 nm of surface than in the bulk material or in inactivated electrodes. Much of the oxygen in this layer was present as C-O bonds, most likely of a phenolic or quinone nature. The formation of these surface functionalities was thought to be as a result of the mild oxidation of the carbon surface during the diamond polishing steps, which may have been assisted by frictional heating. The subsequent alumina and ultrasonic treatments were suggested as serving to remove oil and some

contaminants which were suspected to block active sites and retard rates of electron transfer.

Chemical pretreatment following polishing has also been reported. Taylor and Humffray [6] noted that dipping a freshly polished glassy carbon electrode in chromic acid produced a significant increase in the rate constant for the Fe(III) - Fe(II) system.

Several groups have noted that the performance of carbon electrodes can be improved by electrochemical pretreatment [7-10]. In all cases, the pretreatment included the application of relatively large positive potentials to the working electrode, and frequently, negative potentials were applied as well. The exact amplitude and duration of the applied potentials varied considerably, with many groups recommending the use of potential cycling or alternating current (ac) waveforms.

Engstrom [7] has investigated the effects of preanodisation and precathodisation on the electrochemical oxidation of hydroquinone, ferrocyanide and hydrazine at a glassy carbon electrode. For all three electroactive species, preanodisation at a voltage greater than 1.5 V vs. SCE was required to activate a freshly polished electrode. Ferrocyanide and hydrazine also required precathodisation at -1.0 V vs. SCE to remove an inhibitory layer formed during preanodisation. In all cases, pretreatment resulted in a substantial improvement in the half-wave potential and the reproducibility of the voltammetric wave. The results were interpreted in terms of three different surface conditions that exist on the surface of the glassy carbon electrode during the course of the pretreatment. The first surface condition, prevalent on a freshly polished electrode, is a relatively inactive condition. The electrochemical reaction of the three compounds studied was

poorly catalysed on this surface. The reason for the low activity was suggested to be due to the lack of surface functional groups on the surface or, alternatively, the presence of impurities on the surface that hindered charge transfer. The second type of surface results after anodisation, which activates the surface, in addition to forming a deposited layer of an oxide material. This oxide layer had a strong inhibitory affect on the oxidation of ferrocyanide and hydrazine, but did not affect the oxidation of hydroquinone. It was proposed that the activation of the electrode surface in this second condition must involve either the oxidation of the electrode surface to produce functionalities capable of catalysing the electrochemical reaction, or the oxidative removal of impurities from the surface which inhibited charge transfer. This activation may occur directly by electrochemical oxidation, or indirectly by oxygen produced during anodisation. The third surface condition is that of the activated electrode after the oxide layer has been cathodically reduced. This surface was found to be active toward all the electroactive species studied. Engstrom's procedure was also found useful for enhancing the amperometric detection of hydrazine following LC separation [11].

Electrochemical pretreatment employing an AC waveform has been reported for carbon electrodes [8-10]. Blaedel and Mabbot [10] employed an AC pretreatment of  $\pm 4$  V at 70 Hz for 4 minutes at carbon film and glassy carbon electrodes. The pretreatment enhanced the electrodes response and yielded well-defined, reproducible responses for ferrocyanide and NADH. Gonon et al. [8] used a similar AC pretreatment for the activation of pyrolytic carbon fibre microelectrodes. The procedure invoved the application of a triangular waveform of 0 to 3 V at 70 Hz for 20 seconds. The treated electrodes, used in combination with DPV, were capable of separating ascorbic acid from

catecholamines. This separation is of great importance, particularly in the interpretation of experimental results in in vivo electrochemistry, where the voltammetric response of ascorbic acid usually overlaps with those from the catecholamines. The treated microelectrodes also exhibited an increased sensitivity, of at least one order of magnitude, with respect to several catechols. The lower upper potential limit (i.e. 3 V) required for activation, in comparison to that used by Blaedel and Mabbot, was explained in terms of current density, as the microelectrode was at least 2,000 times smaller in area than the carbon film electrode.

Electrochemical pretreatments are especially noted for their ability to increase the density of carboxyl, quinone, phenolic and other surface oxygen groups on the edge plane of carbon electrodes [2]. In conjunction with cleaning the surface (by removing chemi- and physi-sorbed impurities) and roughening the surface (increasing the geometric area of the electrode), the incorporation of surface functionalities was thought to enhance the rate of heterogeneous electron transfer for various redox couples by acting as a redox mediator [12].

Conversely, the oxygen-depleted surface of carbon electrodes, created by vacuum heat treatments, has also been observed to increase the rate of electron transfer by several orders of magnitude for model redox systems, such as ascorbic acid and dopamine. Fagan et al. [13] have shown that the freshly exposed and unroughened carbon surface obtained after vacuum heat treatment provides a cleaned surface that allows enhanced electrochemical activity. Cyclic voltammograms obtained before and after the heat treatment are shown in Figure 3.2. Additionally, the reduced density of surface functional groups on the surface of the electrode resulted in a diminished background charging current. Even though it was suggested that

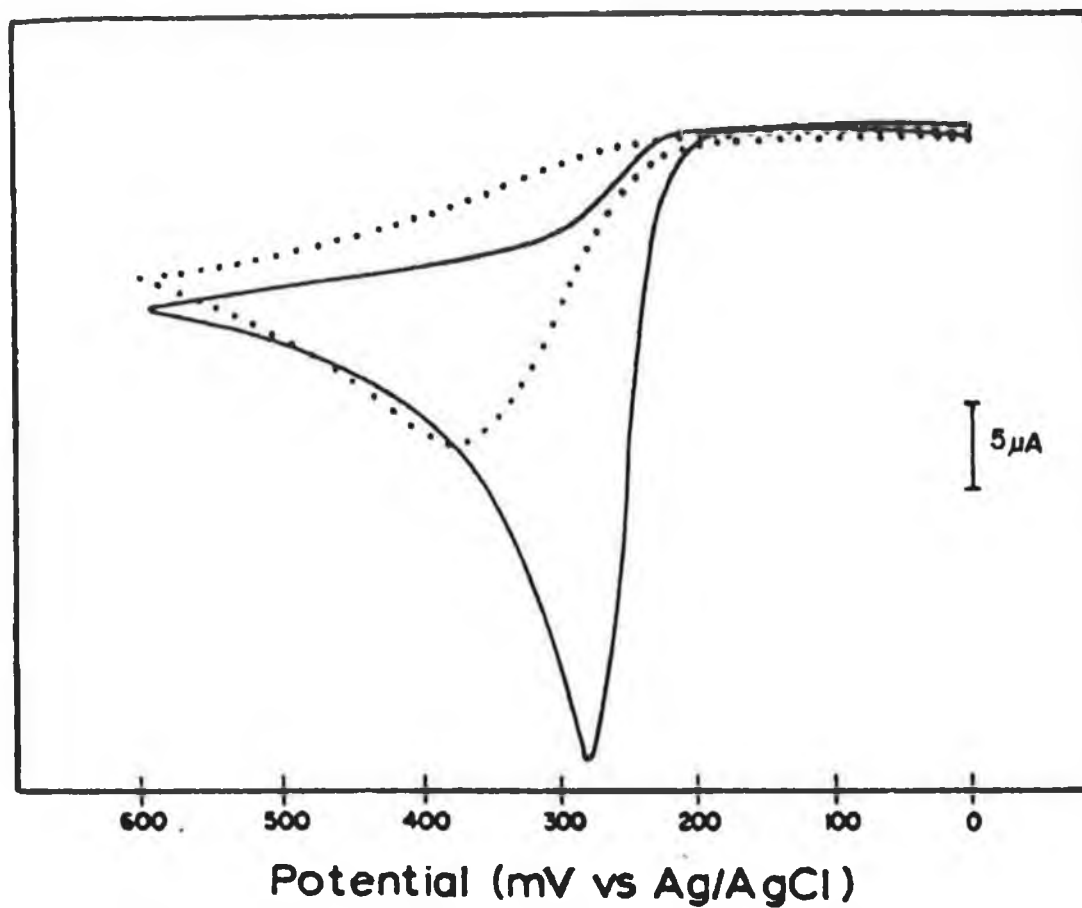


**Figure 3.2:** Cyclic voltammetry for 1 mM ascorbic acid at polished, deactivated glassy carbon electrode (dashed line) and polished, deactivated and vacuum heat treated glassy carbon electrode (full line). Scan rate, 100 mV s<sup>-1</sup> [13].



more redox couples need to be evaluated, especially at more positive potentials where surface redox species could participate in mediating electron transfer reactions, these observations question the role of surface functional groups in electron-transfer mechanisms. The main reasons for activation by this technique was believed to be due to an increase in the active site density as a consequence of the removal of surface contaminants and the exposure of fresh carbon.

In another study which investigated the role of surface functionalities, Nagaoka et al. [14] studied dioxygen reduction at carbon electrodes treated electrochemically and at electrodes on which quinone was adsorbed. Results were compared to see if the surface redox groups introduced on the electrochemically pretreated electrode could serve as mediators. The electrodes behaved very differently for oxygen reduction, especially with respect to pH. For the quinone-adsorbed electrodes, oxygen reduction via quinone was not observed at a pH less than the  $pK_a$  of the semiquinone, for the other electrodes, reduction currents were unchanged in the pH range investigated. Accordingly, from the results obtained in this study, the enhanced activity of electrochemically pretreated electrodes could not be attributed to the mediation by the surface-confined quinones, at least for oxygen reduction.

Edmonds and Guoliang [15] presented conflicting evidence on the importance of surface functionalities induced by electrochemical pretreatment. They examined the effects of electrochemical pretreatment on surface ionisable groups with the aid of pH-stat experiments. Using this technique, the number of exposed ionisable groups on the surface of electrochemically pretreated carbon fibre microelectrodes was calculated. This number, when compared with a typical peak current for the reduction of copper(II), indicated proportionality between the

number of ionisable groups and sensitivity.

Laser pulses have also found application in the activation of solid electrodes. Poon and McCreery [16] reported that the use of laser pulses of short duration (10 ns) and high intensity ( $20 \text{ MW cm}^{-2}$ ) could increase the rate of heterogeneous electron transfer at a glassy carbon electrode by 1 to 3 orders of magnitude. The laser-activated surface was cleaned as well as roughened with visible cracks and defects, similar to those observed on carbon surfaces that have been treated electrochemically [17]. Investigations of these surface defects has been accomplished through the use of Raman spectroscopy, prior to and following activation. Information concerning microcrystalline size and lattice arrangements has permitted McCreery and co-workers to correlate the density of edge sites with the growth of the  $1360 \text{ cm}^{-1}$  Raman vibrational band of the carbon spectra. The  $1360 \text{ cm}^{-1}$  band is spectroscopically indicative of graphitic edge planes. Coupled with capacitance and adsorption studies, this spectroscopic marker allowed them to quantitatively correlate increased rates of electron transfer with the density of edge defects created by laser activation of basal plane regions [18,19]. It was concluded that the active sites for electron transfer are on graphitic edges, inherent in the glassy carbon structure, and the principle function of the laser is exposure of these sites, by removal of chemi- and physisorbed impurities. Illustrated in Figure 3.3 are cyclic voltammograms obtained in this study which led the authors to this conclusion. Curve (a) is a fractured surface of a glassy carbon electrode, used to expose graphitic edges, and like the laser activated surface (curve (c)) exhibited much faster kinetics than the polished surface shown in curve b.

This conclusion by McCreery and co-workers is consistent with the observations of Wightman et al. [2], in which electrochemical reversibility differences were shown to be

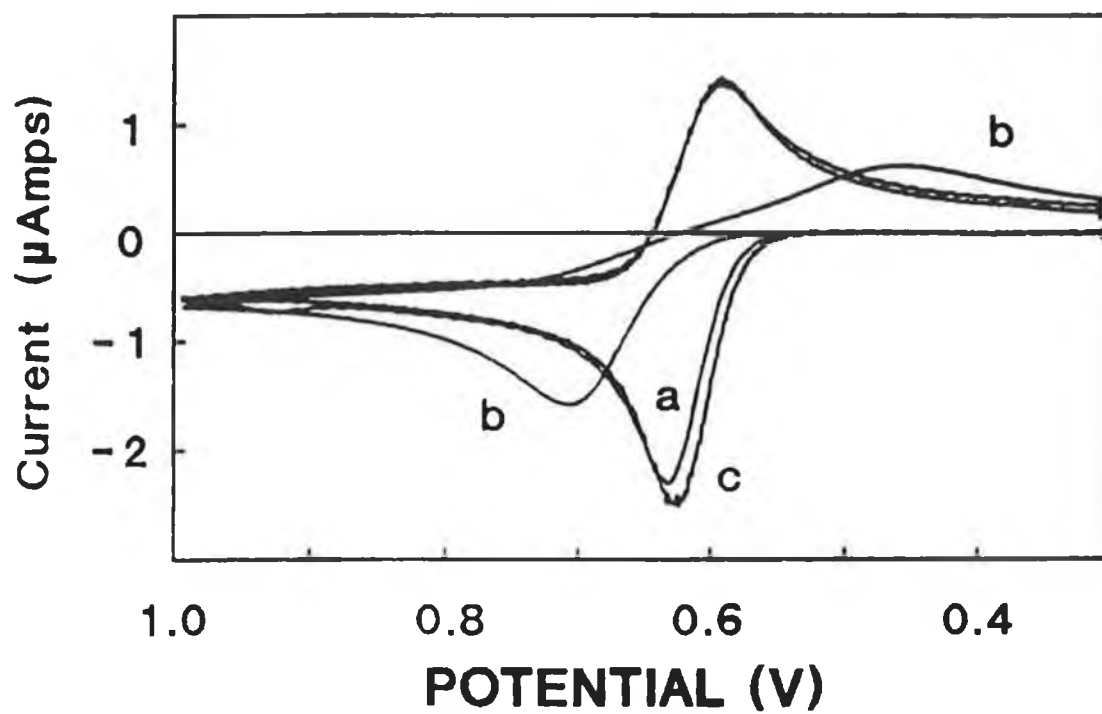


**Figure 3.3:** Cyclic voltammetry of 1.0 mM dopamine at (a) fractured surface, (b) polished surface, (c) polished and laser activated with three 25 MW cm<sup>-1</sup> pulses. Scan rate, 1 V s<sup>-1</sup> [19].

pronounced between the edge and basal planes of pyrolytic graphite. Mild electrochemical pretreatment of the basal plane resulted in a surface that yielded electrochemical behaviour comparable to the edge orientation. Slow rates of electron transfer have also been found at pyrolytic carbon disks; however, the rates can be accelerated by radio-frequency oxygen plasma treatment [20]. Since these treatments roughen the electrode surface with a corresponding increase in edge orientation, the data suggest that charge transfer is impaired at the basal plane, and that the presence of sites of edge orientation is necessary for electron transfer to occur. The slow rate of electron transfer may have several different origins. One conclusion that has been proposed, is that the basal surface is hydrophobic, and thus wetting of the electrode surface by aqueous solution is impaired [21]. The edge orientation is formed by cleaving carbon-carbon bonds. If this is performed in air or aqueous solution, oxygen functional groups can be formed on the surface, resulting in a more polar surface than the basal plane [22]. To further support this hypothesis, electron transfer rates were found to be slower on the cylindrical axis of high modulus carbon fibres when compared to low modulus carbon fibres. It was proposed that this may arise, because high modulus fibres have a greater degree of basal character on the cylindrical axis than the low modulus carbon fibres.

### 3.2 A Study on the Electrochemical Pretreatment of Carbon Fibre Microelectrodes for the Determination of Folic Acid

The purpose of the work reported herein was to investigate various parameters concerning the electrochemical pretreatment of carbon fibre microelectrodes for the determination of a model compound. Electrochemical activation was systematically evaluated with respect to duration of applied potential, frequency of activation regime, potential range and solution conditions.

Folic acid, N-[4[[[2-amino-1, 4-dihydro-4-oxo-6-pteridiny] methyl]amino]benzoyl-L-glutamic acid (I) was chosen as the analyte for this investigation as it is an electroactive compound of considerable biological importance [23]. It has long been recognised as part of the vitamin B complex and is administered in the prophylaxis and treatment of megaloblastic anaemia and other diseases. Simple and sensitive methods are required for its determination in pharmaceutical, clinical and food samples. Published methods for the determination of the vitamin include spectrophotometric [24] and chromatographic procedures [25,26].

To date, the only electrochemical methods reported for this vitamin have utilised the reduction behaviour of this compound at mercury electrodes. Jacobsen and Bjornsen [27] used AC polarography and reported a detection limit of  $2 \times 10^{-8}$  M. A more sensitive procedure was developed by Fernandez et al. [28] using adsorptive stripping voltammetry which permitted a detection limit of  $1 \times 10^{-11}$  M folic acid after a 10 minute accumulation time. Methods based on solid electrodes may, however, be more desirable for electrochemical sensing and flow injection (FI) applications.

### 3.2.1 EXPERIMENTAL

#### 3.2.1.1 Reagents

Analytical grade reagents and deionised water, obtained by passing distilled water through a Millipore Milli-Q water purification system were used in the preparation of all solutions. Folic acid was purchased from Sigma and used without further purification. 1 mM stock solutions of folic acid were prepared in 0.01 M NaOH and stored in the dark at 4 °C. Britton-Robinson (BR) buffers and perchloric acid (0.1 M) were employed as the background electrolytes. The BR buffers were made 0.04 M in acetic acid, boric acid and ortho-phosphoric acid. Individual buffers solutions were adjusted to the required pH with 0.8 M NaOH.

#### 3.2.1.2 Apparatus

The experiments were performed in a standard three electrode configuration in an electrolytic cell in which carbon fibre, platinum and Ag/AgCl electrodes were used as working, counter and reference electrodes respectively. The cell was used in conjunction with an EG&G PAR Model 273 potentiostat/ galvanostat interfaced to an IBM PS/2 Model 30 computer. The software used was the PAR Model 270 Electrochemical Analysis System. Two voltammetric techniques were used; namely differential pulse voltammetry (DPV) and cyclic voltammetry (CV) using a staircase waveform. For DPV, a pulse amplitude of 50 mV and a pulse width of 50 ms were used for all measurements. All electrochemical measurements were carried out at room temperature.

Scanning electron microscopic images were obtained using a Hitachi Model 570-S high resolution scanning electron microscope (SEM).

### 3.2.1.3 Procedures

#### 3.2.1.3.1 Construction of Microelectrodes

Cylindrical carbon fibre microelectrodes were made from carbon fibres (Donnay, Belgium) of 7  $\mu\text{m}$  diameter. The fibres were soaked and washed in dilute nitric acid, followed by acetone and finally with de-ionised water, and then dried at 70°C. The procedure for making the microelectrode involved the insertion of a single fibre into a 100  $\mu\text{L}$  pipette tip. A small drop of epoxy resin (A.R. Spurr, California) was applied to the pipette tip; capillary action draws the resin inside, making an adequate seal. With the aid of a microscope, the seal was then examined after polymerisation and microcylinders were cut to a length of 2 mm. The pipette was backfilled with mercury and electrical contact was established with a steel wire. Resin was then placed over the mercury to prevent its leakage from the pipette.

Disk-shaped microelectrodes were prepared using the cylindrical working electrodes, which were introduced axially along the centre of a cylindrical mould. Spurr resin was then poured into the mould and a rugged support for the fibre was thus prepared. Once cured, the resin could be sliced to expose a disk-shaped working electrode, of 7  $\mu\text{m}$  diameter.

#### 3.2.1.3.2 Microelectrode Pretreatment

Electrochemical pretreatments, which involved the application of a triangular waveform to the microelectrode using the potentiostat, were carried out in a separate cell than that containing the analyte. Following the pretreatment regime, the microelectrode was removed from the cell and washed with deionised water. Voltammetric measurements were then obtained

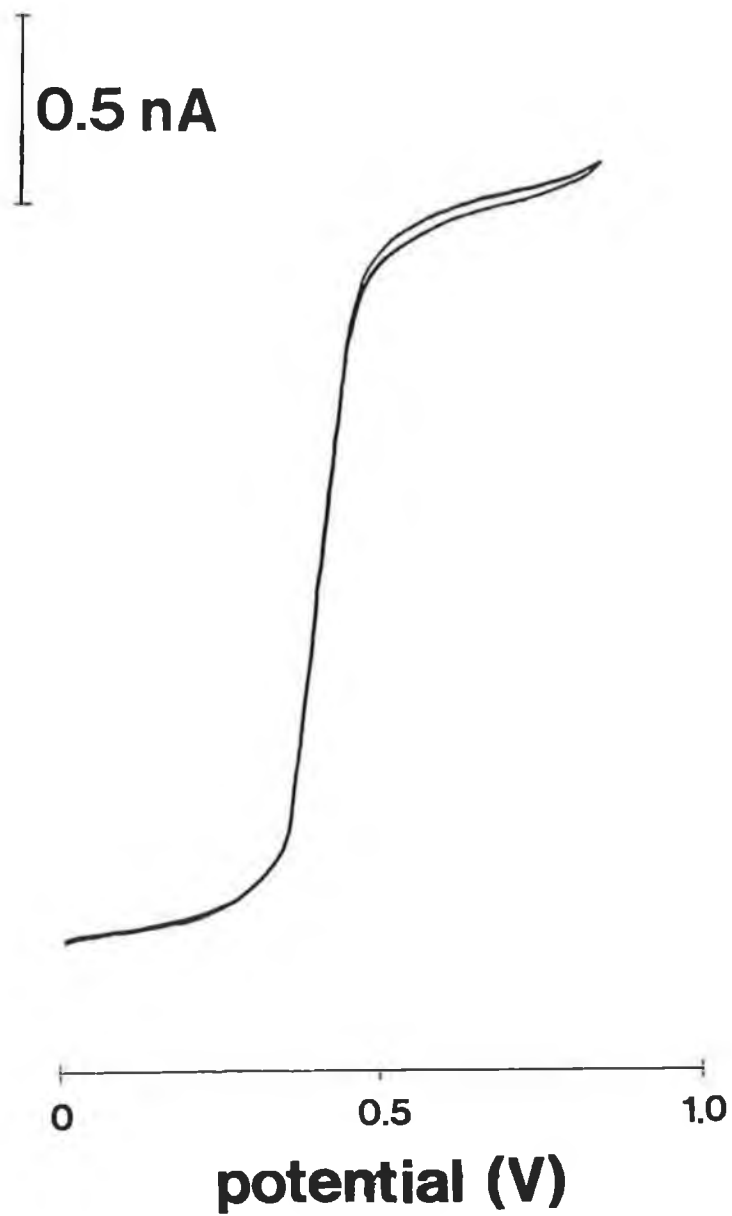


**Figure 3.4:** Cyclic voltammogram of 0.5 mM ferrocene in acetonitrile without added supporting electrolyte. Scan rate,  $10 \text{ mV s}^{-1}$ .



with the freshly treated fibre.

Polishing of the disk-shaped microelectrode was carried out after slicing of the resin mould. First the electrode was polished on emery paper (600 grit) , then with 6  $\mu\text{m}$  diamond paste, followed by successively finer grades of alumina (0.1 and 0.05  $\mu\text{m}$ ). The microelectrode was then sonicated in deionised water for 10 minutes in an ultrasonic bath.

### 3.2.2 RESULTS AND DISCUSSION

#### 3.2.2.1 Polishing Pretreatment

From an analytical standpoint, a pretreatment procedure was sought that would provide a sensitive and reproducible active surface. Polishing has been reported as an effective technique for obtaining a reproducible and well-defined electrochemical response [2,3]. The voltammogram shown in Figure 3.4 was recorded for the oxidation of ferrocene at the disk-shaped microelectrode using the polishing procedure described in the Experimental section. The limiting current, defined by Saito [29] for the limiting steady state current for a disk electrode is described by:

$$i_L = 4nFDc_r \quad (3.1)$$

where  $r$  is the radius of the microelectrode disk and the other terms have their usual meanings. The limiting current obtained for the oxidation of ferrocene was quite accurately defined by Equation 3.1, with a percentage relative standard deviation of  $\pm 8\%$  ( $n = 10$ ). The voltammograms obtained in this study were obtained in acetonitrile without the addition of supporting

electrolyte, which demonstrates one of the advantages of performing electrochemical measurements at microelectrodes.

#### 3.2.2.2 Electrochemical Pretreatment

The procedure of polishing is limited to microelectrodes in a disk configuration, since polishing of cylindrical carbon fibre microelectrodes is not feasible. Although cylindrical microelectrodes may be more fragile than corresponding disk electrodes, they possess several advantages, and were used for the remainder of this study. Firstly, they are much less sensitive to an imperfect seal between electrode and insulator than are disk electrodes, because the integrated current density in the vicinity of the seal is a minute fraction of the total current. Secondly, the area of the cylinder depends not only on its radius but also on its length. Therefore, one can adjust the length of the microcylinder to achieve the desired magnitude current without changing the diffusional characteristics. Thus enhanced diffusional flux can be realised without requiring the measurement of small current signals against noisy backgrounds [30].

As polishing could not be applied to cylindrical microelectrodes, an electrochemical pretreatment procedure was investigated. The first electrochemical pretreatment investigated involved anodisation followed by cathodisation of the microelectrode in BR buffer pH 2. The different potentials examined included 1.2, 1.4, 1.6 and 1.8 V applied for 1 minute followed by cathodisation at -1.5V for 1 minute. This treatment is similar to that used by Engstrom and co-workers [7] for the activation of glassy carbon electrodes. However, simply holding the microelectrodes at high positive potentials generally damaged the fibres and the results obtained were irreproducible. This underlines the value of applying an alternating potential

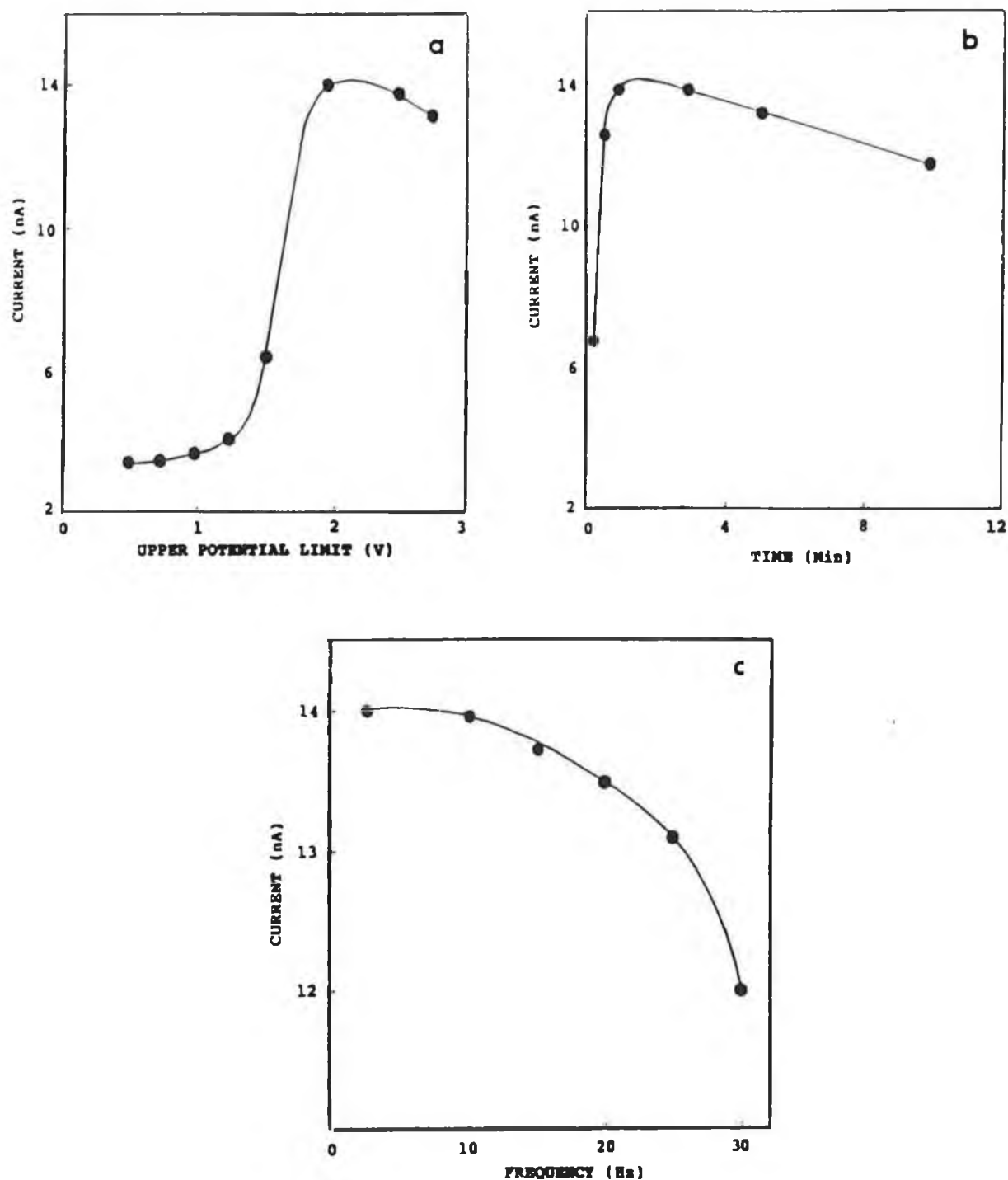


**Figure 3.5:** Effect of pretreatment parameters on the DPV response of  $1 \times 10^{-6}$  M folic acid. (a) Effect of upper potential limit; (b) Effect of duration of potential cycle; (c) Effect of frequency. Duration (a,c), 1 minute ; frequency (a,b), 10 Hz ; upper potential limit (b,c), 2 V. Supporting electrolyte, 0.1 M perchloric acid.

program, in which the potential of the electrode is held at the extreme limits for only a very brief part of the cycle. The application of an alternating potential of a triangular waveform to the microelectrode was then investigated.

The effect of various parameters of the pretreatment, namely potential range, duration and frequency, upon the resulting voltammetric response for folic acid are shown in Figures 3.5A-C. Each data point on the graphs was obtained using a fresh untreated microelectrode to eliminate erroneous data from the accumulative effect of previous treatments.

The effect of the upper potential limit (the initial potential was selected as 0 V in all cases) on the current response for folic acid is shown in Figure 3.5A for one minute at a frequency of 10 Hz. The current for the reduction of folic acid increased gradually from 0.7 to 1.5 V after which it increased dramatically until it reached a maximum at 2.0 V, followed by a gradual decrease in current. When the potential was extended beyond 3.0 V many fibres broke or provided noisy and irreproducible results. An initial potential of -1.5 V, rather than 0 V, was then chosen to include the hydrogen reduction wave; however, this did not result in an improvement in sensitivity.

Typical results for the duration of pretreatment are shown in Figure 3.5B for a potential cycle of 0 to 2 V at a frequency of 10 Hz. After 1 minute there was no improvement in sensitivity, and in fact after 5 minutes a steady decline in sensitivity occurred. An increase in noise was also observed when the pretreatment was continued for periods longer than five minutes.

The influence of the frequency of the potential program was

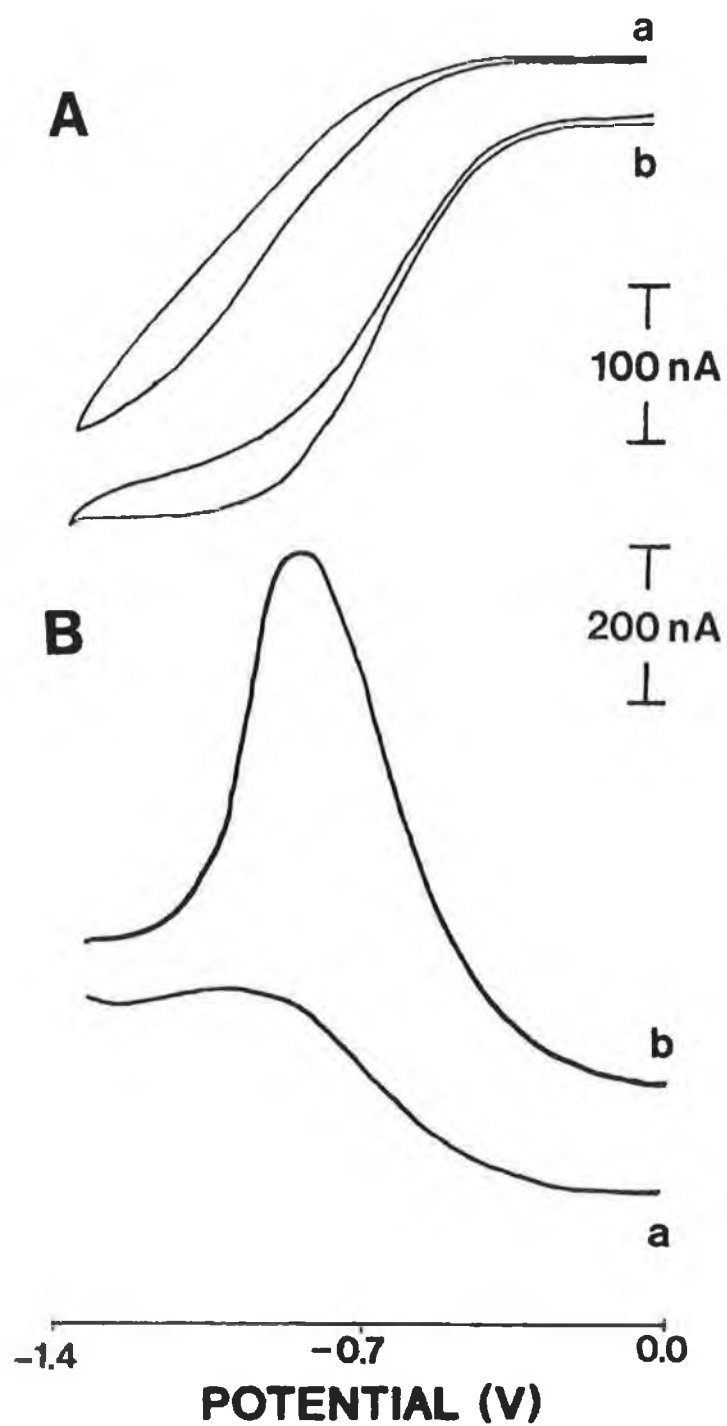


**Figure 3.6:** (A) Cyclic voltammograms and, (B) differential pulse voltammograms of air-saturated BR buffer (pH 2.0). (a) Before pretreatment, and (b) after electrochemical pretreatment. Scan rate, (A)  $100 \text{ mV s}^{-1}$ , (B)  $10 \text{ mV s}^{-1}$ .

examined from 1 to 30 Hz for a potential cycle of 0 to 2 V for one minute. The test voltammograms obtained at the lower frequencies, i.e. 1 to 10 Hz, yielded higher sensitivities than those observed at higher frequencies, as displayed in Figure 3.5C. The optimum frequency was chosen as 10 Hz as it yielded high sensitivity and was fast enough to avoid damage to the fibre.

The effectiveness of pretreatment appeared to be influenced by the supporting electrolyte composition. Hydrochloric acid (0.1 M), perchloric acid (0.1 M) and BR buffers of pH 2 to 12 were all tested, with the highest degree of activation being obtained using BR buffer, pH 2. Such solution-dependent observations have been made previously with conventional carbon electrodes, where anodisation of the electrode in citrate-acetate media resulted in activation, but anodisation in acetate buffer alone was not effective [21].

The pretreatment selected as optimal was a potential cycle from 0 to 2 V at a frequency of 10 Hz for a period of 1 minute in BR buffer pH 2. When 10 consecutive voltammograms were obtained for folic acid without intermediate electrochemical pretreatment, the current response decreased with each successive scan. Using the optimal pretreatment between each DPV scan, the response was constant, with the precision, calculated as the relative standard deviation ( $n = 10$ ), being better than 2.5%.

The pretreatment regime optimised for folic acid was employed to examine its effectiveness for the reduction of oxygen. Cyclic voltammograms for an air-saturated solution of BR buffer (pH 2.0), recorded prior to and after the pretreatment, are shown in Figure 3.6A. The oxygen response, which appears to be irreversible at the untreated electrode (curve (a)), is

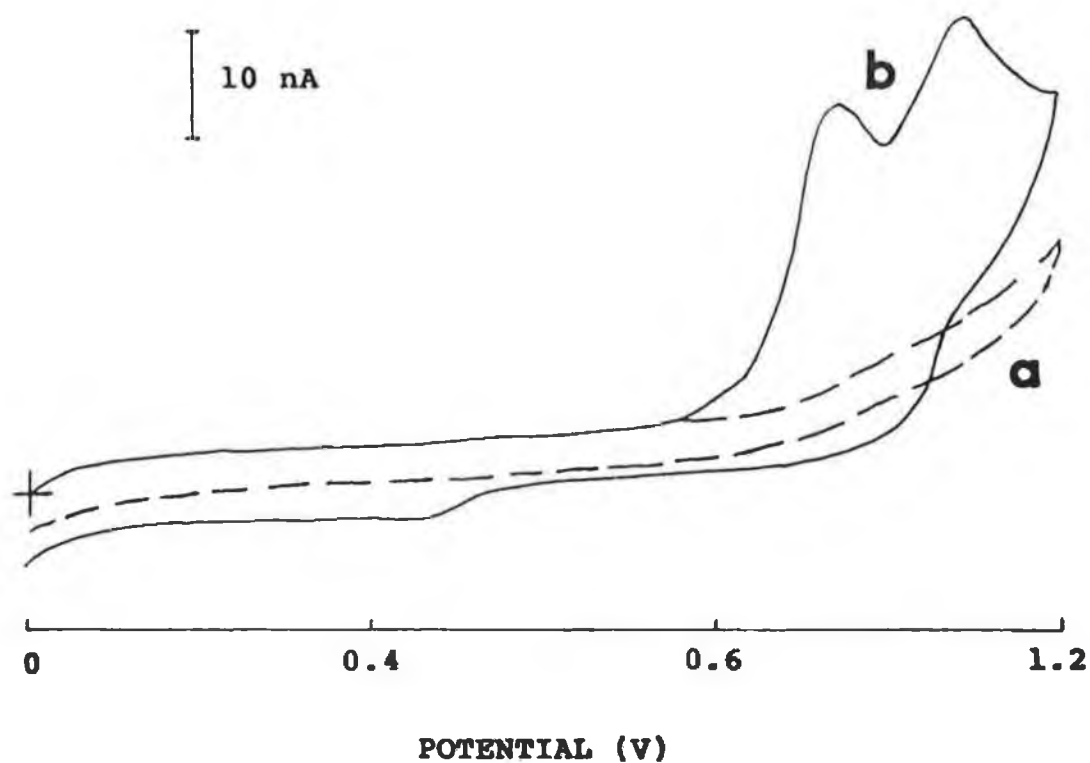


**Figure 3.7:** Effect of pretreatment on the staircase cyclic voltammetric response of  $1 \times 10^{-5}$  M folic acid in 0.1 M perchloric acid at (a) untreated microelectrode, and (b) electrochemically pretreated microelectrode. Scan rate  $100 \text{ mV s}^{-1}$ .

significantly altered to a more reversible response, with an anodic shift in its  $E_p$  value of approximately 150 mV following electrochemical pretreatment (curve (b)). Differential pulse voltammograms from the same study, shown in Figure 3.6B, demonstrate the substantial increase in sensitivity obtained after pretreatment.

A voltammetric study was then carried out to examine the effects of pretreatment on the functional characteristics of the microelectrode. The effect of pretreatment on both the faradaic and charging currents are shown in Figures 3.7 and 3.8 respectively. The increase in charging current obtained after pretreatment could be interpreted as being due to an increase in the surface area of the microelectrode. Bjelica et al. [31] have reported that glassy carbon electrodes subjected to prolonged electrolysis at extreme positive potentials caused roughening of the surface. However, it can be concluded that the faradaic current enhancement resulting from electrochemical pretreatment was not caused solely by increases in microscopic area, as the increase in charging current was much less than the increased faradaic current observed.

SEM images of untreated and electrochemically pretreated carbon fibres revealed that the outer layer of the fibre was caused to 'bubble' and peel away from the surface following the pretreatment. The electrochemical data suggest that this outer surface is unreactive, similar to the basal plane of glassy carbon and pyrolytic carbon [2,18,19], and that the pretreatment exposes a fresh carbon surface for charge transfer to occur. As proposed by McCreery and co-workers [18,19], this removal of an in-active layer may expose 'clean' graphitic edges as active sites for electron transfer to take place.

This activation of the electrode surface as a result of the



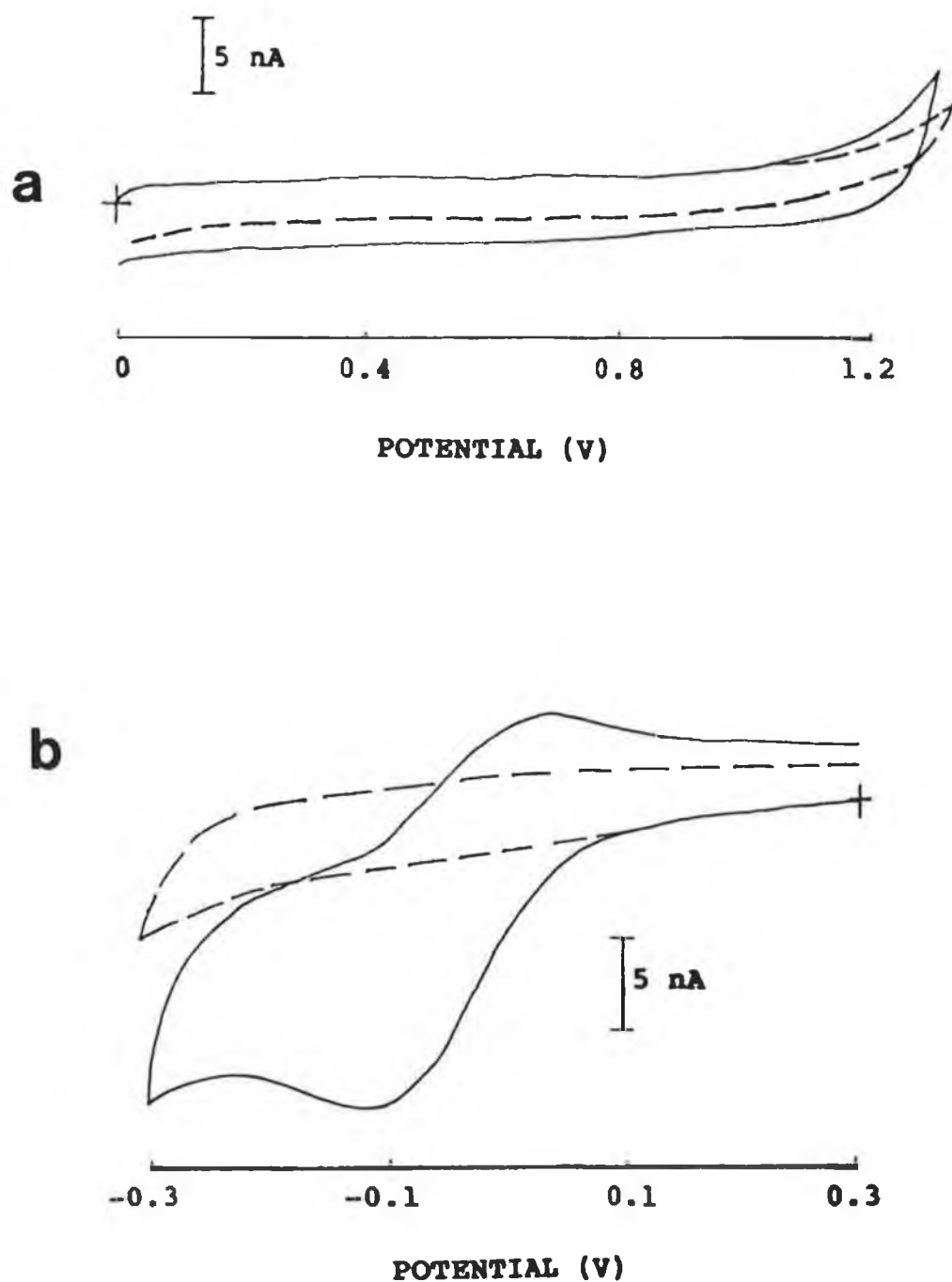


**Figure 3.8:** Staircase cyclic voltammograms of the background electrolyte (BR buffer pH 2) in (a) the anodic and (b) cathodic directions. (The dashed line represents the response before pretreatment and the full line after pretreatment). Scan rate,  $100 \text{ mV s}^{-1}$ .

oxidative removal of an inhibitory or passivating layer from the electrode surface is supported by the results obtained in Figure 3.9. The rapid reduction of the current amplitude illustrated in this figure, after successive scans without intermediate pretreatment, is presumably due to a reduction product of folic acid fouling the electrode surface, which is removed following pretreatment.

In addition, a surface bound quasi-reversible process appeared with a CV peak-to-peak separation potential of 150 mV (Figure 3.8B). The existence of such a process has been observed on glassy carbon electrodes and carbon fibre microelectrodes following electrochemical pretreatment [7,32]. It has usually been attributed to the presence of a surface quinone-hydroquinone system. In this study, the process did not appear until the upper potential reached approximately 1.6 V. The amplitude of the anodic and cathodic peaks also increased as the applied potential range was extended anodically. The potential required to generate the surface group corresponds to the potential required to activate the microelectrode toward folic acid. The coincidence of these results suggest that these two processes are related.

However, while the appearance of surface groups is indicative of activation, contrary reports appear in the literature on their significance. Edmonds et al. [15] support the view that surface quinoidal functionalities generated by electrochemical pretreatment were responsible for the increased sensitivity observed for carbon fibre microelectrodes. Other workers [14] have reported that quinone groups introduced onto the surface of glassy carbon electrodes do not serve as electron mediators for oxygen reduction. However, the most convincing evidence reported against their involvement, is the independence of vacuum heat treatments or laser activation on the surface

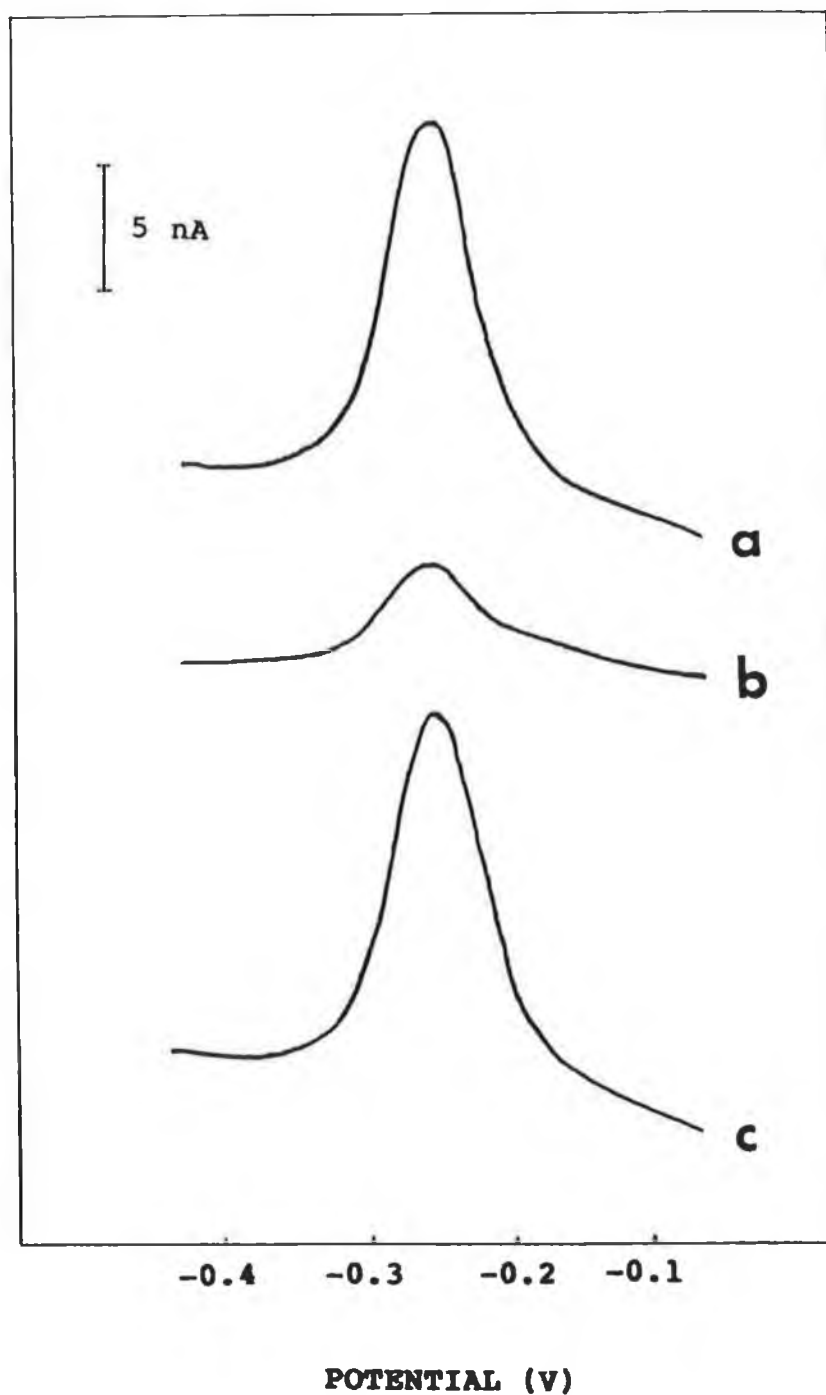


**Figure 3.9:** Differential pulse voltammograms of  $1 \times 10^{-6}$  M folic acid in 0.1 M perchloric acid. (a) Response after pretreatment; (b) response from fifth scan without intermediate pretreatment; and (c) response after second pretreatment carried out after (b). Scan rate,  $10 \text{ mV s}^{-1}$ .

oxygen content [13,16].

#### 3.2.2.3 Determination of Folic Acid

The voltammetric behaviour of folic acid was investigated using the activated microelectrodes in the range -1.2 to 1.2 V, using both DPV and staircase CV waveforms, and examining the behaviour of the vitamin in BR buffers of pH 1-12. There were two possible processes of analytical use; one at 1.03 V and the other at -0.25 V, both of which gave a maximum current response at pH 1. The reduction peak at -0.25 V in 0.1 M perchloric acid (see Figure 3.9) was considered best for analytical purposes, owing to its symmetrical morphology and the fact that it is far from an electrolyte decay curve. This peak is likely to be due to the 2-electron reduction of folic acid to 5,8-dihydrofolic acid. The peak potential varies linearly with pH in the range 1 to 12 with a slope of  $-55 \text{ mV pH}^{-1}$ . A calibration curve was constructed using the results from differential pulse voltammetry and a dynamic linear range was obtained between  $2 \times 10^{-8}$  to  $1 \times 10^{-6} \text{ M}$  with a correlation coefficient of 0.9996 ( $n = 10$ ). The slope of the calibration curve was  $11 \text{ nA } \mu\text{M}^{-1}$  with an intercept of  $1.07 \text{ nA}$  ( $\pm 0.04 \text{ nA}$ ). The detection limit was estimated as  $1 \times 10^{-8} \text{ M}$ , from the voltammograms obtained of  $2 \times 10^{-8} \text{ M}$  folic acid, based on a  $S/N = 3$ .

#### 3.3 CONCLUSION

In conclusion, it was demonstrated that electrochemical pretreatment greatly improves the voltammetric response for folic acid (and oxygen), and is a simple method (requiring the use of only a scanning potentiostat or a waveform generator) for obtaining consistent, well-defined voltammetric responses from carbon fibre microelectrodes. The data presented appears to be

consistent with a mechanism where the pretreatment results in the removal of an inhibitory layer, allowing charge transfer to take place, whether it is initially the removal of an inactive layer from the 'as-received' carbon fibre, or the subsequent removal of electrochemical reaction products which foul the electrode surface.

However, electrochemical pretreatment must also cause chemical changes in the electrode surface, beyond those associated with a simple cleaning process, as evidenced by the appearance of surface functionalities. Therefore the possibility of the existence of mediated electron transfer cannot be eliminated.

This is the first report in the literature that deals with the detection of folic acid at a bare carbon surface. The range of linearity and the detection limit compares favourably with that reported by Jacobsen et al. [27] who employed AC polarography. Although a much lower detection limit was obtained by Fernandez et al. [28], who utilised the adsorptive stripping process of folic acid at a mercury electrode, this approach has the possible advantages of being used as a detection system in HPLC or FIA, or for in vivo studies.

### 3.4 REFERENCES

1. R.N. Adams, *Electrochemistry at Solid Electrodes*, Marcel Dekker, New York, 1969.
2. R.M. Wightman, M.R. Deakin, P.M. Kovach, W.G. Kuhr and K.J. Stutts, *J. Electrochem. Soc.*, 131 (1984) 1578.
3. G.N. Kamau, W.S. Willis and J.F. Rusling, *Anal. Chem.*, 57 (1985) 545.
4. J.F. Evans and T. Kuwana, *Anal. Chem.*, 51 (1979) 358.
5. J. Zak and T. Kuwana, *J. Am Chem. Soc.*, 104 (1982) 5514.
6. R.J. Taylor and A.A. Humffray, *J. Electroanal. Chem.*, 42 (1973) 34.
7. R.C. Engstrom, *Anal. Chem.*, 54 (1982) 2310.
8. F.G. Gonon, C.M. Fombarlet, M.J. Buda and J.F. Pujol, *Anal. Chem.*, 53 (1981) 1386.
9. L. Falat and H.Y. Cheng, *Anal. Chem.*, 54 (1982) 2108.
10. W.J. Blaedel and G.A. Mabbot, *Anal. Chem.*, 50 (1978) 933.
11. K. Ravichandran and R.P. Baldwin, *Anal. Chem.*, 55 (1983) 1782.
12. I.F. Hu, D.H. Karweik and T. Kuwana, *J. Electroanal. Chem.*, 188 (1985) 59.
13. D.T. Fagan, I.F. Hu and T. Kuwana, *Anal. Chem.*, 57 (1985) 2759.
14. T. Nagaoka, T. Sakai, K. Ogura and T. Yoshine, *Anal. Chem.*, 58 (1986) 1953.
15. T.E. Edmonds and J. Guoliang, *Anal. Chim. Acta*, 151 (1983) 99.
16. M. Poon and R.L. McCreery, *Anal. Chem.*, 58 (1986) 2745.
17. P.M. Kovach, M.R. Deakin and R.M. Wightman, *J. Phys. Chem.*, 90 (1986) 4612.
18. R. Bowling, R. Packard and R.L. McCreery, *J. Electrochem. Soc.*, 135 (1988) 1605.

19. R. Bowling, R. Packard and R.L. McCreery, J. Am. Chem. Soc., 112 (1990) 4617.
20. J.F. Evans and T. Kuwana, Anal. Chem., 58 (1986) 2745.
21. F. Marcos, J. Phys. Chem., 57 (1972) 1801.
22. R.E. Panzer and P.J. Elving, J. Electrochem. Soc., 119 (1972) 864.
23. A.L. Lehninger, Principles of Biochemistry, Worth, New York, 1982, pp 772.
24. G.R. Rao, G. Kanjilal and K.R. Mohan, Analyst, 103 (1978) 993.
25. M.W. Dong, J. Leopore and T. Tarumoto, J. Chromatogr., 442 (1988) 81.
26. C. Paveenbampen, D. Lamontanaro, J. Moody, J. Zaremto and C.J. Rehm, J. Pharm. Sci., 75 (1986) 1192.
27. E. Jacobsen and M.W. Bjornsen, Anal. Chim. Acta, 96 (1978) 345.
28. J.M. Fernandez, A.C. Garcia, A.J. Miranda and P.T. Blanco, J. Electroanal. Chem., 225 (1987) 241.
29. Y. Saito. Rev. Polarogr., 15 (1968) 177.
30. S.T. Singleton, J.J. O'Dea and J. Osteryoung, Anal. Chem., 61 (1989) 1211.
31. L. Bjelica, R. Parsons and R.M. Reeves, Croat. Chem. Acta, 151 (1983) 99.
32. J. Wang, P. Tuzhi and V. Villa, J. Electroanal. Chem., 234 (1987) 119.

## CHAPTER 4

### THE DESIGN AND EVALUATION OF SOME DETECTION TECHNIQUES FOR CAPILLARY ELECTROPHORESIS



#### 4.1 INTRODUCTION

Electrophoresis has been used by biochemists for many years to separate amino acids, peptides, proteins and polynucleotides. Despite impressive advances, modern open-bed gel electrophoresis is a collection of manually intensive methodologies that cannot be readily automated. Casting of gels, application of samples, running of gels, and staining are time-consuming tasks prone to irreproducibility and poor quantitative accuracy. In the past ten years rapid instrumental methods for performing electrophoretic separations in capillary tubes have been developed, which holds the promise of putting capillary electrophoresis (CE) on the same instrumental footing as other separation techniques such as LC.

Initial work on electrophoresis in open tubes was presented in 1974 by Virtanen [1] who reported the potentiometric detection of analytes, electrophoretically separated, in 200 to 500  $\mu\text{m}$  i.d. glass tubes. His research dealt with zone electrophoresis and discussed many of the unique advantages of using small diameter tubes. In 1979 Mikkers and co-workers [2] used this technique with narrow-bore teflon tubes. Jorgenson and Lukacs [3] then reported the use of glass capillary columns with an on-column fluorescence detector, which created the impetus for further developments in this technique.

CE provides a simple solution to the problem of joule heating, which results in poor resolution in conventional electrophoresis. The microchannel of a capillary has such a high surface-to-volume ratio that heat is efficiently dissipated by transfer through the capillary walls. Such heat removal nearly eliminates convection, so that peaks approach the theoretical limit of being broadened only by diffusion [3]. This heat

dissipation permits the use of high potentials for separation, which leads to extremely efficient separations combined with a dramatic decrease in analysis time. These advantages have resulted in CE becoming one of the most promising new techniques available to the analytical scientist.

In the following section, a brief overview of this technique is given, including the more commonly used detection schemes. This is followed by a description of a method developed for the analysis of amino acids in brain tissue using CE. Also presented in this chapter is the construction and evaluation of an amperometric detector for CE.

#### 4.1.1 Modes of Capillary Electrophoresis

The most frequently used modes of CE have been capillary zone electrophoresis, micellar electrokinetic capillary chromatography, capillary gel electrophoresis, isotachopheresis and isoelectric focusing. Isotachopheresis and isoelectric focussing are beyond the scope of this discussion and have been reviewed by Jorgenson [4].

##### 4.1.1.1 Capillary Zone Electrophoresis (CZE)

A typical CZE system, as illustrated in Figure 4.1, consists of a buffer filled capillary, both ends of which are placed in buffer reservoirs that also accomodate electrodes. A power supply furnishes the high voltage (HV) input, typically of the order of 15 to 30 kV, and an on-column detector completes the system. Sample injection is perfomed either through electromigration or hydrostatically using pressure, vacuum or gravity. Sample volumes are in the nanolitre or picolitre range.

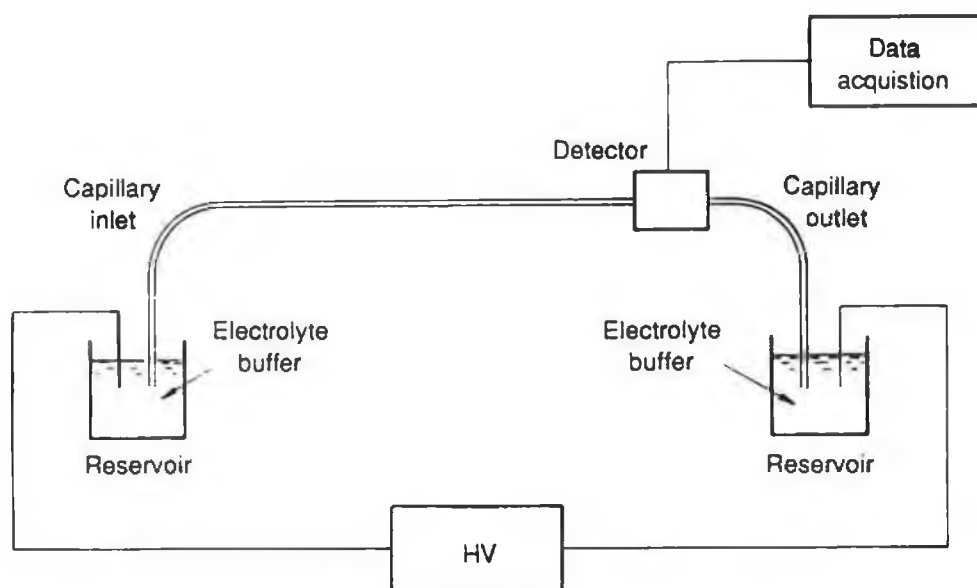


**Figure 4.1:** Generic diagram of a capillary electrophoresis system

The flow of solvent in a capillary when a tangential potential field is applied is termed 'electroosmosis' [5] and this is an important process in CZE. Any solid-liquid interface is surrounded by solvent and solute molecules that are not orientated as in the bulk of solution. Under normal aqueous conditions with small binary electrolytes, the walls of the fused silica capillaries have an anionic charge resulting from the ionisation of surface silanol groups. In solution, equivalent counter ions are arranged into two layers. The layer next to the surface is tightly bound by electrostatic forces and is termed the 'compact layer'. Thermal motion causes some of these ions in the compact region to diffuse further out into solution to form the 'diffuse region' of the double layer. The potential difference thus created across the layers is termed the 'zeta potential'. If an electrical field is imposed tangentially to the surface, the cationic counter ions in the diffuse layer migrate toward the cathode, and, because these ions are solvated, they drag solvent molecules with them. This process is called 'electroosmotic flow'. The extent of the potential drop across the double layer governs the rate of flow.

In addition to the bulk flow of the electrolyte, electrophoresis also takes place, that is, the applied electric field exerts a force on the cations to cause them to move to the cathode and anions to the anode. As a result, ionic solutes injected onto the capillary column separate into distinct zones, based on their respective charge. Consequently species migrate in the direction of the electroosmotic flow and are detected as each discrete zone passes a suitable detector located downstream from the capillary inlet. A graphical representation of this process is illustrated in Figure 4.2. The term  $\psi_0$  is the electrical potential at the interface between solid and liquid. Out into solution this potential decreases as shown by the curve. It decreases linearly in the compact region and then

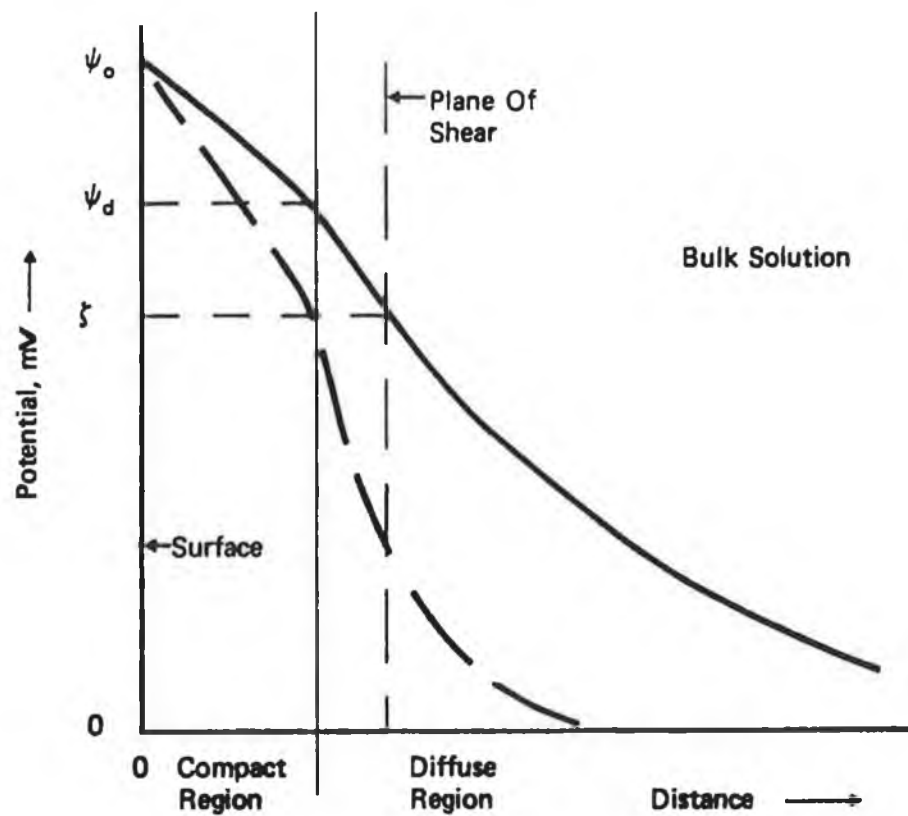


**Figure 4.2:** Graph representing the relationship between potential and distance from the surface, in the double layer [6].

exponentially in the diffuse layer. The term  $\psi_d$  is the potential at the interface between the compact and diffuse regions of the double layer. If the bulk of solution flows tangentially to the surface, 'a plane of shear' is established at or just outside the interface between the compact and diffuse regions. The plane of shear is not at the surface of the solid because the ions in the compact region have associated solvation spheres that are held stationary. The potential at the plane of shear is the zeta potential. The addition of electrolyte to the bulk solution compresses the double layer as represented by the dashed curve in Figure 4.2. The processes affecting a species in an electrophoretic separation are depicted in Figure 4.3A. The extremely small size of the double layer leads to a flow that originates at the walls of the capillary, resulting in a flat flow profile (Figure 4.3B). Flat flow profiles are expected when the capillary radius is greater than seven times the double layer thickness [6]. This profile contrasts with the characteristic parabolic velocity profile resulting from laminar flow. In CZE this flow profile, and lack of need for a stationary phase, result in a system of extremely high efficiency. Separations of dansylated amino acids that have been optimised for efficiency have been reported with efficiencies greater than two million [7].

#### 4.1.1.2 Micellar Electrokinetic Capillary Chromatography (MECC)

Neutral molecules present a special problem for CZE as they do not separate from each other but migrate as a group. In 1984 Terabe and co-workers [8] introduced the use of electroosmotically pumped micelles in a CE system to effect chromatographic separations of neutral compounds. These micelles act as a partitioning agent for the neutral molecules that are internalised according to their hydrophobic nature. The separation is based on the differential distribution of the

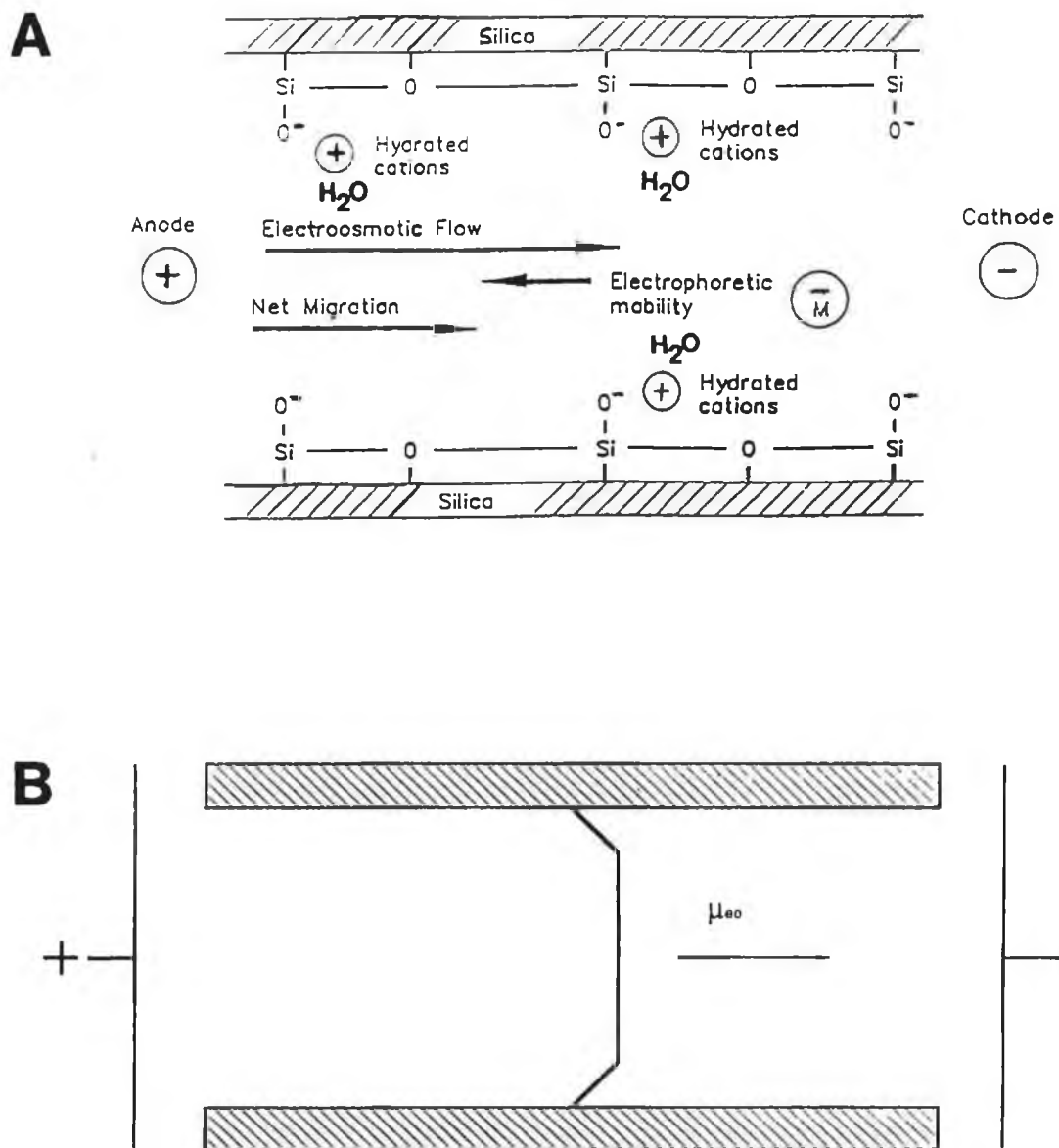


**Figure 4.3:** Schematics illustrating (A) the basic principle of CZE and (B) the flow profile resulting from electroosmotic flow in capillaries.

solute molecule between the electroosmotically pumped aqueous phase, and the slower moving electrophoretically retarded micellar phase. Although MECC was developed as a means for separating neutral solutes, micelles have also been used to enhance markedly the separation of charged species [9].

#### 4.1.1.3 Capillary Gel Electrophoresis (CGE)

Proteins present a major difficulty for separation by CZE due their adsorption to the capillary wall. Gel filled capillaries have demonstrated great potential for protein separations [10,11]. Cohen and Karger [11] developed a procedure to covalently bind polyacrylamide gels to the fused silica walls of capillary columns. This modification has permitted them to perform capillary SDS-PAGE (sodium dodecyl sulphate-polyacrylamide gel electrophoresis), a common procedure in conventional open-bed electrophoresis. The protein-SDS complexes migrate with a velocity dependent only on the size of the complex. Gel filled columns offer several advantages over open-bed gel electrophoresis, including higher resolution, reduced analysis time, and increased sensitivity, as well as the ability to use greater potential fields and to use on-line sample detection without the requirement of staining procedures.

#### 4.1.2 Detection Methods

One of the main areas of research in CE is the development of sensitive methods of detection. The small column dimensions and narrow zone widths place stringent requirements on the detection system. Indeed, this feature has been identified by Jorgenson and Lukas [3] as the greatest obstacle to further development and utilisation of capillaries. Several of the detection systems commonly used in LC have been successfully adapted to CE, and will be briefly reviewed in this section.



#### 4.1.2.1 Optical Detection

Optical detectors based on both UV/VIS absorbance and fluorescence spectrometry are currently the most common means of monitoring CE separations. In both cases detection is often made on-column and the construction involved is generally simple as most workers use polyimide-coated fused capillaries. A section of this coating is removed to reveal an on-column flow cell that is transparent throughout the UV and visible range.

The main drawback with optical detection is the small optical pathlength associated with on-column detection. The UV detector, the more universal of the two optical detectors, exhibits detection limits between  $10^{-6}$  and  $10^{-4}$  M of analyte depending on its molar absorptivity. Recently two novel procedures have been reported to improve these limitations. Tsuda and co-workers [13] utilised rectangular-shaped capillaries to increase the pathlength and reported an improvement of one order of magnitude in the limit of detection over circular capillaries. Wang et al. [14] designed a multireflective absorption cell which resulted in a 40-fold decrease in the detection limit when compared to a single-pass cell.

Fluorescence detection typically affords a hundred to a thousand fold improvement in sensitivity compared with UV absorbance detection. Laser induced fluorescence is currently the most sensitive detection method for CE. In these systems the capillary is used as the flow cell, the laser illumination is perpendicular to the capillary, and a photomultiplier tube monitors the fluorescence produced. Dovichi et al. [15,16] developed a more sensitive method that has the same excitation geometry but uses a sheath flow cuvette as the sample cell, thereby eliminating much of the scattered light and luminescence

from the fused silica capillary. With this technique, detection limits in the low zeptomoles ( $10^{-21}$  moles) region have been reported.

The fundamental limitation of fluorescence detection is that relatively few molecules fluoresce. To overcome this limitation, fluorescence detection has been extended to non-fluorescent analytes by the use of derivatising reagents. Fluorescent tagging has been accomplished by precolumn [3,17], on-column [18] and post-column [19] derivatisation. An alternative method of detecting non-fluorescent analytes was developed by Kuhr and Yeung [20] using an indirect fluorescence procedure. A fluorophore was added to the electrolyte and the non-fluorescent ions detected through charge displacement of the fluorophore.

#### 4.1.2.2 Conductivity Detection

Conductivity measurement is well recognised as a universal detection system in LC and was first employed as a detection method in CE by Mikkers and co-workers [2]. As is true of all bulk property detectors, the conductivity detector is less sensitive than detectors that respond to physical properties of the analyte. Nevertheless, conductivity detection has proven useful in the determination of several classes of ions, including organic acids [2,21], metal ions [22] and inorganic ions [21].

The designs used for CE conductivity detectors are on-column and end-column structures. Foret et al. [21] used a microscale moulding method to construct an on-column detector. Huang and co-workers [23] used another scheme for constructing an on-column detector which involved drilling a hole directly through the capillary column with a laser. Two platinum electrodes sealed in the resulting holes, on opposite sides of

the column, served as sensing electrodes. Recently, Huang and Zare [24] described the construction of an end-column detector. The detection system employs one electrode at the capillary outlet, and a drilled hole beside the electrode which provides an outlet for the separation buffer into the cathodic buffer reservoir where the ground electrode is located, to complete the detector. The design is an improvement over earlier end-column conductivity detectors described by the same workers, as it is simpler in construction and results in less zone broadening.

#### 4.1.2.3 Amperometric Detection

Amperometric detection is complicated by the fact that the current running through the capillary is typically several orders of magnitude greater than the faradaic current measured at the electrode. To circumvent this problem, Wallingford and Ewing [25] employed a porous glass joint to couple two pieces of capillary together. This joint was immersed in the cathodic buffer reservoir where it permits the flow of ions but not bulk electrolyte flow, enabling the detection section of the capillary to be isolated from the applied electrical field. The electroosmotic flow serves to 'pump' the electrolyte and analytes past the joint to the end of the detection capillary. Carbon fibre microelectrodes have been generally used for detection due mainly to their small dimensions. They can be inserted into the end of the column with the aid of a micro-manipulator and a microscope. Wallingford and Ewing [26] have demonstrated the high sensitivity obtainable with such a detection system and have reported  $1 \times 10^{-8}$  M detection limits for several catecholamines.

Amperometric detection has also been utilised in MECC [27,28]. In these studies it was shown that the concentration of the surfactant, SDS, has a direct effect on the sensitivity of

the system. Increasing the concentration of SDS led to a decrease in the limiting current for several catechol compounds to a constant value. It was proposed that this was caused by the adsorption of micelles onto the surface of the electrode which formed a selectively permeable barrier to the oxidation of hydrophobic catechols. In a further study, Wallingford and Ewing [29] modified the surface of the carbon fibre with Nafion which appeared to minimise the SDS adsorption and allowed lower detection limits to be obtained.

Olefirowicz et al. [29] demonstrated the feasibility of indirect amperometric detection for CE. Dihydroxybenzylamine (DHBA) was used as the cationic 'electrophore'. A stable background was obtained when the carbon fibre microelectrode was held at 0.7 V vs. SSCE at concentrations of 10  $\mu$ M DHBA in the presence of electrolyte buffer. Several amino acids and peptides were detected using this system, with detection limits in the femtomole range.

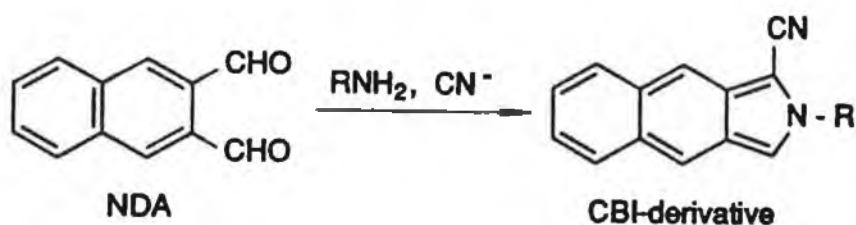
The use of a modified copper wire amperometric detector for CE was reported recently [30]. The formation of copper(I) oxide on the surface of the electrode was induced by the application of a positive potential. Specific analytes form a complex with this film, which results in a dissolution of the copper(I) oxide in an analyte-dependent oxidation current. This electrode was used to detect amino acids and dipeptides with sub-femtomole detection limits being reported.

#### 4.2 THE DETERMINATION OF AMINO ACID NEUROTRANSMITTERS IN RAT BRAIN HOMOGENATE BY CAPILLARY ELECTROPHORESIS WITH UV DETECTION

There are four amino acids in a mammalian brain that have been definitively shown to possess a role in neurotransmitter functions. Glutamate and aspartate are the principal excitatory

transmitters, while gamma-aminobutyric acid (GABA) and glycine are the principal inhibitory transmitters [31]. These neurotransmitters have been implicated in many neurological and psychiatric disorders, such as Huntington's disease, Parkinson disease, epilepsy, schizophrenia and senile dementia [32]. Therefore, there is great interest in developing methods which permit the quantitation of these amino acids in the brain.

Many analytes of biological interest, including amino acids, lack properties for direct determination at physiologically relevant levels. To circumvent this limitation, chemical derivatisation is generally employed to enhance detection sensitivity. A derivatising reagent developed at the University of Kansas [33] was specifically designed for primary amines. Naphthalene-2,3-dicarboxaldehyde (NDA) reacts with primary amines in the presence of cyanide to produce cyano[f]benzoinindole (CBI) derivatives which are both fluorescent and electroactive. The reaction scheme is given below:



Of the various analytical methods currently used, LC has been routinely used with much success, and appears to be the current method of choice for the analysis of derivatised amino

acids [34]. However, the use of CE for this particular separation should prove advantageous due to its high separation efficiency, small volume capability (particularly important for brain samples), low cost, and rapid analysis times.

#### 4.2.1 EXPERIMENTAL

##### 4.2.1.1 Reagents

All amino acids and amines were purchased from Sigma and used as received. Naphthalene-2,3-dicarboxaldehyde (NDA) was supplied by Oread Laboratories (Kansas). Sodium cyanide and sodium borate were obtained from Fisher Scientific (New Jersey). Solutions were prepared in NANOpure water (Sybron- Barnstead, Massachusetts) and passed through a membrane filter (0.45  $\mu$ m pore size) before use.

##### 4.2.1.2 Apparatus

Electrophoresis in the capillary was driven by a high-voltage dc (0 to 30 kV) power supply (Spellman High Voltage Electronics Corp., New York). The anodic high-voltage end of the capillary was isolated in a laboratory-built plexiglas box equipped with an interlock device for operator safety. Two platinum wires were employed, one of which served as the anode and the other as the cathode. The column used for all separations was a fused silica capillary (115 cm length, 50  $\mu$ m i.d., and 360  $\mu$ m o.d.), with a detection window at 95 cm. The window was prepared by the removal of a 1 cm length section of the protective polyimide coating using hot concentrated hydrochloric acid. This method was preferred over a flame procedure as it resulted in a less fragile optical window. An Isco Capillary Electrophoresis Model CV<sup>4</sup> (Isco, Nebraska) UV/VIS absorbance detector was operated at 420 nm. Sample

introduction was accomplished by electrokinetic injection using 5 kV for 12 seconds. Under these conditions, an injection precision of a few percent was possible; the precision is limited primarily by the reproducibility in the length for which the injection potential is applied. This injection technique introduces bias in the analysis; analytes with high electrophoretic mobility travel at greater speed and thus are introduced to a greater extent than slower moving analytes.

#### 4.2.1.3 Procedures

##### 4.2.1.3.1 Sample Derivatisation

Typically 10 to 100  $\mu\text{L}$  of sample was mixed with 700 to 790  $\mu\text{L}$  of 20 mM sodium borate solution. A 100  $\mu\text{L}$  of 10 mM NaCN was then added, followed by 100  $\mu\text{L}$  of 10 mM NDA in acetonitrile to give a final volume of 1 mL. (For higher concentrations of amino acids that occur in the brain homogenate sample 20 mM NaCN and 20 mM NDA were used in order to completely derivatise all the primary amines present). The resulting solution was thoroughly mixed and enclosed in a darkened vial to protect from photodegradation. The sample was allowed to fully derivatise at room temperature ( $25^{\circ}\text{C}$ ) for thirty minutes before analysis was carried out. This procedure was easily scaled down to give total sample volumes of 10  $\mu\text{L}$ .

##### 4.2.1.3.2 Brain Homogenate Preparation

Rats were sacrificed by cervical dislocation, and the brain removed and washed to remove extraneous matter. Subsequently, a weighed amount of brain tissue (approximately 0.5 g) was placed in 3 mL of 20 mM sodium borate and sonicated in an ice bath for 15 minutes using an Artix Sonic Dismembrator (Artix Systems Corp., New York). Following this, 100  $\mu\text{L}$  of 4.9 mM

alpha-aminoadipic acid, which acted as the internal standard (IS), was added to 885  $\mu\text{L}$  of the homogenate and the mixture acidified with 15  $\mu\text{L}$  of concentrated perchloric acid to precipitate any protein present. The mixture was then centrifuged at 16,000 rpm and the supernatant filtered through a 0.45  $\mu\text{m}$  pore size membrane before sample derivatisation. The above procedure has been successfully scaled down to accommodate samples as small as 0.019 g of brain in 150  $\mu\text{L}$  of buffer.

#### 4.2.1.3.3 Determination of Electrophoretic Mobility

The electrophoretic mobility was determined by the measurement of the migration times relative to that of a neutral marker. The marker used was NDA-labelled tyrosine as it is neutral at the pH employed in this study (pH 9.0). Equations 4.1 and 4.2 describe the relationship between the electrophoretic velocity ( $V_{\text{ep}}$ ,  $\text{cm s}^{-1}$ ), electroosmotic velocity ( $V_{\text{eo}}$ ,  $\text{cm s}^{-1}$ ), total velocity of the analyte ( $V_{\text{t}}$ ,  $\text{cm s}^{-1}$ ), and electrophoretic mobility ( $U_{\text{ep}}$ ,  $\text{cm}^2 \text{V}^{-1} \text{s}^{-1}$ ) where  $t_{\text{m}}$  is the migration time of the analyte (s),  $t_{\text{nm}}$  is the migration time of the neutral marker (s),  $l$  is the length of the capillary to the detector (cm),  $E$  is the electrical field strength ( $\text{V cm}^{-1}$ ),  $L$  is the total length of the capillary (cm), and  $V$  is the separation voltage (V).

$$V_{\text{ep}} = V_{\text{t}} - V_{\text{eo}} = l t_{\text{m}}^{-1} - l t_{\text{nm}}^{-1} \quad (4.1)$$

$$U_{\text{ep}} = V_{\text{ep}} E^{-1} = V_{\text{ep}} L V^{-1} \quad (4.2)$$



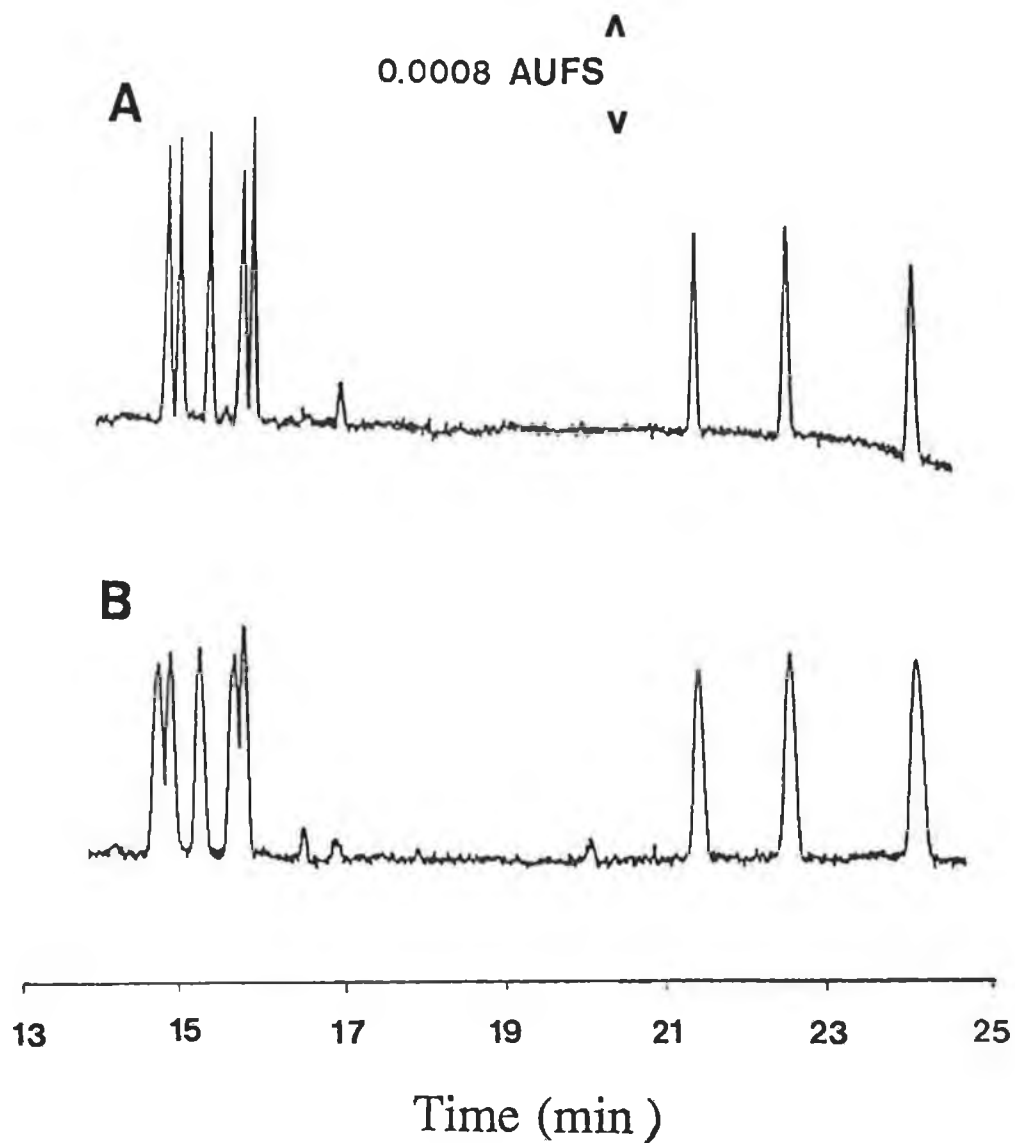


**Figure 4.4:** Electropherogram of seven NDA-labelled amino acids. Separation conditions: 0.02 M sodium borate buffer (pH 9.0); voltage, 30 kV; column length, 115 cm; detection wavelength, 420 nm. Samples derivatised in sodium borate buffer (pH 9.0) of concentration (A) 20 mM (B) 50 mM.

## 4.2.2 RESULTS AND DISCUSSION

### 4.2.2.1 Analysis of Amine Standards

Successful analysis of the major amino acid neurotransmitters, i.e. GABA, glycine, glutamate and aspartate, requires that these compounds be separated not only from each other but also from other primary amines which occur in the brain and are converted to CBI derivatives during sample derivatisation. Thus, the amino acid neurotransmitters should be separated from the other commonly occurring amino acids (which are also derivatisable), as well as from other neurotransmitters, including norepinephrine, dopamine and DOPA, and phosphoethanolamine (PEA). In addition, for the procedure to be successful in the analysis of real samples, an internal standard needs to be employed. Of those investigated, the amine, alpha-aminoadipic acid, served the purpose well since it eluted at a position at which there are no endogenous peaks in the brain samples. To achieve this demanding separation, a relatively long column was required with the separation voltage operated at its maximum (30 kV).

The derivatisation reaction required a pH above 8 to give reasonable yields, and typically borate buffers near pH 9 were employed [34]. Performing the derivatisation reaction in solutions of higher pH resulted in no improvement in separation. However, the resolution of NDA-labelled amines depended markedly on the concentration of the borate buffer used in the derivatisation procedure. Illustrated in Figure 4.4 is the effect of performing the derivatisation in 50 mM versus 20 mM borate buffer. As can be seen, the peaks obtained using the higher concentration of borate are much broader than those from the more dilute solution. A similar effect has been previously reported where solutions of a lower ionic strength than the

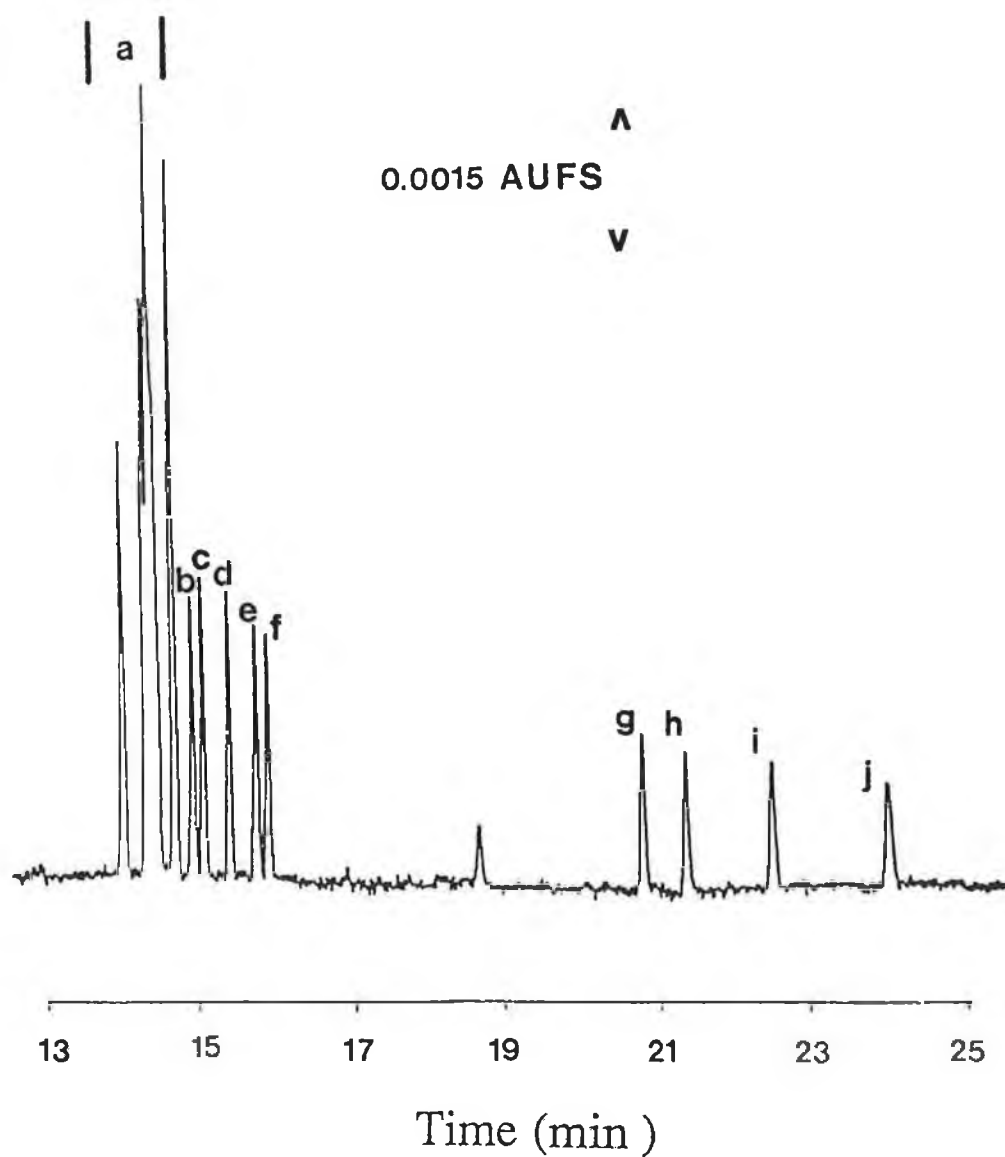


**Figure 4.5:** Electropherogram of NDA-labelled amino acids; (a) Trp, Phe, His, Gln, Leu, Ile, Met, Tyr, Thr, Val, Asn, (b) GABA (c) Ser, (d) Ala, (e) Taur, (f) Gly, (g) PEA, (h) IS, (i) Glu, (j) Asp. Separation conditions as outlined in Figure 4.4.

separating buffer resulted in narrower peaks [35]. In this study if borate buffers less than 20 mM were used, the derivatisation procedure did not go to completion, especially for those amino acids with acidic side chains, such as aspartate and glutamate. Therefore, 20 mM sodium borate was found to provide the optimum concentration for subsequent analyses.

Using the optimum conditions, the major amino acid neurotransmitters were separated from each other and the other common amino acids, as shown by the electropherogram in Figure 4.5. Separation of the neurotransmitters, norepinephrine and dopamine, as well as their metabolic precursor, DOPA, from each other and the other amino acids is illustrated in Figure 4.6. The high separation efficiency of CE is demonstrated in this figure as indicated by the resolution of 16 different derivatives from each other.

As a further study, the correlation of electrophoretic mobility of the amino acids with their physicochemical properties was investigated. This is complicated both by the lack of a well developed theory for the expected relationships and by the difficulties in evaluating the physicochemical parameters. When a species is placed in the buffer medium, in addition to the electrophoretic migration, the net velocity must also include an additional term related to the frictional drag. The net electrophoretic mobility is achieved when the force due to the electrostatic attraction is balanced by the frictional drag of the medium. Most conclusions from experimental explorations have used simplified assumptions. For instance, the species were usually considered to be spherical, and Stokes law was used to estimate frictional forces [36]. Rickard and co-workers [37] have recently examined the assumptions underlying the available theoretical predictions of electrophoretic mobility and explored the ability to correlate

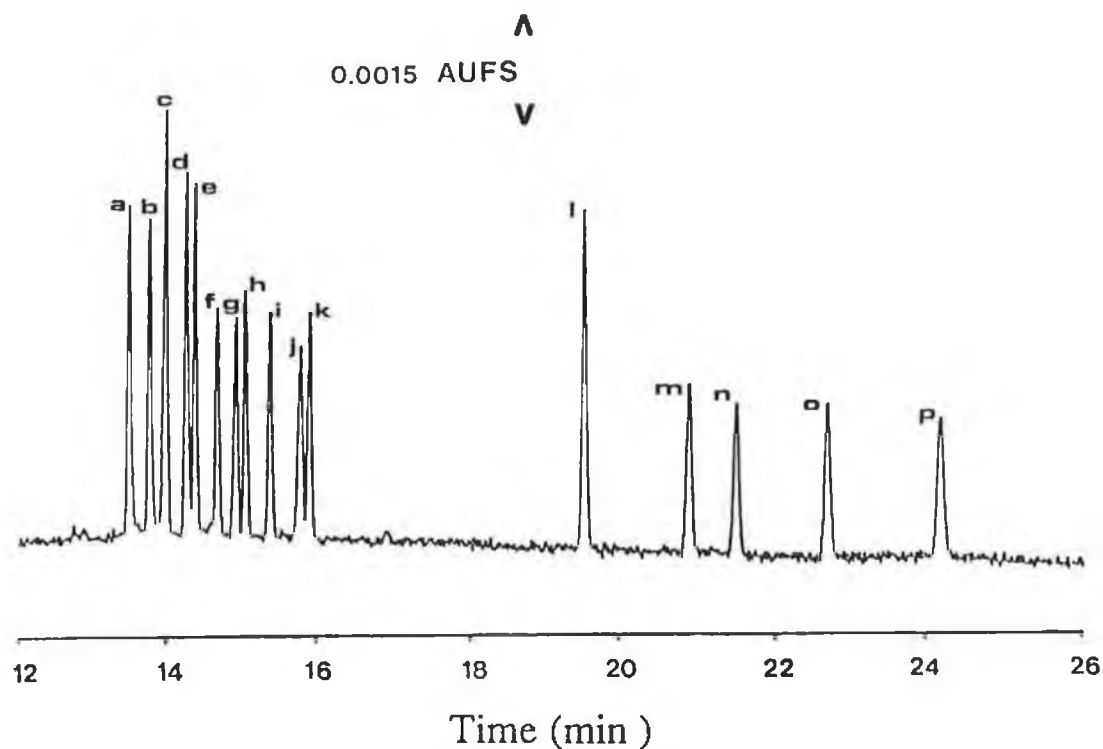


**Figure 4.6:** Electropherogram of NDA-labelled amino acids and amines: (a) norepinephrine, (b) dopamine, (c) Trp, (d) Phe, (e) Tyr, (f) Asn, (g) GABA, (h) Ser, (i) Ala, (j) Taur, (k) Gly, (l) DOPA, (m) PEA, (n) IS, (o) Glu, (p) Asp. Separation conditions as outlined in Figure 4.4.

the mobility with the physicochemical properties of the analytes and the separation buffer. In one of the mobility models they employed, it was predicted, using Stokes law, that the frictional drag is related to the radius of the species, which is proportional to the 1/3 power of the molecular weight. The amino acids separated were plotted in Figure 4.7 as the observed electrophoretic mobility vs. the quantity of calculated charge divided by the molecular weight to the 1/3 power (Figure 4.6). The linear least square fit resulted in a correlation coefficient of 0.998. Thus, this mobility model is suitable to facilitate the elucidation of optimum separation strategies and the identification of amino acid mixtures.

Quantitation of the NDA-labelled derivatives of GABA, glycine, glutamate, aspartate, serine, alanine, taurine and PEA was achieved using response factors based on peak heights obtained from the concentration range of  $2 \times 10^{-5}$  to  $5 \times 10^{-5}$  M. The detection limits calculated based on a  $S/N = 3$  are given in Table 4.1. In addition, the separation efficiency was determined by calculating the number of theoretical plates from migration times and peak half-widths. These results are also presented in Table 4.1.

Since the injection of cations and anions involves both electrophoresis and electroosmotic flow, the apparent injection volume for these ions is different than the liquid volume injected. Thus an apparent volume must be determined to calculate the number of moles detected. This apparent volume of injection,  $V$ , can be calculated by the following equation;

$$V = (U_{ep} + U_{eo})Et_{inj} \quad (4.3)$$

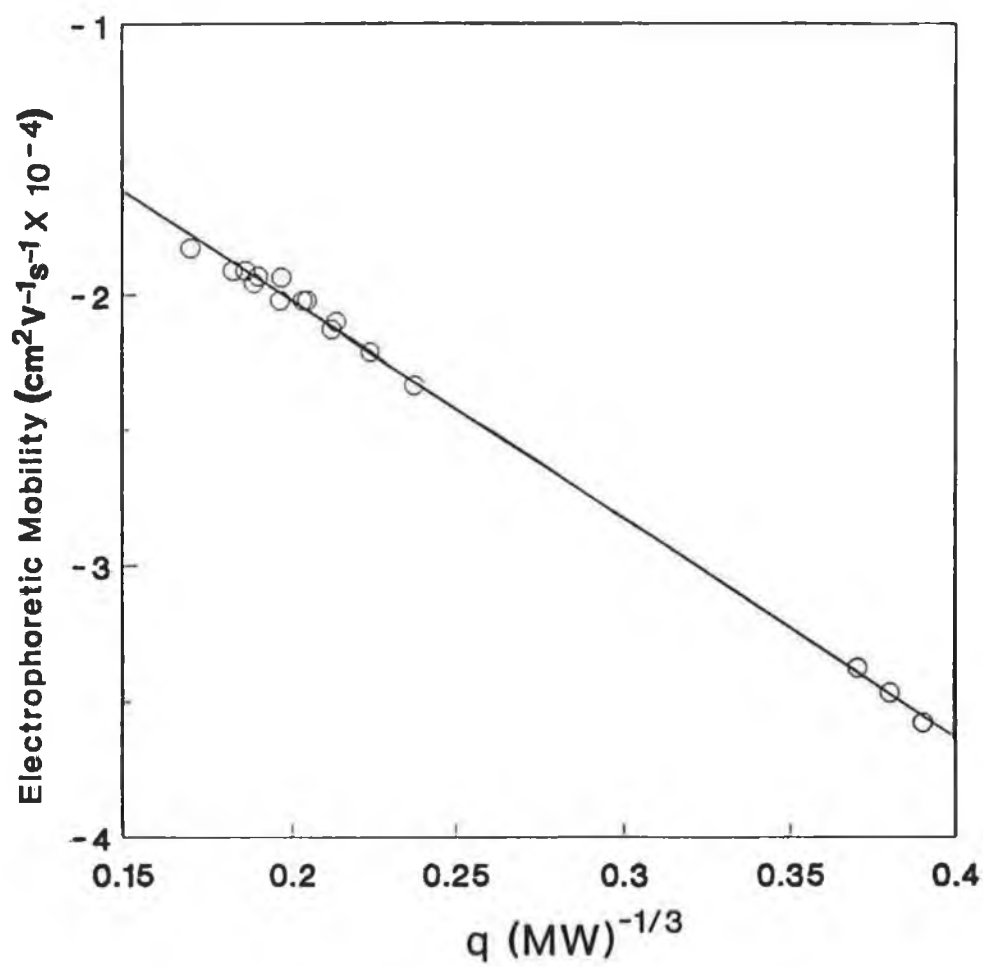


Figure 4.7: Fit of electrophoretic mobility vs. charge to size parameter

where  $U_{ep}$  is the electrophoretic mobility,  $U_{eo}$  is the coefficient of electroosmotic flow,  $E$  is the applied field strength,  $A$  is the cross-sectional area of the capillary bore, and  $t_{inj}$  is the injection time [38].

Table 4.1: Limit of detection and separation efficiency

Amino acid	Apparent volume (nL)	Detection limit		Efficiency
		( $\mu$ M)	(fmol)	
GABA	6.31	3.8	24.0	344,000
SER	6.27	3.5	21.9	425,000
ALA	6.14	3.7	22.7	445,000
TAUR	6.00	4.4	26.4	360,000
GLY	5.95	4.3	25.6	444,000
GLU	4.21	8.7	36.6	414,000
ASP	3.96	10.2	40.4	385,000

#### 4.2.2.2 Quantitation of Amino Acids in Rat Brain

Capillary electrophoresis was performed on the NDA derivatised sample of a rat brain homogenate using the protocol described in the Experimental section. The resulting electropherogram, showing the separation of the NDA-labelled amino acids, is given in Figure 4.8. All peaks were identified, both by comparison of standard and sample migration times and by spiking with standards. Use of the internal standard and the



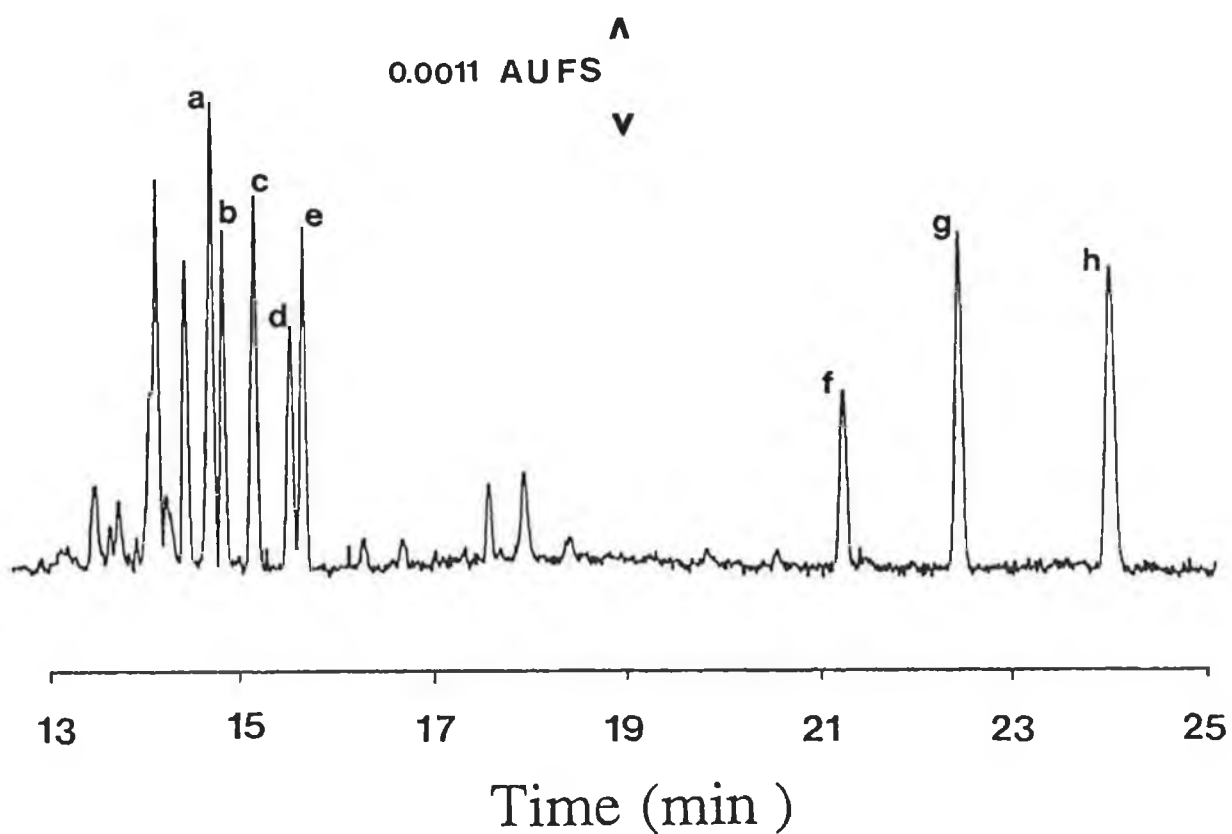


**Figure 4.8:** Electropherogram of NDA-labelled rat brain homogenate; (a) GABA, (b) Ser, (c) Ala, (d) Taur, (e) Gly, (f) IS, (g) Glu, (h) Asp. Separation conditions as in Figure 4.4.

response factors calculated enabled quantitation of these amino acids. Listed in Table 4.2 are the concentrations of the amino acids in the homogenate and the corresponding concentrations in the brain.

Table 4.2: Concentration of amino acids in rat brain

Amino acid	Concentration			
	mean <sub>(5)</sub>	Homogenate ( $\mu$ M)		Brain ( $\mu$ mol/g)
		RSD <sub>(5)</sub>	%RSD	
GABA	557.4	18.7	3.4	3.42
SER	512.4	9.3	1.8	3.15
ALA	392.4	9.1	2.3	2.41
TAUR	422.4	10.0	2.4	2.59
GLY	487.2	7.4	1.5	3.00
GLU	1353.6	10.3	0.8	8.31
ASP	1384.8	15.4	1.1	8.50

#### 4.2.3 CONCLUSION

In conclusion, the capillary electrophoretic separation of several NDA-labelled amino acids has been demonstrated. The procedure developed was successfully applied to the determination of the amino acids involved in neurotransmitter roles and several other amino acids in the brain. Although the procedure

exhibited excellent separation efficiencies (of the order of 400,000 theoretical plates), the detection limits, although adequate for the quantitation of amino acids in the brain homogenate, were relatively high, and limits other analytical applications. However, the detection limits are typical of other reported CE methods utilising UV/VIS detection, and as previously discussed, is as a direct result of the short pathlengths used in CE. In a later study described in chapter 5, the detection of the same NDA-labelled amino acids with an electrochemical detector, which enabled lower detection limits to be achieved, is described.

#### 4.3 THE DESIGN AND EVALUATION OF AN AMPEROMETRIC DETECTOR FOR CAPILLARY ELECTROPHORESIS

In CE, one of the main areas of research is the development of sensitive detection systems. As a consequence of the small sample volumes involved, high sensitivity and small volume detectors are necessary for analysis of many real samples. Much of the work on CE and most commercial instruments use UV detection. However, since this is an optical technique and is pathlength dependent, its sensitivity is limited when using small diameter capillaries. Laser-based fluorescence detectors are more sensitive, but are expensive, limited to certain wavelengths, and require derivatising reagents for many applications. Electrochemical detection has an advantage over these techniques in that the response is not dependent on pathlength; therefore, very small capillary diameters can be used without sacrifice in signal. It also utilises relatively inexpensive instrumentation [25,26].

Wallingford and Ewing [25,26] have developed an off-column electrochemical detector using a porous glass frit to isolate the detection end of the column from the applied electrical field. The fabrication of this joint assembly is quite difficult and intricate. Unless perfect realignment of both sections of capillary is achieved, considerable band broadening can occur. This joint does not appear durable, as the porous glass is extremely fragile and must be kept submerged in solution. An additional limitation of the design is that the porous glass capillary is not readily available. Huang and Zare [39] designed an on-column frit which also served to isolate the final section of the capillary column from the applied electrical field. However, the authors described the drawbacks of the design, including lack of capillary-to-capillary reproducibility, leakage of the frit and difficulty of fabrication (requiring the

use of a CO<sub>2</sub> laser). Recently, Huang et al. [24] have reported that it is not necessary to isolate the microelectrode from the high voltage if capillaries with very small internal diameter (5 µm) are employed. In such capillaries, the current generated by the CE separation is low enough that it does not adversely affect the electrochemical detection. However, as a result of the small size of the microelectrodes employed, the concentration detection limits are not as low as those reported with larger internal diameter capillary columns.

This section describes an alternative construction procedure in which the detection end of the capillary column is isolated from the high applied voltage. The capacity of the developed system for the analysis of real samples is explored, as well as the use of voltammetric characterisation as a method of compound identification.

#### 4.3.1 EXPERIMENTAL

##### 4.3.1.1 Reagents

Hydroquinone, p-chlorogenic acid, caffeic acid, p-coumaric acid and sinapic acid were purchased from Sigma and used as received. All other chemicals were analytical reagent grade. All solutions were prepared in NANOpure water (Sybron-Barnstead, Massachusetts) and filtered through a 0.45 µm pore size membrane filter before use.

##### 4.3.1.2 Apparatus

###### 4.3.1.2.1 Construction of the joint assembly

Fused silica capillaries with an i.d. of 50 µm and an o.d. of 360 µm were obtained from Polymicro Technologies (Arizona). A

capillary cutter (Supelco, Pennsylvania) was used to score the polyimide coating approximately 1.5 cm from the end of the capillary column. A 1 cm length of Nafion tubing of i.d. 330  $\mu\text{m}$  and o.d. 510  $\mu\text{m}$  (Perma Pure Products, NJ) was carefully threaded over the score mark. Both ends of the Nafion tubing were then sealed to the capillary column using Shell 815 epoxy resin (Mid-Con Plastics, Kansas) with 20% (v/v) triethylenetetramine. This was cured overnight. Once cured, gentle pressure was applied to either end of the Nafion tubing, causing the capillary to fracture at the score. The Nafion tube holds the capillary joint securely in place and insures correct alignment. For additional support, the joint was epoxied to a small section of glass. A schematic diagram of the joint is illustrated in Figure 4.9. It was found that the construction could be completed with a 100% success rate.

#### 4.3.1.2.2 CE apparatus

Electrophoresis in the capillary was driven by a high voltage dc (0-30 kV) power supply (Glassman High Voltage Inc., New Jersey). The anodic high-voltage end of the capillary was isolated in a plexiglas box fitted with an interlock for operator safety. A digital microampere current meter was positioned between the platinum wire ground cathode and ground. Experiments were performed at ambient air temperature (24°C). For UV work the absorbance detector described in section 4.2.1.2 was employed. Sample introduction was performed using pressure injection, which was found to be reproducible and avoided bias associated with electrokinetic injection. The injection volume was calculated in a continuous fill mode by recording the time required for the sample to reach the detector.

The Nafion joint was manipulated through two openings in opposite sides of a plastic beaker and subsequently sealed in

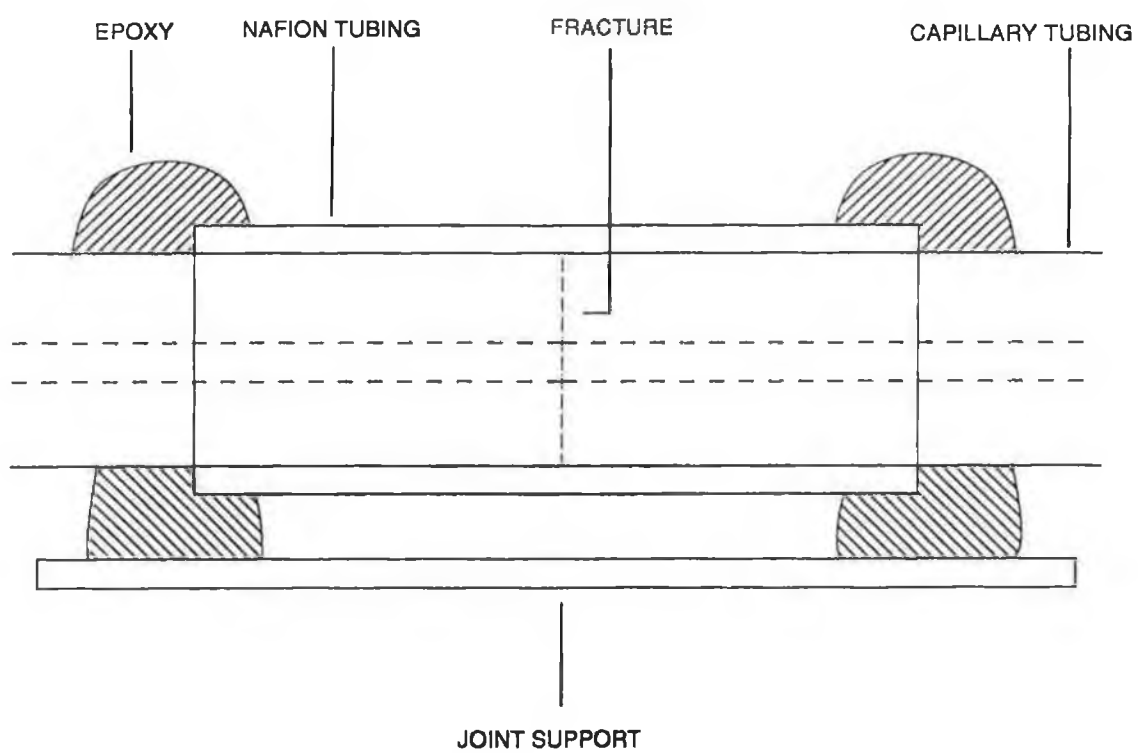


**Figure 4.9:** Schematic of the Nafion joint.

place with epoxy resin. The joint was immersed in buffer solution and this assembly served as the cathodic buffer reservoir. The detection capillary section was then inserted into the electrochemical detection cell. An illustration of the complete system is shown in Figure 4.10.

Previous investigations by Wallingford and Ewing [25] reported that the back pressure in the detection section is a significant contributor to zone broadening. However, they demonstrated that if the length is shorter than 2 cm, peak distortion is negligible. Accordingly, in this study, the Nafion joint was positioned 1.5 cm from the detection end of the column. A small section of polyimide coating was removed from the end of the detection capillary to provide better visualisation of the insertion of the microelectrode.

#### 4.3.1.2.3 Electrochemical Detection System

Cylindrical carbon fibre microelectrodes were constructed by aspiration of a 33  $\mu\text{m}$  diameter fibre (Avco Speciality Products, Massachusetts) into a pulled 1.0 mm i.d. capillary tube. The capillary tube was pulled with a vertical pipette puller (Medical Systems, New York) to a tip diameter of approximately 50 to 75  $\mu\text{m}$ . Silicone rubber adhesive was applied to the tip of the capillary where the fibre protruded. Once cured, the sealant forms an intact seal around the fibre which was found to be resistant to all buffer solutions used. In addition, due to the physical nature of the sealant, added flexibility was imparted to the fibre, which aided in the insertion of the fibre into the capillary column. The fibre was then cut to the required length, 150 to 250  $\mu\text{m}$ , using surgical scissors. Electrical contact was established via a copper wire cemented to the carbon fibre using silver epoxy.



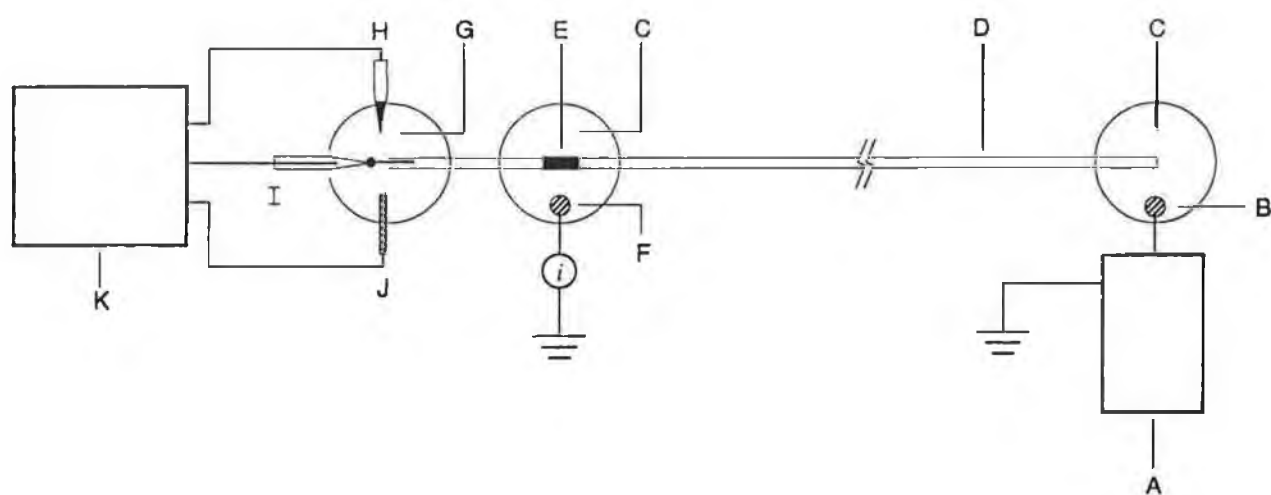


**Figure 4.10:** Schematic of the complete system: (A) high voltage power supply, (B) anode, (C) buffer reservoirs, (D) capillary column, (E) Nafion joint, (F) cathode, (G) detection cell, (H) reference electrode, (I) carbon fibre microelectrode (J) auxillary electrode, (K) amperometric detector.

The microelectrode was then mounted onto a X-Y-Z micromanipulator and positioned into the electrochemical cell. The electrochemical cell is similar to those described previously [25,40]. With the aid of an optical microscope, the microelectrode was aligned and inserted into the capillary column. The cell was operated in a three electrode configuration, with a platinum wire and a laboratory-built Ag/AgCl electrode serving as the auxiliary and reference electrodes, respectively. Electrode connections were made to a BAS Model LC-4C (Bioanalytical Systems, Indianapolis) amperometric detector. The low currents generated at the microelectrode necessitated that the electrochemical cell was shielded in a Faraday cage to reduce noise contributions from external sources.

#### 4.3.1.3 Procedures

In order to analyse the phenolic acids in apple juice, the compounds were first separated from possible interferents by passing 4 mL of juice through a Sep-Pak C<sub>18</sub> cartridge and washing the column with 10 mL of NANOpure water. A 2 mL volume of 0.01 M sodium borate solution (pH 9.25) was then used to elute the phenolic acids. Neutral phenols remained on the column. This extract was directly injected onto the column.

#### 4.3.2 RESULTS AND DISCUSSION

Several tests were performed to evaluate the Nafion joint and to characterise the effects of this modification. No substantial difference (< 1%) in the current measurement was observed between capillaries that did not contain the joint and those that had been modified when the same applied field strength and buffer were used.

No difference in electroosmotic flow was obtained when grounding was conducted either through the joint or at the detection end of the capillary column. As this experiment could not be carried out with the electrochemical detector, a UV/VIS detector was employed. Current measurements taken at both these grounded positions were essentially the same. Reproducibility of joint-to-joint construction was examined based on the measurement of electroosmotic flow for six modified columns. The percent relative standard deviation was calculated as 6.8%. No deterioration of the operation of a modified column was apparent following daily use over a two month period.

Although the Nafion joint completes the electrical circuit, the detection end of the column does not appear to be at true ground, as noise levels were found to be proportional to the applied voltage. Furthermore, when buffers were used which exhibited higher electrophoretic currents (i.e., buffers of lower resistance), detector noise was observed to increase. This has also been reported by Ewing's group [25]. In order to minimise this effect, buffers of high resistance should be employed.

#### 4.3.2.1 Linearity and Detection Limit for Hydroquinone

To ascertain the detector response using the described system, hydroquinone was chosen as the test analyte. Using 0.01 M sodium acetate buffer (pH 6.0) and a separation voltage of 425 V cm<sup>-1</sup>, linear regression analysis for concentrations ranging from  $7 \times 10^{-8}$  to  $1 \times 10^{-4}$  M provided a calibration curve with a correlation coefficient of 0.998 ( $n = 10$ ). The high separation efficiency achievable with CE was apparent, with the the number of theoretical plates calculated from the peak half-width for hydroquinone being of the order of 185,000. The detection limit for this compound was calculated from the

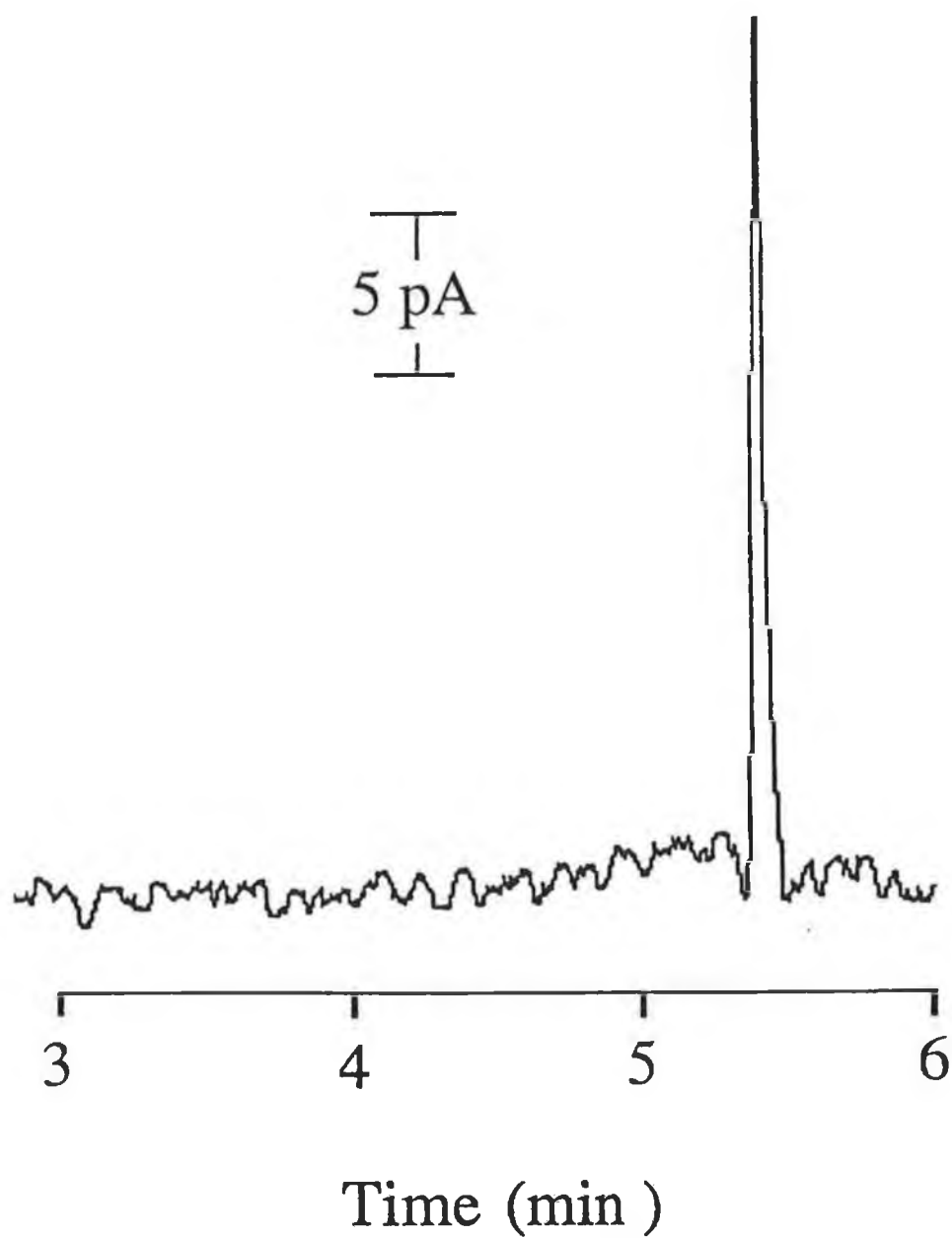


**Figure 4.11:** Electropherogram of  $7 \times 10^{-8}$  M hydroquinone. Separation conditions: 0.01 M sodium acetate buffer (pH 6.0); separation voltage, 425 V  $\text{cm}^{-1}$ ; detection potential, +750 mV vs. Ag/AgCl.

electropherogram shown in Figure 4.11 and was determined to be  $9 \times 10^{-9}$  M based on  $S/N = 3$ . From a review of literature, this is the lowest concentration limit of detection reported using CE with electrochemical detection. Using 5.8 nL as the injection volume, the detection limit corresponds to 34.8 attomoles. Percent relative standard deviations for the reproducibility of migration time and detector response for hydroquinone were 0.7% and 1.8% respectively ( $n = 8$ ).

The coulometric efficiency of the detector was also examined. This involved the determination of the quantity of charge passed through the electrochemical cell during electrolysis. Faraday's law relates the measured charge to the amount of material electrolysed:

$$N = Q (nF)^{-1} \quad (4.4)$$

where  $N$  is the number of moles electrolysed,  $Q$  is the the total charge passed,  $n$  is the number of electrons passed per molecule, and  $F$  is Faraday's constant. Insertion of a 33  $\mu\text{m}$  o.d. carbon fibre into a 50  $\mu\text{m}$  i.d. capillary column produces an annular flow width of approximately 8.5  $\mu\text{m}$ . This, and the high sensitivity obtained, are indicative of a thin-layer flow cell of high coulometric efficiency. To measure the coulometric efficiency as a function of flow velocity, a known volume of  $1 \times 10^{-4}$  M hydroquinone was injected. Different flow velocities were achieved by adjustment of the applied electrophoretic voltage between 65  $\text{V cm}^{-1}$  and 400  $\text{V cm}^{-1}$ . The coulometric efficiency could be determined by knowing the number of moles, current sensitivity, chart speed, and that the oxidation of hydroquinone involves 2 Faradays per mole. The efficiency was determined at several flow rates. The data acquired in this

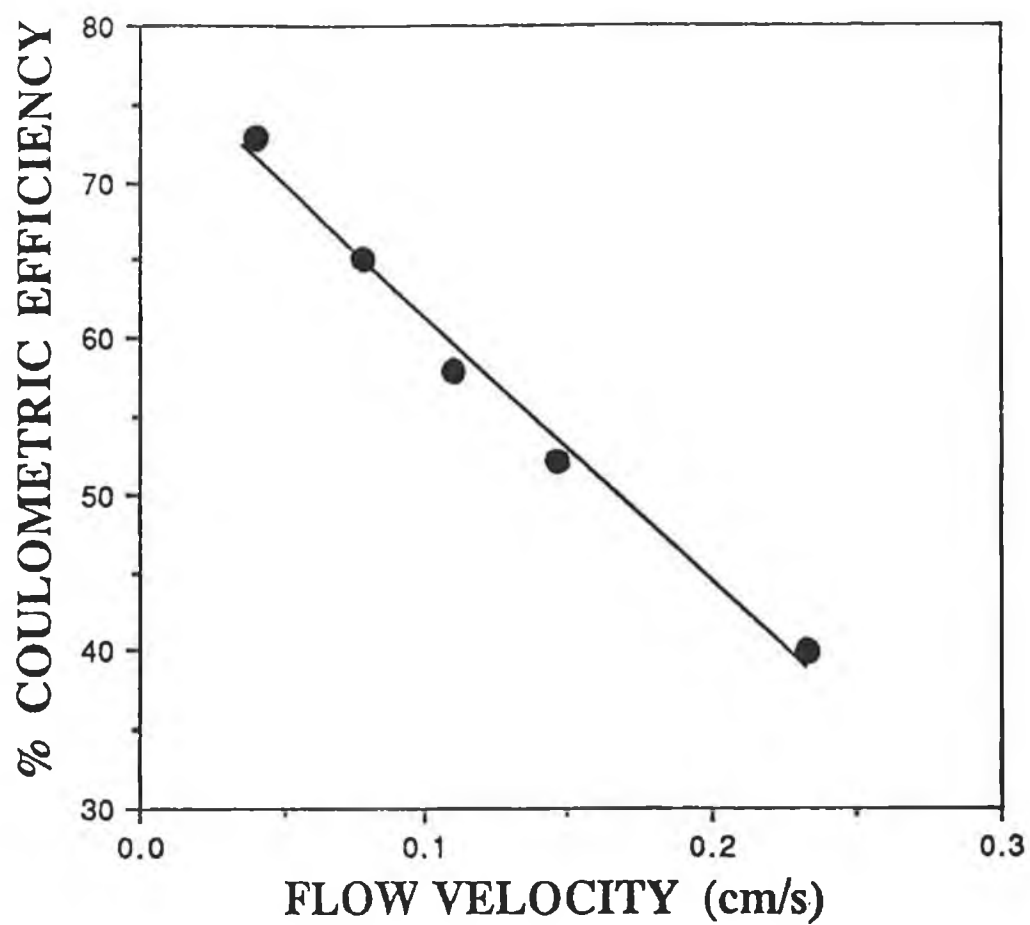


Figure 4.12: Coulometric efficiency as a function of flow velocity for  $1 \times 10^{-4}$  M hydroquinone. Separation conditions as outlined in Figure 4.11.

study is presented in Figure 4.12 and, as expected, demonstrates the high coulometric efficiencies obtained for flow rates typically utilised in CE separations.

#### 4.3.2.2 Analysis of Apple Juice

The application of this system to 'real' sample matrices was then explored. An electropherogram obtained for the apple juice extract is shown in Figure 4.13. Based on migration times, peaks A, B, and C were identified as chlorogenic acid, p-coumaric acid and caffeic acid, respectively. However, migration time is not always a reliable indicator of peak identity, particularly in CE where the sample matrix can have a considerable effect on the mobility of the sample constituents. For further verification of peak identity/purity assessment, the electrochemical detector was employed to evaluate the voltammetric behaviour of the compounds of interest. Identification of compounds during hydrodynamic voltammetry experiments is based on two characteristics of the current-potential curve of the analyte. Generally the most important feature is the  $E_{1/2}$  value of the compound, the potential where the current is half of its diffusion limited value. The  $E_{1/2}$  potential defines the potential region where the current response is most dependent on the electrode potential. An additional identifying feature is the general shape of the current-potential curve. For instance, those compounds with fast electron transfer kinetics will exhibit a dramatic increase in current response for a small change in potential. The  $E_{1/2}$  value and shape of the current-potential curve obtained with a hydrodynamic system are dependent on the experimental parameters and this dependence underlines the importance of obtaining such data under conditions identical for standards and sample compounds. Voltammetric characterisation of eluting compounds can be achieved during a series of experiments in which the

amperometric detector potential is incrementally increased.

It has been demonstrated that it is not necessary to obtain the entire voltammogram of the analyte in order to characterise sample components; the comparison of current response in the region where it changes most rapidly is sufficient [41]. To do this, the current response obtained at a potential near  $E_{1/2}$  (where the current is most dependent on potential) is ratioed to the current response at the potential where the current is no longer dependent on potential (mass transport limited value). Since each phenolic acid has a different hydrodynamic response curve in terms of voltage and shape, the ratio is unique to each compound. Current ratios have been employed extensively for voltammetric characterisation of compounds in complex samples [41-44]. In this study, the current responses for both standards and sample peaks were measured at +550, +750, and +950 mV.

Current ratios (ratioed to +950 mV) recorded are given in Table 4.3. The ratios for p-coumaric acid and caffeic acid were virtually identical to those of the sample components eluting at the same time. However, peak A and chlorogenic acid did not exhibit similar voltammetric behaviour, indicating the presence of an impurity. This was further verified when sinapic acid, another phenolic constituent of apple juice, was found to co-elute with chlorogenic acid.



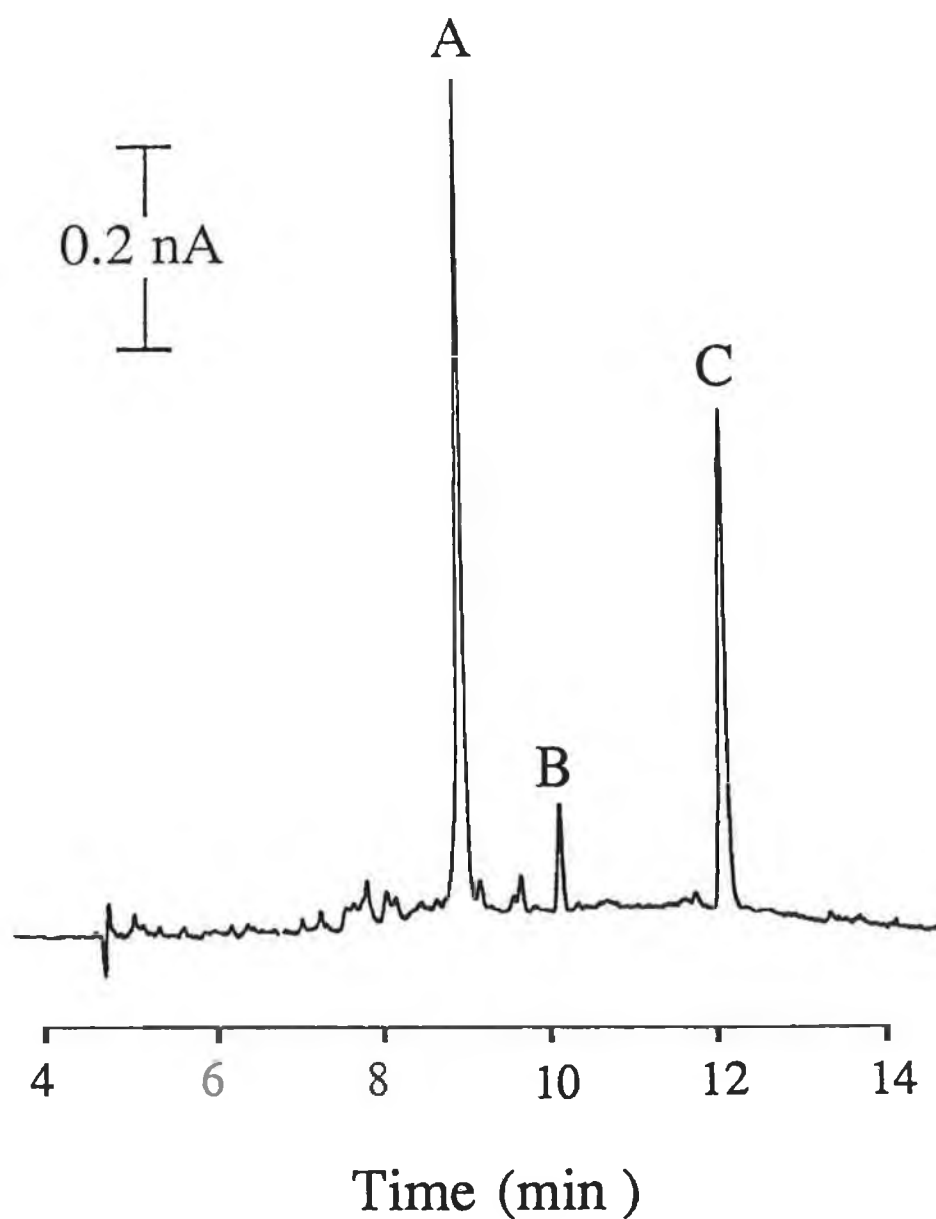


**Figure 4.13:** Electropherogram of apple juice extract. Separation conditions: 0.01 M sodium borate buffer (pH 9.5); separation voltage, 425 V cm<sup>-1</sup>; detection potential, +650 mV vs. Ag/AgCl.

Table 4.3: Voltammetric characterisation of apple juice components

Compound	Migration Time (min)	550 mV/950 mV	750 mV/950 mV
Chlorogenic acid	8.0	0.053	0.263
Peak A	8.0	0.011	0.171
p-Coumaric acid	9.0	0.026	0.246
Peak B	9.1	0.025	0.254
Caffeic acid	10.4	0.306	0.523
Peak C	10.5	0.313	0.543

#### 4.3.3 CONCLUSION

The design of an electrochemical detection system was described which is more easily constructed than those previously reported in the literature. The design was evaluated and found to be extremely durable with no adverse effects on the CE separation. The resulting system exhibited high sensitivity, with detection limits for hydroquinone in the low attomole range. An additional advantage of the electrochemical detector was also demonstrated using voltammetric characterisation which permitted the verification compound identity and purity.

The simplicity of construction of this system should make electrochemical detection for CE a more widely exploited analytical tool. The design also lends itself readily to sample collection and interfacing to other end column detectors including mass spectroscopy.

#### 4.4 REFERENCES

1. R. Virtanen, Acta. Polytech. Scand., 123 (1974) 1.
2. F.E.P. Mikkers, F.M. Everaerts and Th.P.E.M. Verhaggen, J. Chromatogr., 169 (1979) 11.
3. J.W. Jorgenson and K.D. Lukacs, Anal. Chem., 53 (1981) 1298.
4. J.W. Jorgenson, Anal. Chem., 58 (1986) 743A.
5. C.L. Rice and R. Whitehead, J. Phys. Chem., 69 (1965) 4017.
6. T.S. Stevens and H.J. Cortes, Anal. Chem., 55 (1983) 1365.
7. R.D. Smith, J.A. Olivares, N.T. Nguyen and H.R. Udseth, Anal. Chem., 60 (1988) 436.
8. S. Terabe, K. Otsuka, K. Ichikawa and T. Ando, Anal. Chem., 56 (1984) 436.
9. R.A. Wallingford and A.G. Ewing, J. Chromatogr., 441 (1988) 299.
10. S. Hjerten, J. Chromatogr., 270 (1983) 1.
11. A.S. Cohen and B.L. Karger, J. Chromatogr., 397 (1987) 409.
12. A.G. Ewing, R.A. Wallingford and T.M. Olefirowicz, Anal. Chem., 61 (1989) 292A.
13. T. Tsuda, J.V. Sweedler and R.N. Zare, Anal. Chem., 62 (1990) 2149.
14. T. Wang, J.H. Aiken, C.W. Huie and R.A. Hartwick, Anal. Chem., 63 (1991) 1372.
15. Y. F. Cheng and N.J. Dovichi, Science, 242 (1988) 562.
16. S. Wu and N.J. Dovichi, J. Chromatogr., 480 (1989) 141.
17. P. Gozel, E. Gassmann, H. Michelson and R.N. Zare, Anal. Chem., 59 (1987) 44.
18. S.L. Pontoney, X. Huang, D.S. Burgi and R.N. Zare, Anal. Chem., 60 (1988) 2625.

19. D. Rose and J.W. Jorgenson, *J. Chromatogr.*, 447 (1988) 117.
20. W.G. Kuhr and E.S. Yeung, *Anal. Chem.*, 60 (1988) 1832.
21. F. Foret, M. Deml, V. Kahle and P. Bocek, *Electrophoresis*, 7 (1986) 430.
22. X. Huang and R.N. Zare, *Anal., Chem.*, 63 (1991) 2193.
23. X. Huang, T.K. Pang, M.J. Gordon and R.N. Zare, *Anal. Chem.*, 59 (1987) 2747.
24. X. Huang, R.N. Zare, S. Sloss and E.G. Ewing, *Anal. Chem.*, 63 (1991) 189.
25. R.A. Wallingford and A.G. Ewing, *Anal. Chem.*, 59 (1987) 1762.
26. R.A. Wallingford and A.G. Ewing, *Anal. Chem.*, 61 (1989) 98.
27. R.A. Wallingford and A.G. Ewing, *Anal. Chem.*, 60 (1988) 258.
28. R.A. Wallingford and A.G. Ewing, *J. Chromatogr.*, 441 (1988) 299.
29. T.M. Olefirowicz and A.G. Ewing, *J. Chromatogr.*, 499 (1990) 713.
30. C.E. Engstrom-Silverman and A.G. Ewing, *J. Microcol. Sep.*, 3 (1991) 141.
31. *Basic Neurochemistry*, G.J. Siegal (Ed.), Raven Press, New York, 1989, pp 132.
32. *The Biochemical Basis of Neuropharmacology*, J.R. Cooper, F.E. Bloom and R.H. Roth, Oxford Press, New York, 1986, pp 125.
33. P. deMontigny, J.F. Stobaugh, R.S. Givens, R.G. Carlson, K. Srinivasachar, L.A. Sternson and T. Higuchi, *Anal. Chem.*, 59 (1987) 1096.
34. S.M. Lunte and O.S. Wong, *LC-GC*, 7 (1990) 908.
35. D.S. Burgl and R. Chien, *J. Microcol. Sep.*, 3 (1991) 199.
36. P.D. Grossman and D.S. Sloane, *Anal. Chem.*, 62 (1990) 1592.

37. E.C. Rickard, M.M. Strohl and R.G. Nielson, Anal. Biochem., 197 (1991) 197.
38. T.M. Olefirowicz and A.G. Ewing, Anal. Chem., 62 (1990) 1872.
39. X. Huang and R.N. Zare, Anal. Chem., 62 (1990) 443.
40. L.A. Knecht, E.J. Guthrie and J.W. Jorgenson, Anal. Chem., 56 (1984) 479.
41. D.A. Roston and P.T. Kissinger, Anal. Chem., 53 (1981) 1695.
42. S.M. Lunte, K.D. Blankenship and S.A. Read, Analyst, 113 (1988) 99.
43. D.A. Roston, R.E. Shoup and P.T. Kissinger, Anal. Chem., 54 (1982) 1417A.
44. C.E. Lunte and P.T. Kissinger, Anal. Chem., 55 (1983) 1458.

CHAPTER 5

CAPILLARY ELECTROPHORESIS WITH  
ELECTROCHEMICAL DETECTION OF  
MICRODIALYSIS SAMPLES FOR  
IN VIVO STUDIES.

## 5.1 INTRODUCTION

One of the main advantages of CE is its capability of handling picolitre to nanolitre volumes. This has been exploited by Ewing's group [1], which have used CE with electrochemical detection to study biological environments such as single cell cytoplasm. Sampling of the cytoplasm was accomplished by insertion of the high voltage end of the electrophoresis capillary into a single nerve cell. This end of the capillary was etched with hydrofluoric acid to form a microinjector for obtaining samples of cytoplasm. The technique has the possibility of being applied to the investigation of hormone levels, intracellular messenger concentrations, and general metabolism, as well as the study of the immune system at the single cell level.

Another application, where the small sample volume requirement should prove advantageous, is the coupling of CE with microdialysis sampling. Microdialysis sampling, the subject of a recent review [2], is a new technique for the *in vivo* study of pharmacokinetics, drug metabolism and neurochemical processes. The concept of microdialysis originated in the early 1970's, but it has only seen widespread application recently, as a result of the commercial availability of microdialysis probes [3]. The technique is accomplished by insertion of a microdialysis probe into a living system. A variety of probe geometries are commercially available, and a common design of such is illustrated in Figure 5.1. The body of the probe is usually constructed of a stainless steel needle tubing, fused silica or a combination of the two. The dialysis membrane through which low molecular weight substances can easily diffuse are generally composed of polycarbonate, polyacrylonate and regenerated cellulose. A fluid, known as the perfusion medium,

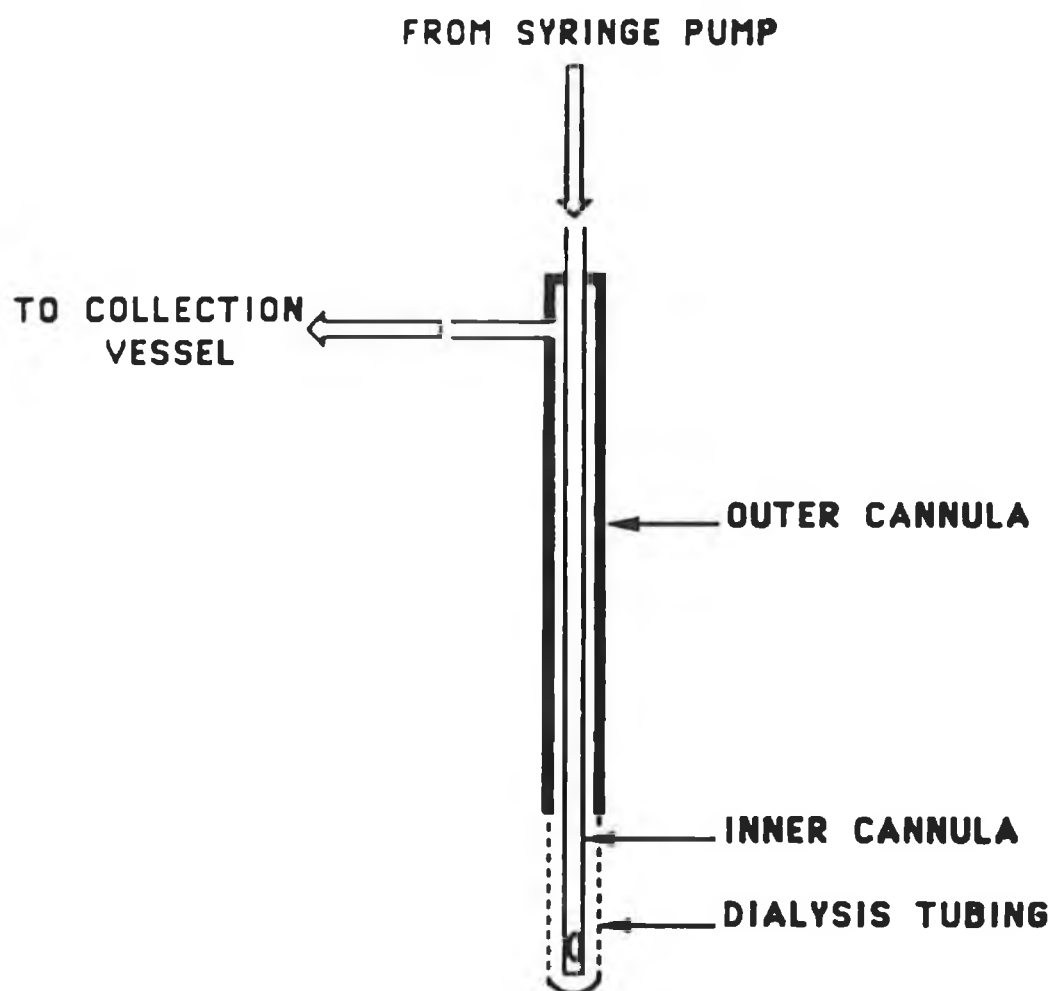


Figure 5.1: Schematic diagram of a cannula-type microdialysis probe.



whose macroscopic composition closely resembles that of the extracellular space, is pumped through the probe. Ideally, the ionic strength and pH of the perfusion medium will match those of the extracellular space. Ringer's solution is therefore commonly used. A precisely controlled flow rate allows chemicals to be predictably introduced into or removed from the extracellular space by establishment of a diffusional steady state across the membrane wall. A typical microdialysis experimental system is illustrated in Figure 5.2.

Microdialysis provides several advantages over conventional techniques which typically involve blood sampling. Large protein molecules are excluded from crossing the dialysis membrane. Therefore, microdialysis samples are amenable to direct analysis with no deproteinisation step required. In vitro enzymatic reactions are also eliminated, as enzymes are excluded from crossing the membrane. As there is no net fluid exchange, continuous collection for long periods of time with no change in blood volume is possible. Additionally, in pharmacokinetic studies, only the pharmacologically significant free fraction of a drug is sampled because protein-bound drug is also excluded from diffusing across the dialysis membrane.

The microdialysis process competes with or supplements other experimental protocols such as cell culturing, tissue slicing, tissue homogenising and conventional sampling of biological fluids (including blood, urine and spinal, lymphatic and ocular fluids). The fact that no fluid is removed from or introduced into the system is especially advantageous. In addition, it is possible to monitor multiple analytes by coupling other analytical techniques to the microdialysis system. With these systems the dialysis probe can be rapidly employed for a variety of analytes; there is no need to engineer a new probe for each one.

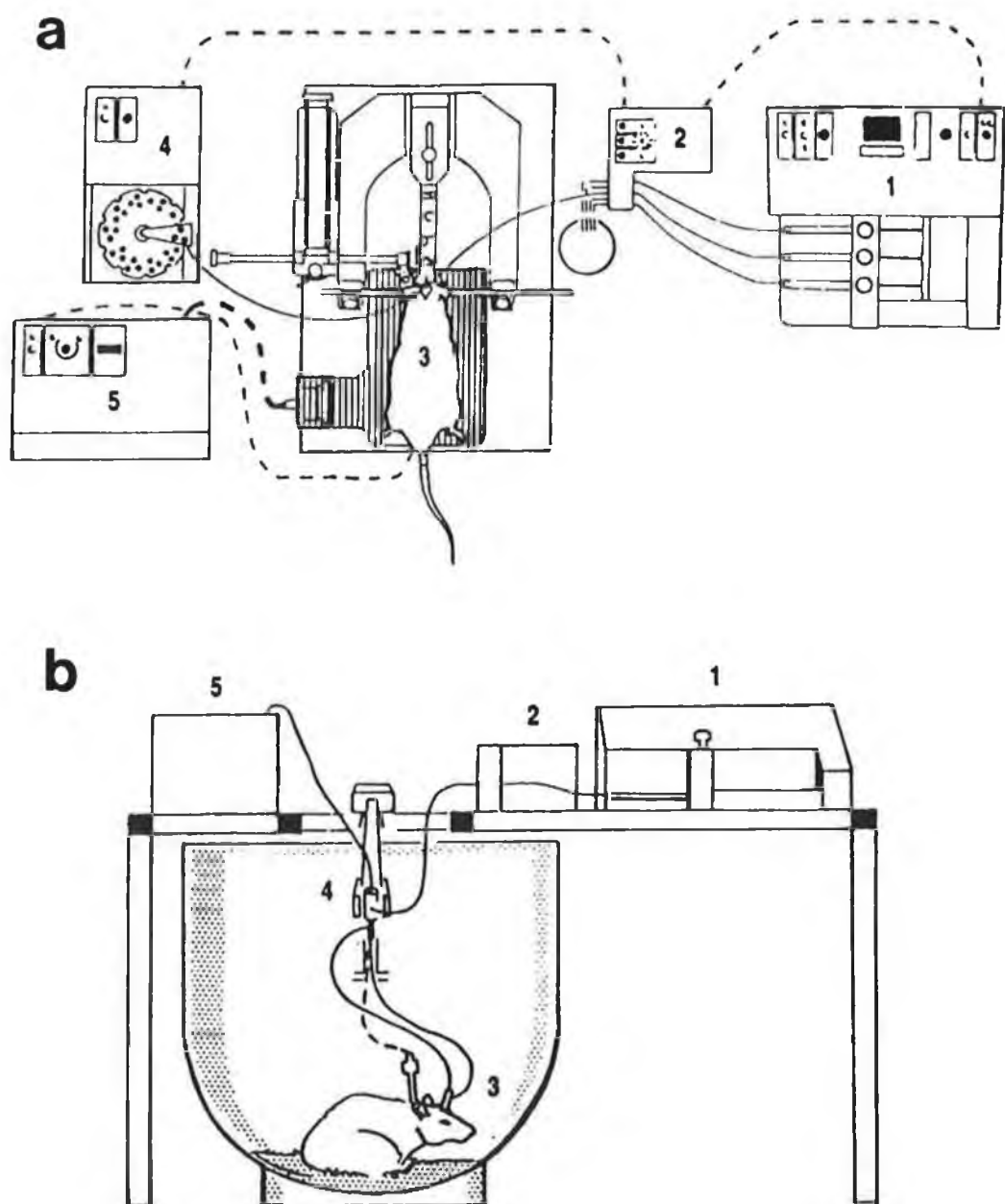


**Figure 5.2:** Schematic diagram of a microdialysis system illustrating the setup for (a) anaesthetised animals, and (b) conscious, freely moving animals. (1) microinjection pump, (2) syringe selector, (3) microdialysis probe, (4) microfraction autosampler, (5) temperature controller.

A microdialysis probe can be utilised not only for sampling but also for the administration of a compound. By using the probe for both dosing and sampling, a specific area of an organ can be dosed and the localised effect within that area can be studied. Alternatively, an animal may be given a systematic dose of a compound and microdialysis probes can be placed concurrently in various tissues to examine the distribution and varying effects of the compound.

The greatest number of applications reported using this technique, to date, involves neurochemical studies, but more recently it has been recognised as a powerful new technique for the study of in vivo pharmacokinetics and the metabolism of drugs.

#### 5.1.1 Neurochemical Applications

The requirement for an in vivo technique for the study of neurochemical events has always generated a high level of interest. In 1974, Ungerstedt and Pycock [5] developed a hollow dialysis fibre mounted on a steel cannula. This probe was implanted in the brain tissue to analyse neurotransmitter release in vivo. At the time of these first microdialysis experiments, analytical techniques capable of detecting low concentrations of endogenous neurotransmitters (picomole range) were almost non-existent. For example, to perform experiments involving the dopamine system in the brain, the tissue had to be preloaded with a radioactively labeled compound to enable detection. By the end of the 1970's, sensitive LC methods for the determination of neurotransmitter substances had been developed. This made it possible to study many different events in the extracellular fluid of the central nervous system. The neurotransmitters dopamine, DOPAC, serotonin and

norepinephrine, and the amino acids aspartate, glutamate, glutamine, serine, taurine and GABA, have all been extensively investigated in vivo using microdialysis, with analysis being predominately performed by LC. The neurochemical applications of microdialysis have been thoroughly reviewed [4,6].

#### 5.1.2 Pharmacokinetics and Drug Metabolism

The pharmacokinetics of a drug are typically determined by the administration of a known dosage and the withdrawal of blood samples at timed intervals. The samples are then analysed for the drug of interest to derive a concentration-time curve. This approach presents several problems in terms of both the determination of the drug concentration in the blood and the pharmacokinetic parameters derived from the data. Removal of blood results in a decrease in total blood volume which may lead to alterations in the observed distribution and elimination of a drug. To minimise this loss, the sampling frequency may be reduced; however, this results in a loss of temporal resolution and subtle changes in the concentration-time curve may be lost. Whole blood samples are also difficult to analyse as they contain protein. This requires a sample preparation step for protein removal which typically leads to a release of protein-bound drug. Therefore, pharmacokinetic parameters derived will correspond to total drug concentration and not the more meaningful free drug concentration.

Lunte's research group [7,8] first demonstrated the utility of microdialysis sampling for pharmacokinetic studies, of acetaminophen and its sulphate and glucuronide metabolites. Well defined kinetic curves were presented from which the pharmacokinetic parameters were derived. Also demonstrated was the use of simultaneous sampling using multiple dialysis probes to determine the relative rates of clearance from various

organs. In further research [9], they investigated the pharmacokinetics of acetylsalicylic acid (ASA) using microdialysis. This drug presents a particularly difficult problem for pharmacokinetic determinations as it is rapidly metabolised to salicylic acid in the blood. ASA is hydrolysed by enzymes in the blood, so that simply removing the sample from the animal does not stop metabolism. In order to minimise these reactions continuing in vitro, special precautions have been employed. However, these procedures are all operator intensive, complicate the analytical procedure, and are less than completely effective. Using microdialysis sampling it was demonstrated that this complication was eliminated, as the enzymes involved in ASA metabolism are excluded from the microdialysis samples.

Scott and co-workers [10] used in vivo microdialysis for the study of the hepatic metabolism of phenol. Xenobiotic metabolism is generally studied using preparations which may not reflect actual in vivo metabolism. In vitro tissue incubations can provide information about early metabolic steps but can be perturbed by the necessity of artificially providing components of the system lost during sample preparation. In many cases, compartmentalisation of the cells is lost in sample preparation which can lead to profound effects on the observed metabolism. Additionally, no insight into interaction between organs can be obtained on experiments on isolated organs. Using in vivo microdialysis, it was demonstrated how this technique offered a promising alternative for the study of xenobiotic metabolism. Because the integrity of the biological system is maintained and endogenous levels of cofactors are used, such experiments more accurately reflect actual metabolic reactions from exposure to xenobiotics. Indeed, in their investigation, considerable differences were reported between in vivo and in vitro experiments.

This chapter will present in two sections the application of microdialysis sampling coupled to CE with electrochemical detection. The first study involves a pharmacokinetic study of the drug L-dopa. The second is a neurochemical analysis of amino acid neurotransmitters.

## 5.2 PHARMACOKINETIC STUDY OF L-DOPA BY MICRODIALYSIS SAMPLING COUPLED TO CAPILLARY ELECTROPHORESIS WITH ELECTROCHEMICAL DETECTION

L-dopa is used in the treatment of Parkinson disease, in which the symptoms are related to the depletion of striatal dopamine. L-dopa is the levorotary isomer of dihydroxyphenyl-alanine (dopa) which is a metabolic precursor of dopamine. This drug can cross the blood-brain barrier where it is subsequently metabolised to dopamine. Long term treatment with the drug is associated with a variety of untoward effects, including 'end of dose' hypokinesia or wearing-off phenomenon, dyskinesia and dystonia. Investigations into the pharmacokinetic behaviour of L-dopa have greatly contributed to the understanding of these response fluctuations. Age related delayed gastric emptying, dietary factors, and variable transit time are some of the contributory factors to the decreased bioavailability of the drug leading to unpredictable patterns of motor fluctuation [11]. The bioavailability of L-dopa is not routinely evaluated for individual patients as yet because of the lack of fast, reliable and sensitive assays required during long-term monitoring periods. Recently, a report has been published which describes a method for the *in vivo* monitoring of L-dopa using microdialysis and LCEC [12]. However, the method suffers from poor temporal resolution, and dialysate samples must be diluted to yield usable quantities for LC analysis. The purpose of the present study was to demonstrate the increased temporal resolution achievable using CE analysis.

### 5.2.1 EXPERIMENTAL

#### 5.2.1.1 Reagents

L-dopa and alpha-methyldopa were purchased from Sigma and used as recieved. All other chemicals were of analytical reagent grade. All solutions were prepared in NANOpure water and passed through a membrane filter (0.2  $\mu\text{m}$  pore size) before use. Stock solutions of the standards were prepared in 0.05 M HCl containing 0.1%  $\text{Na}_2\text{S}_2\text{O}_5$  and 0.02%  $\text{Na}_2\text{EDTA}$ . Subsequent working dilutions were prepared in a Ringer's solution consisting of 155 mM NaCl, 5.5 mM KCl and 2.3 mM  $\text{CaCl}_2$ .

#### 5.2.1.2 Apparatus

##### 5.2.1.2.1 CE System

The system used is the same as described in chapter 4, section 4.3.1.2.2. A separation voltage of 30 kV and a column length of 75 cm was used. A 0.01 M borate buffer, pH 8.3, was used in all experiments. The detection potential was operated at +800 mV vs. Ag/AgCl.

##### 5.2.1.2.2 Cyclic Voltammetry

Cyclic voltammetry experiments were conducted in a three electrode cell configuration using a Cypress Model CYSY-1 computerised electrochemical analyser (Cypress Systems, Kansas).

##### 5.2.1.2.3 Microdialysis System

Microdialysis was carried out using a Carnegie Medicine microinjection pump (BAS) coupled to a flexible dialysis probe. The construction of the probe (Figure 5.3) has been described

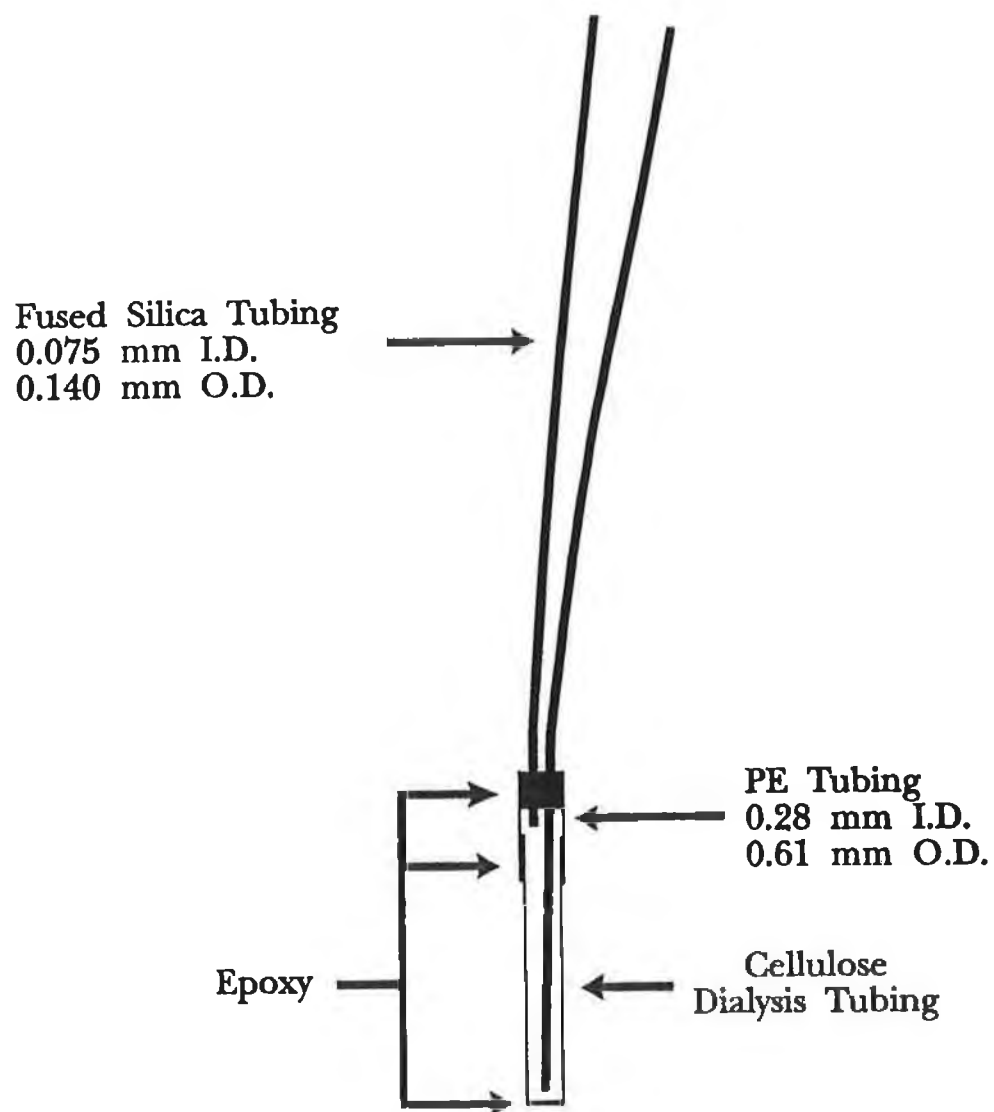


**Figure 5.3:** Schematic diagram of the flexible microdialysis probe and parallel i.v. cannula.



elsewhere [13]. The dialysis tubing used was regenerated cellulose fiber of 232  $\mu\text{m}$  i.d. and 250  $\mu\text{m}$  o.d. and molecular weight cut-off of 5,000 daltons (Dow Chemicals, Michigan). A cannula of PE-10 tubing was inserted parallel to the dialysis probe for the i.v. administration of L-dopa. This cannula was inserted such that it did not overlap the dialysis membrane.

#### 5.2.1.3 Procedures

##### 5.2.1.3.1 Microdialysis Probe Characterisation

In order to determine the in vivo concentration of amino acids giving rise to the concentrations detected in the perfusion medium, it was necessary to know the recovery of the dialysis probe. The recovery is defined as 'the ratio of the analyte concentration measured in the dialysate to the actual concentration of the analyte in the sample solution'. Determination of the recovery was performed by placing the dialysis probes in a standard solutions of L-dopa. The probe was then perfused at 1  $\mu\text{L min}^{-1}$  and samples of the perfusate collected and analysed. Recoveries were determined from several standards over the range 0.1 to 100  $\mu\text{g mL}^{-1}$  in Ringer's solution, which has been shown to provide the same results as calibration in whole blood [14]. The average recovery for L-dopa was  $31.5 \pm 4.3\%$  ( $n = 12$ ) and was independent of concentration. The recovery of the probe was determined both before and after implantation, and no substantial difference ( $< 6\%$  relative standard deviation) was obtained.

##### 5.2.1.3.2 In Vivo Pharmacokinetic Experiments

Male Sprague-Dawley rats weighing 0.37 to 0.45 kg and approximately 5 months old were used. The rats were anaesthetised with the inhalation of the anesthetic isoflurane,

which does not affect renal or hepatic function. Surgery for the insertion of the probe and cannula into the jugular vein has been previously described [13]. The rats were then placed in an awake animal system (CMA/BAS) which allows the animal full freedom of motion.

The implanted dialysis probe was perfused with Ringer's solution at a rate of  $1 \mu\text{L min}^{-1}$ . Dialysis samples were collected over 5 minute intervals. Blanks were collected for 1 hour. The animals were then given an i.v. bolus administration of 0.5 mL of L-dopa solution through the cannula. The injection solution was prepared by appropriately diluting a  $100 \text{ mg mL}^{-1}$  solution of L-dopa in 0.1 M HCl solution to give a dose of  $25 \text{ mg kg}^{-1}$ . Dialysis sampling was continued for at least 3 hours after administration of L-dopa.

#### 5.2.1.3.3 Electrochemical Pretreatment

The microelectrode was subjected to electrochemical pretreatment, which was achieved using a 50 Hz square-wave waveform of a 2 V amplitude. These parameters were optimised in the manner described in chapter 3. The pretreatment was accomplished using a function generator connected to the external input of the BAS LC-4C amperometric detector. An oscilloscope was used to monitor the voltage and frequency of the applied waveform. Using this arrangement, pretreatment could be performed without removing the the microelectrode from the capillary column. Pretreatment was carried out while buffer was flowing past the electrode surface.

## 5.2.2 RESULTS AND DISCUSSION

### 5.2.2.1 Electrochemical Pretreatment

As discussed in Chapter 3, electrochemical pretreatment is known to have a pronounced effect on the electron transfer properties of many solution species; in particular, enhancement of the electrochemical response. Cyclic voltammetry was used to examine the voltammetric response of a carbon fibre microelectrode to the oxidation of L-dopa prior to and following the electrochemical regime described in the Experimental Section. The results obtained for these experiments are illustrated in Figure 5.4. As can be observed, no response for L-dopa was obtained at the untreated electrode (Figure 5.4A), in contrast to the well-defined curve obtained following pretreatment (Figure 5.4B). Following multiple scans, the response was found to diminish, which is indicative of electrode fouling. The effect is illustrated in Figure 5.4C which shows the fifth voltammogram recorded after electrochemical pretreatment had been performed.

Experiments were then carried out to investigate whether electrochemical pretreatment between each measurement of L-dopa would result in a reproducible response. Figure 5.5A shows the result for several measurements of  $25 \mu\text{g mL}^{-1}$  injections of L-dopa. A rapid decrease over 5 injections was observed. However, if the pretreatment was applied between each successive injection, a reproducible response was obtained, as illustrated in Figure 5.5B. The optimum duration of the pretreatment was investigated. For 15, 30, 60 seconds duration, the RSD ( $n = 6$ ) for a concentration of  $25 \mu\text{g mL}^{-1}$  was 1.93, 1.35 and 1.36 % respectively. For further experiments, a 30 second application of the pretreatment was employed.

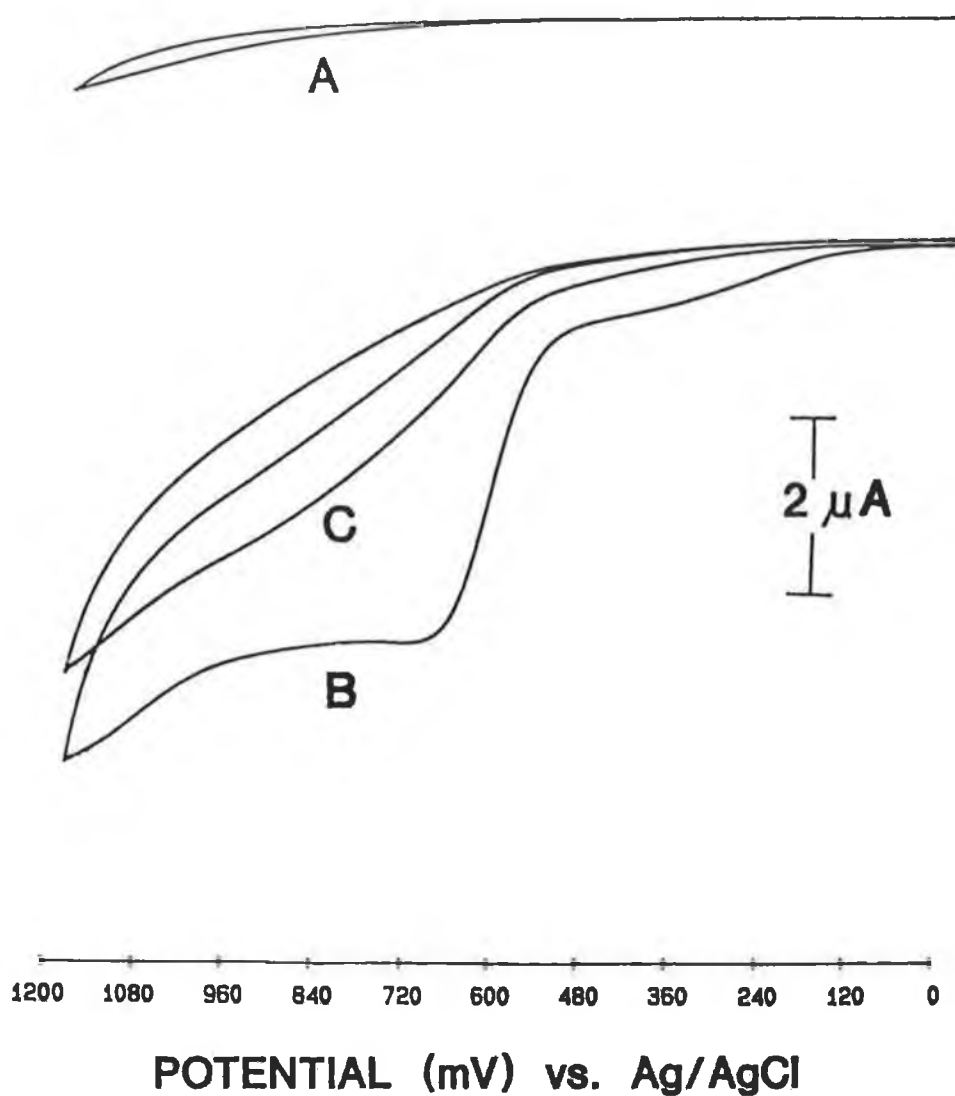


**Figure 5.4:** Cyclic voltammograms of  $8 \times 10^{-4}$  M L-dopa in 0.1 M borate buffer (pH 8.3). (A) Response at untreated microelectrode; (B) response at electrochemically pretreated microelectrode; (C) fifth voltammogram obtained after pretreatment.

#### 5.2.2.2 Linearity and detection limit

A calibration curve prepared over the range  $5.08 \times 10^{-8}$  ( $10 \text{ ng mL}^{-1}$ ) to  $6.1 \times 10^{-4} \text{ M}$  ( $120 \mu\text{g mL}^{-1}$ ) resulted in a correlation coefficient of 0.9998 ( $n = 9$ ). Peak areas of L-dopa standards, rather than peak heights were utilised which avoided inaccuracy from variation in migration time between standards and samples. The limit of detection was calculated from the electropherograms of  $10 \text{ ng mL}^{-1}$  L-dopa and was determined to be  $3 \times 10^{-8} \text{ M}$  ( $5.91 \text{ ng mL}^{-1}$ ) based on a  $S/N = 3$ . This limit of detection is lower than previous values reported in the literature for the determination of L-dopa using LCEC [12,15-18]. Using 7.8 nL as the injected volume, the mass detection limit corresponds to 234 amol. Wallingford and Ewing [18] reported a detection limit of  $2.2 \times 10^{-6} \text{ M}$  or 39 amol for L-dopa using CE with electrochemical detection. For that study, a 9  $\mu\text{m}$  i.d. capillary column was used for the CE analysis, which results in a lower mass detection limits but suffers from higher concentration detection limits.

As the microdialysis probe recovers only 31.5% of the concentration of L-dopa in the extracellular fluid, the limit of quantitation of the drug from dialysis samples was  $12.5 \text{ ng mL}^{-1}$  blood. Standards of L-dopa were analysed periodically between dialysate samples to ensure that the detection response remained reproducible over the course of the pharmacokinetic experiment.

#### 5.2.2.3 Electrophoretic Analysis of Dialysis Samples

Typical electropherograms of blood dialysate obtained by the in vivo microdialysis sampling are shown in Figure 5.6. Dialysis samples were amenable to direct injection onto the capillary column. A blank obtained prior to dosing of the animal with

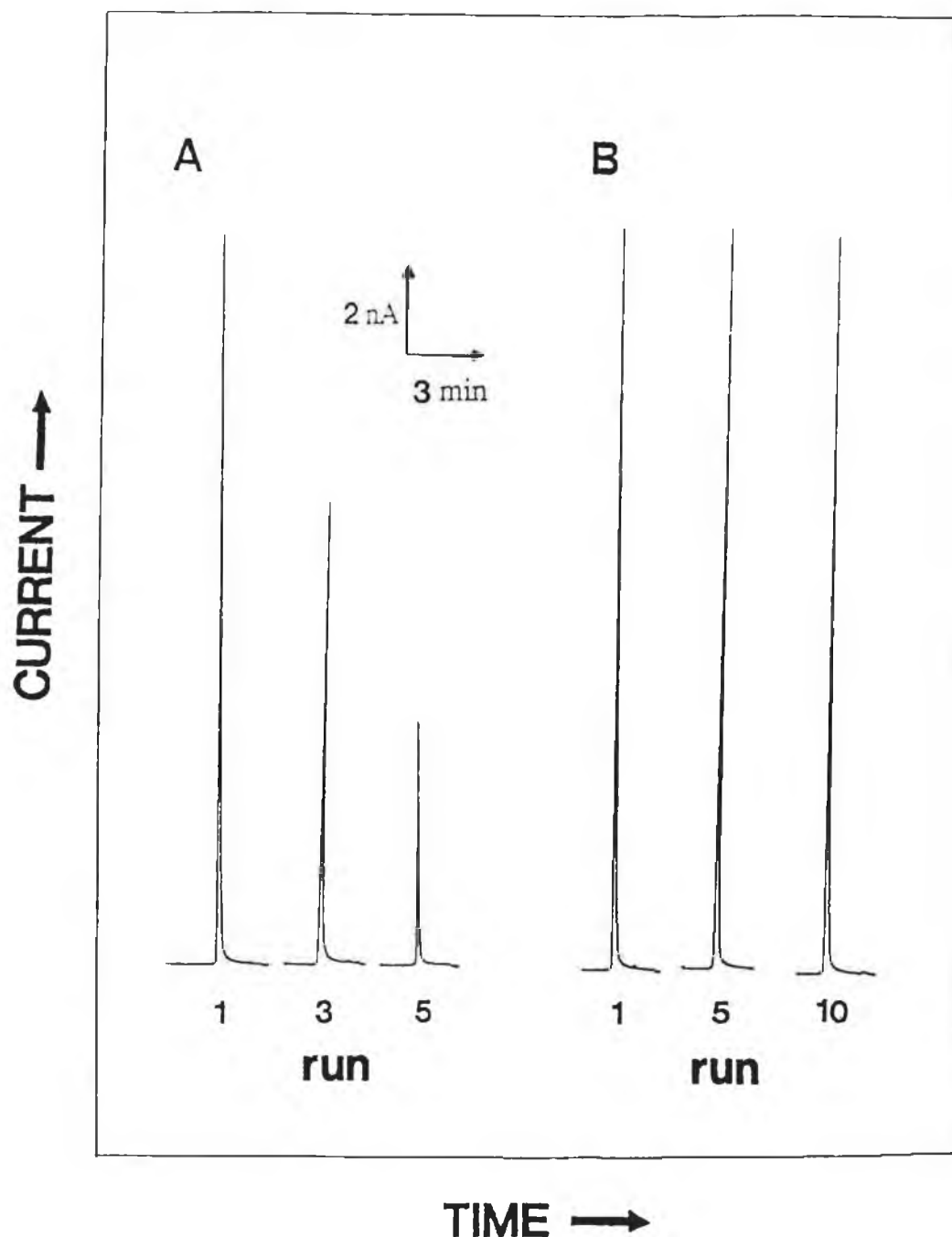


**Figure 5.5:** Electropherograms of  $25 \mu\text{g mL}^{-1}$  L-dopa. Separation conditions: 0.01 M borate buffer (pH 8.3); voltage, 30 kV; column length, 75 cm; detection potential, +800 mV vs. Ag/AgCl. (A) Electropherograms of successive injections (1,3,5) of L -dopa; (B) electropherograms of successive injections (1,3,5) with intermediate pretreatment.

L-dopa is shown in Figure 5.6A and, as illustrated, no interference occurs in the region of the L-dopa elution. Figure 5.6B shows the electropherogram obtained 5 minutes after i.v. administration of L-dopa. The L-dopa peak is fully resolved in just over 10 minutes.

#### 5.2.2.4 Voltammetric Characterisation

While the preliminary identification of L-dopa in the perfusate was based on its migration time, as stated in the previous chapter, this is not always a reliable indicator of peak identity. Therefore, to further verify the identification/purity of L-dopa in the dialysate, the electrochemical detector was employed to evaluate the voltammetric behaviour of this compound. The current ratios were calculated by measurement of the responses at 500 and 650 mV (where the current is the most dependent on potential) which were ratioed to the response obtained at 800 mV (mass transport-limited value). Electropherograms, at these detection potentials, of a dialysis sample obtained 40 minutes after administration of L-dopa are shown in Figure 5.7. The resulting current ratios are listed in Table 5.1.

The ratios for the dialysis sample peak 2, and the authentic L-dopa are virtually identical, confirming its identity. Alpha-methyldopa is one of the major metabolites of L-dopa and has been linked to a possible cause of hypokinesia [19] and to 'off-periods' [20] in patients with Parkinson's disease. Its determination, therefore, could provide useful information in the study of L-dopa treated patients. Based on its migration time, peak 1 (Figure 5.7) was tentatively identified as alpha-methyldopa. To further confirm its identity, the dialysate sample was spiked with alpha-methyldopa and peak 1 was observed to increase. However, on examination of the results obtained

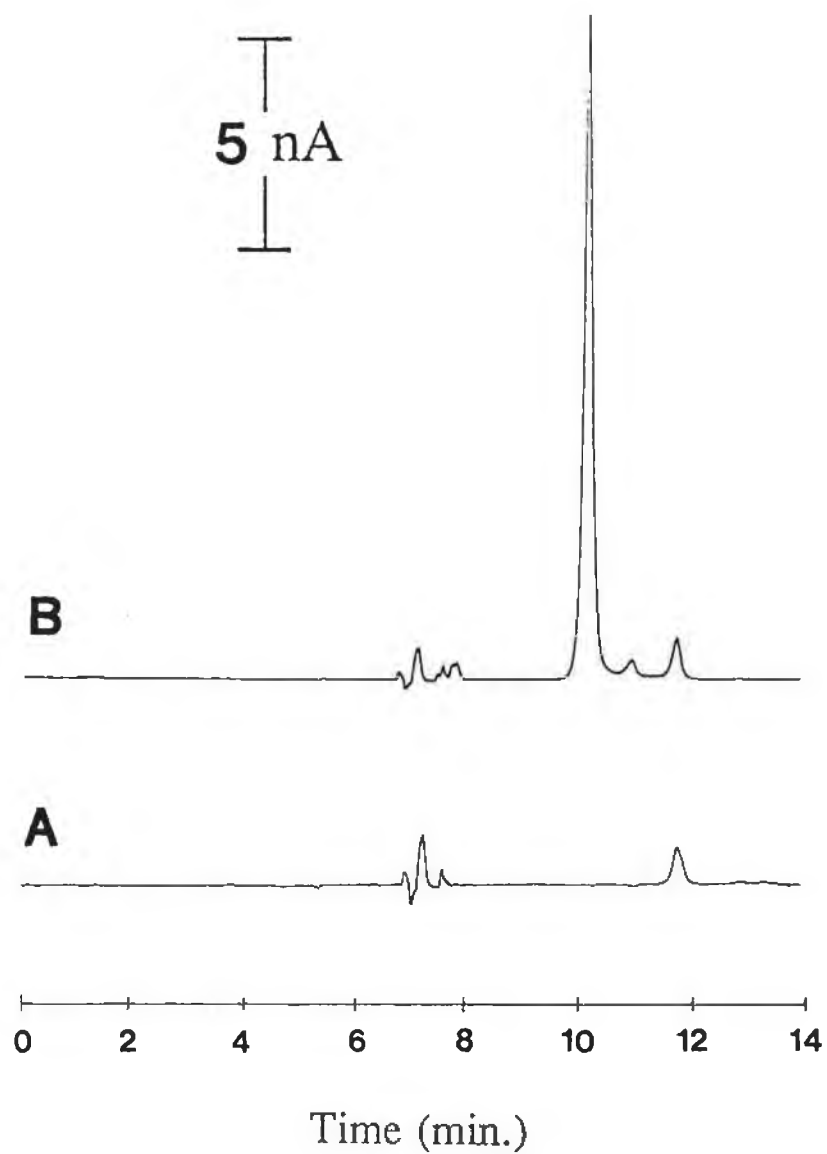


**Figure 5.6:** Typical electropherograms of i.v. microdialysis samples. (A) Blank prior to dosing; (B) 5 minutes after a 25 mg mL<sup>-1</sup> i.v. dose of L-dopa. Separation conditions as outlined in Figure 5.5.



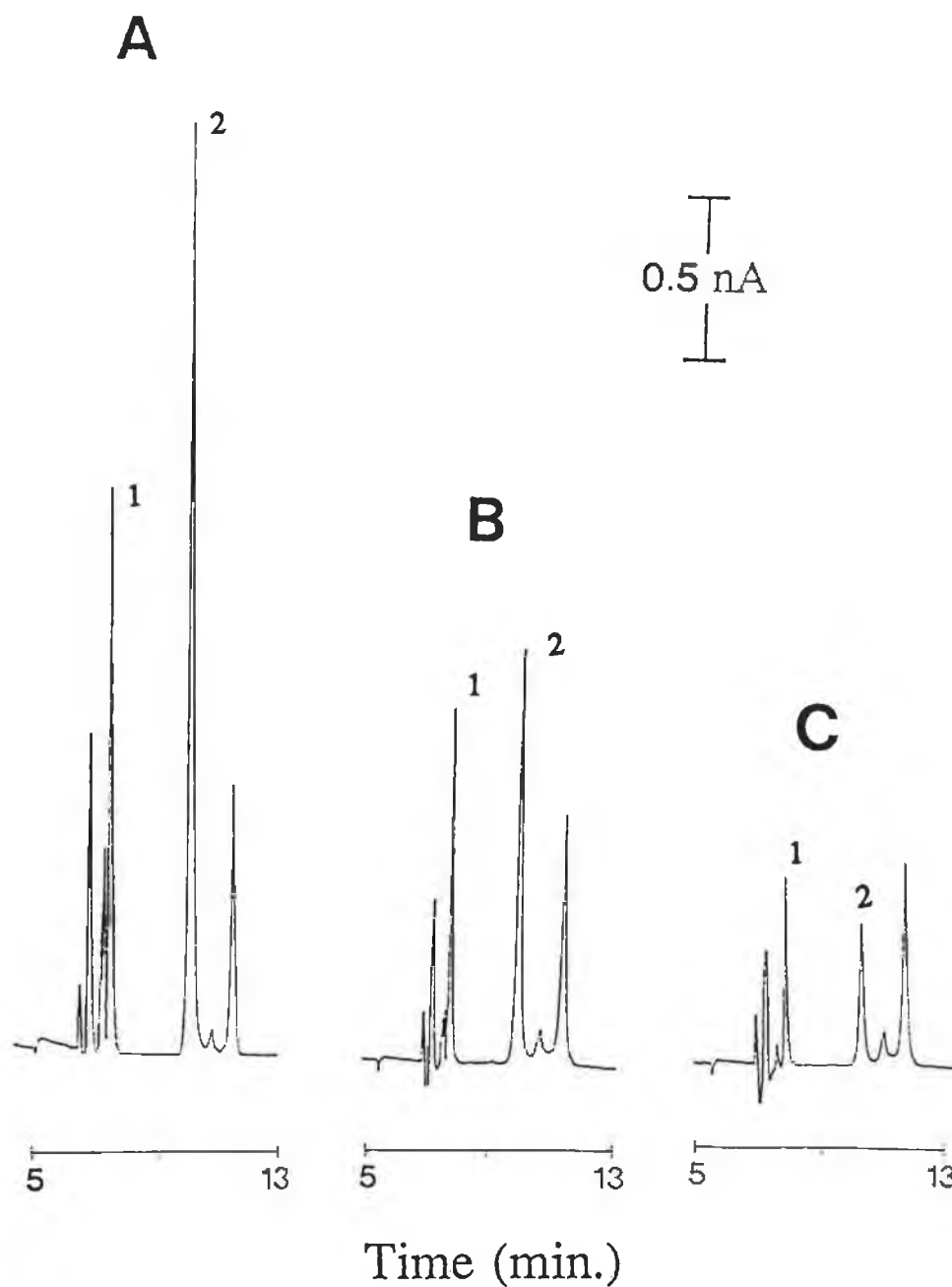
from the voltammetric characterisation (Table 1), the current ratios for the standard alpha-methyldopa and peak 1 were significantly different. It may be assumed from a lack of a peak in the blank prior to L-dopa administration that peak 1 is due to alpha-methyldopa and another co-eluting metabolite of L-dopa.

Table 5.1: Voltammetric Characterisation

Component	Current Ratios	
	+500 mV/+800 mV	+650 mV/+800 mV
Peak 1	0.26	0.63
alpha-methyldopa	0.19	0.52
Peak 2	0.23	0.44
L-dopa	0.24	0.43

#### 5.2.2.5 Pharmacokinetic Experiments

In vivo microdialysis samples were continuously collected for at least three hours after administration of L-dopa. From these samples the concentration-time profile was developed and pharmacokinetic parameters calculated. The in vivo concentration of L-dopa was calculated by determining the concentration in the dialysate from a calibration curve and then adjusting for the



**Figure 5.7:** Electropherograms of the dialysate, obtained 40 minutes after administration of L-dopa, used for the voltammetric characterisation study. Separation conditions as outlined in Figure 5.5, except for the detection potential (A) +800 mV, (B) +660 mV, and (C) +500 mV vs Ag/AgCl.

recovery of the microdialysis probe. A typical concentration curve is presented in Figure 5.8. The data was fitted to an exponential representing first-order elimination kinetics of the form:

$$C(t) = Ae^{-\alpha t} + Be^{-\beta t} \quad (5.1)$$

using a non-linear least-squares fit. The elimination half life was determined from the elimination rate constant ( $\beta$ ) and found to be  $10.3 \pm 1.1$  minutes ( $n = 4$ ). This is lower than the approximate 15 minutes reported by Leppert et al. [17]. However, their experiments were performed on anaesthetised rats, which may have resulted in slower elimination than in awake, freely moving rats.

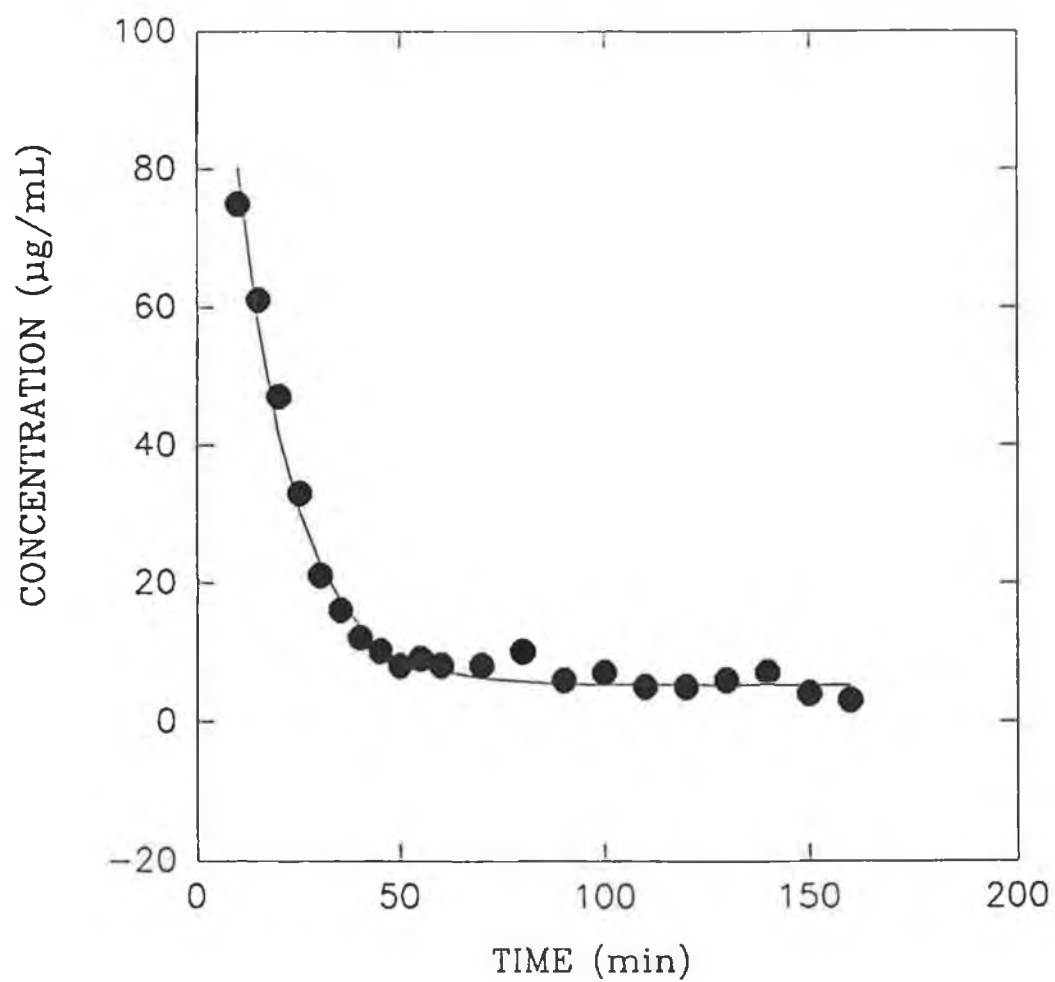


**Figure 5.8:** Concentration vs. time profile for a  $25 \text{ mg kg}^{-1}$  dose of L-dopa in an awake, freely moving rat.

### 5.3 NEUROCHEMICAL APPLICATION OF MICRODIALYSIS SAMPLING COUPLED TO CAPILLARY ELECTROPHORESIS WITH ELECTROCHEMICAL DETECTION

In this study, microdialysis sampling and CE with electrochemical detection was employed for the continuous monitoring of amino acids in the brain. The ability of the probe to sample a tissue, as well as to deliver a test compound to the tissue, is demonstrated by the  $K^+$ -induced stimulation of excitatory amino acid release. The procedure described in chapter 4 for the determination of the major NDA-labeled amino acids involved in neurotransmitter roles using CE with UV detection was the preliminary study investigated to ascertain the feasibility of this project. The detection limits obtained with this technique were sufficient for the analysis of a brain homogenate; however, a more sensitive technique is required for the detection of the levels found in brain dialysate.

#### 5.3.1 EXPERIMENTAL

##### 5.3.1.1 Reagents

All amino acids were purchased from Sigma and used as received. NDA was supplied by Oread Laboratories. Sodium cyanide and sodium borate were obtained from Fisher Scientific. Solutions were prepared in NANOpure water and passed through a membrane filter (0.2  $\mu$ m pore size) before use.

10 mM sodium borate solutions, amino acid stock solutions (5 mM) and sodium cyanide ( $1 \times 10^{-3}$  M) were prepared in NANOpure water. Stock solutions of NDA ( $1 \times 10^{-3}$  M) were prepared in acetonitrile. The Ringers solution consisted of 147 mM NaCl, 4.0 mM KCl and 2.3 mM  $CaCl_2$ . For potassium-evoked overflow, a Ringer's solution of 51 mM NaCl, 2.3 mM  $CaCl_2$  and 100 mM KCl was used.

### 5.3.1.2 Apparatus

#### 5.3.1.2.1 CE System

The CE system is the same as described in chapter 4, section 4.3.1.2.2. A separation voltage of 30 kV and a column length of 1 m were used for all separations. The capillary columns were obtained from Polymicro Technologies and were 50  $\mu\text{m}$  i.d. and 360  $\mu\text{m}$  o.d.. The operating buffer was 0.02 M borate (pH 9.0). The detection potential was operated at +800 mV vs. Ag/AgCl.

#### 5.3.1.2.2 Cyclic Voltammetry

Cyclic voltammetry experiments were conducted using the instrumentation described in section 5.2.1.2.2. For these studies, excess amino acid was employed in the derivatisation step to prevent interference from any impurities or side reactions.

#### 5.3.1.2.3 Microdialysis System

Microdialysis sampling was performed using a Sage Instruments syringe pump coupled to a BAS/Carnegie Medicine 4 mm dialysis fibre probe in the brain and a catheter in the jugular vein. Perfusion was carried out with Ringer's solution at 1  $\mu\text{L min}^{-1}$ .

### 5.3.1.3 Procedures

#### 5.3.1.3.1 Dialysis Probe Characterisation

This was carried out as outlined in section 5.2.1.3.1

#### 5.3.1.3.2 In Vivo Experiments

Male Sprague-Dawley rats of six months or older weighing 400 to 700g were used. The animals were initially anaesthetised by inhalation of the anaesthetic isoflurane to simplify weighing and administration of chloral hydrate. Between 0.5 and 1.0 mL of 400 mg mL<sup>-1</sup> chloral hydrate in isotonic saline was administered i.p. to anaesthetise rats for surgery. Anaesthesia was maintained during the experiment by infusion of 1  $\mu$ L min<sup>-1</sup> of 200 or 400 mg mL<sup>-1</sup> chloral hydrate in saline, via the catheter in the right jugular vein. In some cases, boosts of isoflurane were required during surgery. Caution was exercised when using this combination of anaesthetics, as it can cause respiratory depression.

The rat was positioned in the stereotaxic apparatus, its scalp was shaved, and a sagittal incision was made from just in front of the ears to just behind the eyes. The scalp and underlying soft tissues were folded back to expose the skull. A hole less than 0.5 mm in diameter and 2.5 mm forward and 2.5 mm to the right of the bregma was drilled, just through the skull. A 25-gauge hypodermic needle in the probe carrier of the stereotaxic unit was lowered until it just touched the membrane covering the brain. The hole for the dialysis probe (2.5 mm deep) was created with the needle, since this causes minimal damage to the tissue. The needle was then withdrawn, and the dialysis probe inserted, thus centering it in the frontoparietal cortex [22]. The scalp was closed with tissue staples and the wound covered with paper soaked with isotonic saline to prevent tissue dehydration.

#### 5.3.1.3.3 Derivatising Procedure

To carry out the reaction, 1.8  $\mu\text{L}$  of sodium borate and 0.9  $\mu\text{L}$  of sodium cyanide were added to 3  $\mu\text{L}$  of dialysate sample containing 1.5  $\mu\text{L}^{-1}$  of the internal standard, alpha-aminoadipic acid (varying between 2.5 and 22.5  $\mu\text{M}$  final concentration, depending on the anticipated concentration of aspartate and glutamate in the dialysate), followed by 1.8  $\mu\text{L}$  of NDA. The reaction was allowed to proceed for 30 minutes.

#### 5.3.1.3.4 Electrochemical Pretreatment

Electrochemical pretreatment of the microelectrode was accomplished as outlined in section 5.2.1.3.3

### 5.3.2 RESULTS AND DISCUSSION

#### 5.3.2.1 Electrochemical Pretreatment and Behaviour

Initial studies concerned the investigation of the electrochemical behaviour of NDA-labeled amino acids. The voltammetric response for glutamate at an untreated microelectrode is shown in Figure 5.9A. A broad response was obtained with an  $E_p$  of approximately +680 mV. Following electrochemical pretreatment, a better defined peak shape and nearly a five-fold increase in peak current was obtained with a cathodic shift in the  $E_p$  value to +650 mV (Figure 5.9B). The other NDA-labeled amino acids studied exhibited similar voltammetric behaviour.

Electrochemical pretreatment was found to be necessary between each CE run, as the amino acid derivatives appeared to foul the electrode surface. A diminution of approximately 10 to 20% in peak height between successive injections was observed.



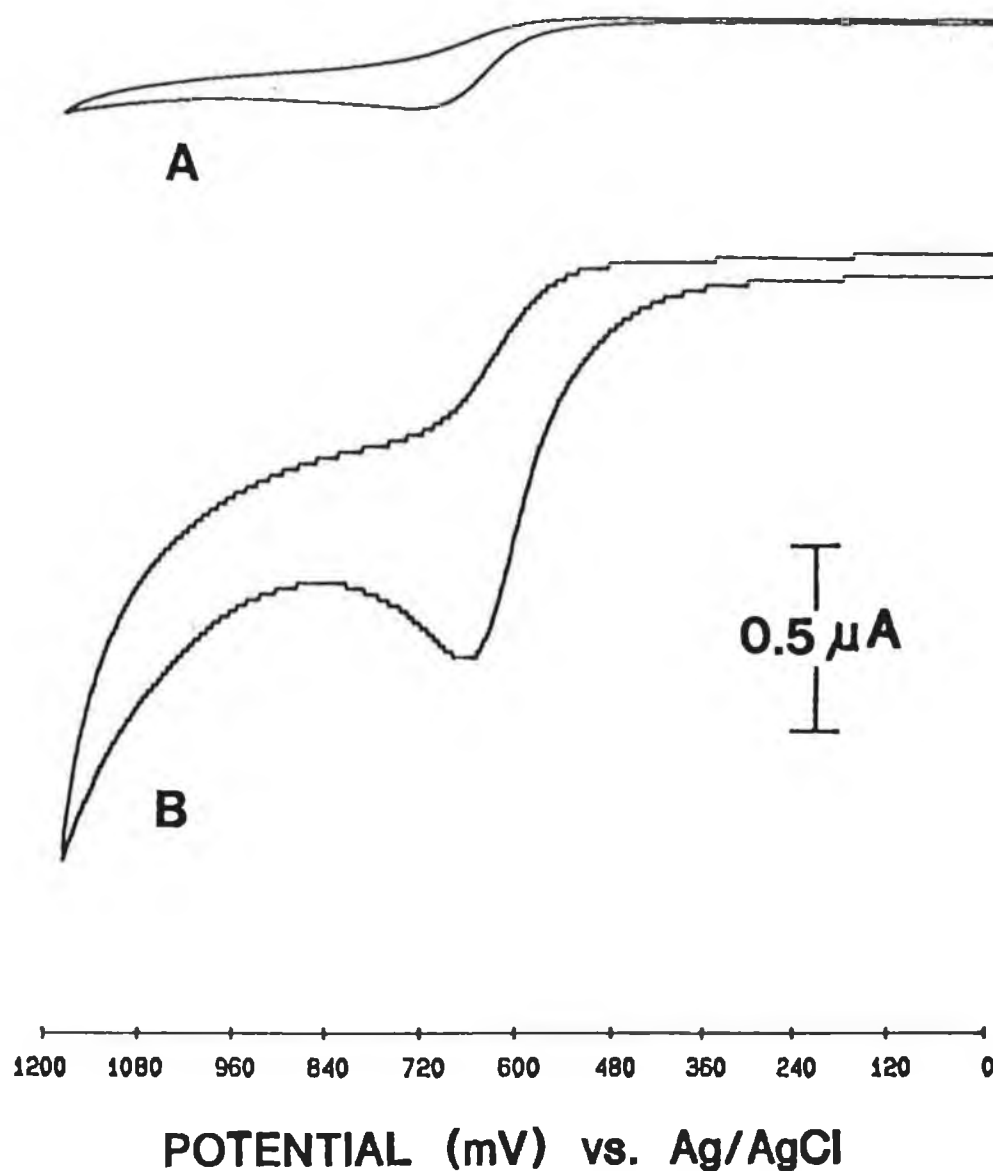


**Figure 5.9:** Cyclic voltammograms of  $5 \times 10^{-4}$  M NDA-labeled glutamate (excess glutamate was used in the derivatisation procedure) in 0.01 M borate buffer (pH 9.0). Scan rate,  $100 \text{ mV s}^{-1}$ . (A) Response at untreated microelectrode, and (B) response at electrochemically pretreated microelectrode.

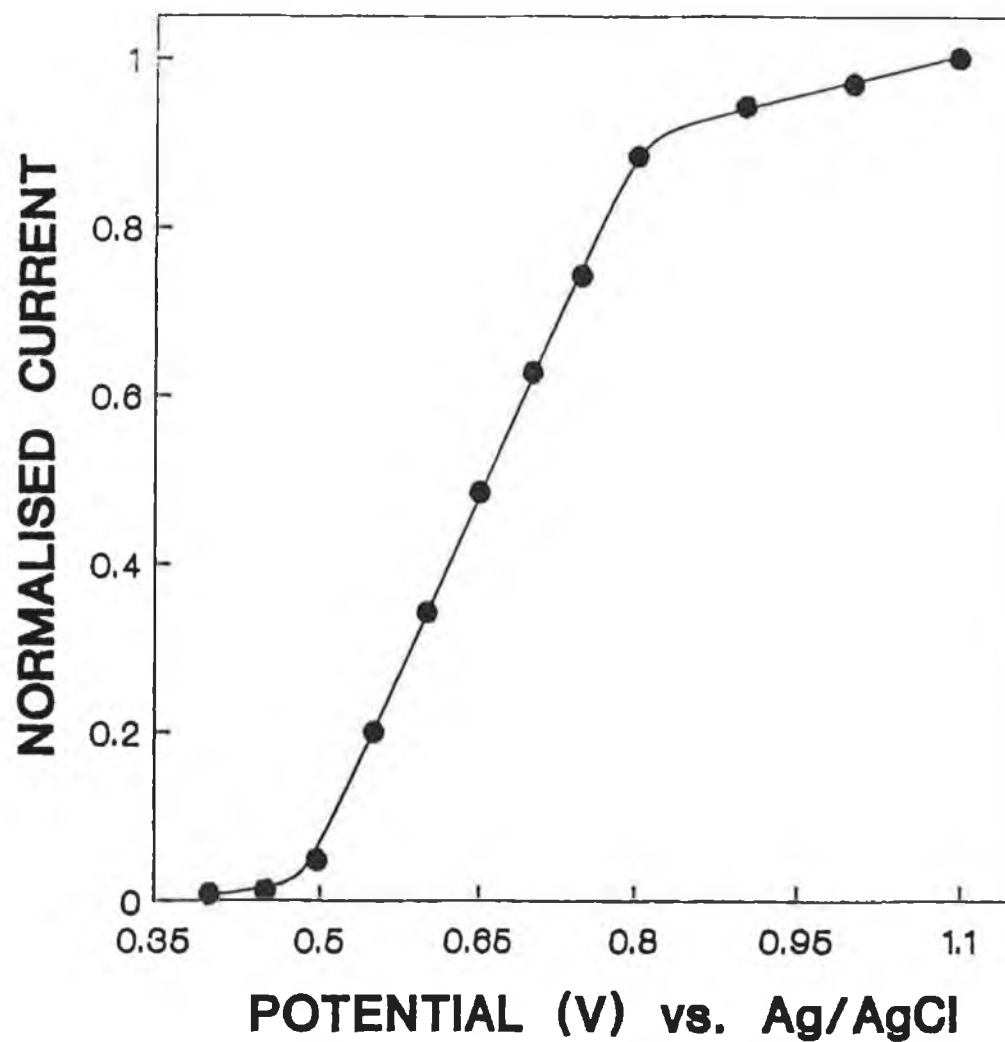


**Figure 5.10:** Hydrodynamic voltammogram of  $5 \times 10^{-5}$  M NDA-labelled glutamate. Separation conditions: 0.02 M borate buffer (pH 9.0); voltage, 30 kV; column length, 1 m.

A similar effect was reported by Oates and Jorgenson [21] who employed carbon fibre microelectrodes for the detection of NDA-labelled amino acids following open tubular chromatography. However, using the electrochemical pretreatment regime between each injection, a reproducible response was obtained with a RSD of 1.2% ( $n = 7$ ). Hydrodynamic voltammetry (HDV) was then investigated, and  $E_{1/2}$  values were obtained for several NDA-labelled amino acids. The HDV recorded for NDA-labelled glutamate is shown in Figure 5.10. The other amino acids studied included GABA, alanine, glycine, glutamine, aspartate and glutamate, and the values obtained were 600, 610, 626, 635, 640, and 650 mV respectively. These values are in agreement with those given in a report by Nussbaum et al. [23] which indicated that acidic derivatives were more difficult to oxidise than the basic derivatives. On the basis of these studies an applied potential of +800 mV was selected for subsequent investigations.

#### 5.3.2.2 Detection Limit

The separation of NDA-labelled alanine, glutamate and aspartate, and the internal standard alpha-aminoadipic acid is shown in Figure 5.11. Quantitation was achieved using response factors which were based on peak areas and were obtained in the range  $2 \times 10^{-7}$  M and  $1 \times 10^{-4}$  M. The limit of detection ( $S/N = 3$ ) for all the NDA-labelled amino acids was extrapolated from the electropherograms at  $2 \times 10^{-7}$  M levels. For alanine, glutamate and aspartate, the limits of detection calculated were  $4.95 \times 10^{-8}$  M,  $1.08 \times 10^{-7}$  M and  $7.88 \times 10^{-8}$  M respectively. Using 8.0 nL as the injection volume, the corresponding mass detection limits are 0.40, 0.86, and 0.63 fmol, respectively. It should be stated that the detection limits were calculated from concentrations that were derivatised without dilution. Therefore they will be higher than those obtained in studies where high concentrations of amino acids

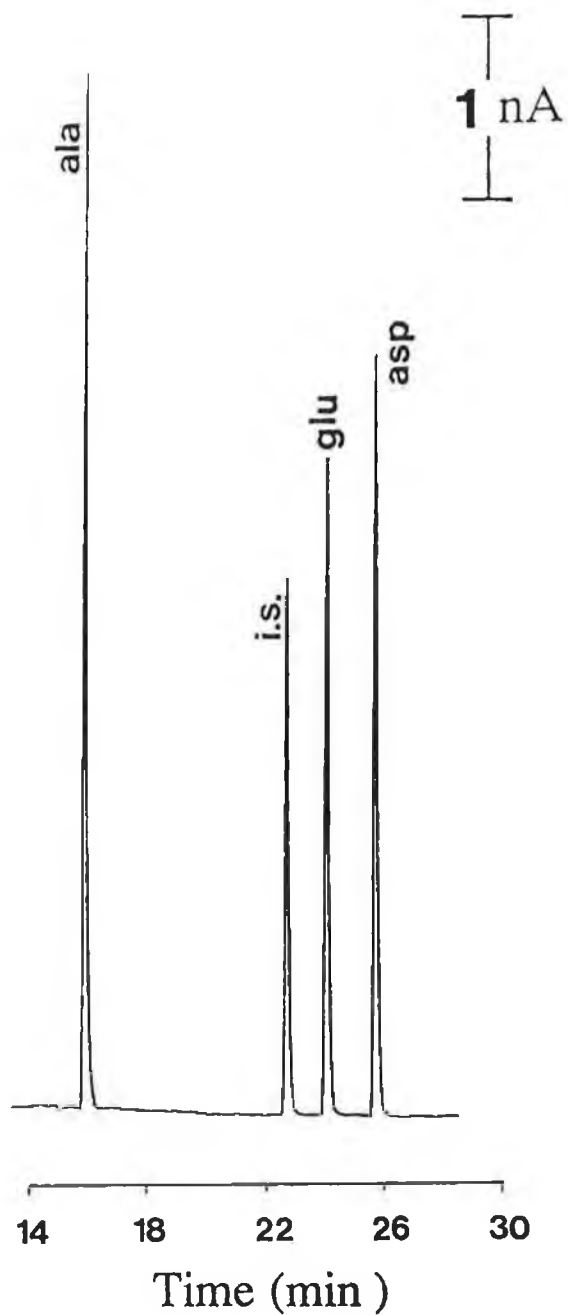
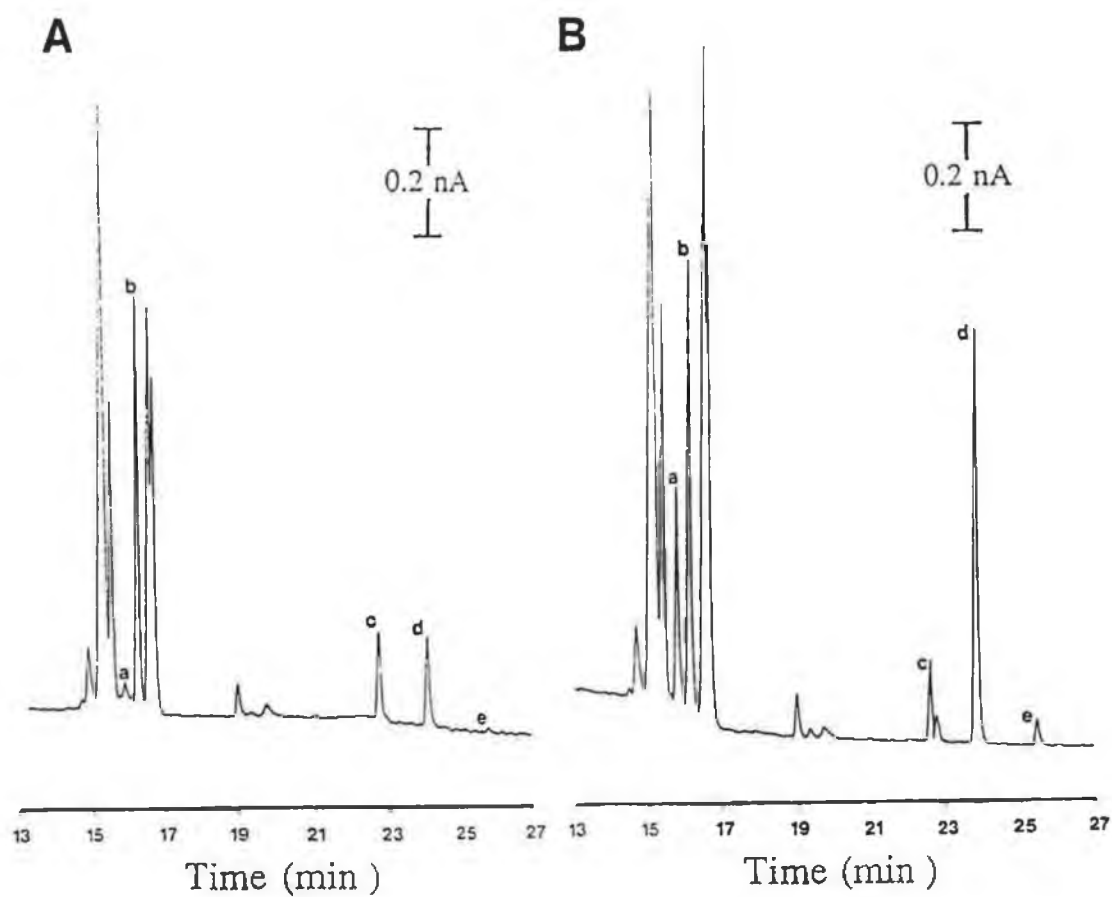


**Figure 5.11:** CE separation of  $1 \times 10^{-4}$  M standards of alanine, alpha-aminoadipic acid (IS), glutamate and aspartate. Separation conditions: detection potential, +800 mV vs. Ag/AgCl; other conditions as outlined in Figure 5.10.

were derivatised and then diluted. In that case, many of the interferences due to side reactions and reagent impurities are also diluted [24]. Based on the recoveries of alanine, glutamate and aspartate from the dialysis probe, which were  $24.3 \pm 3.7\%$ ,  $20.8 \pm 4.3\%$  and  $21.1 \pm 3.7\%$  respectively ( $n = 3$ ), the limit of quantitation for alanine, glutamate and aspartate was  $1.96 \times 10^{-7}$  M,  $5.19 \times 10^{-7}$  M and  $3.73 \times 10^{-7}$  M respectively. Standards of the amino acid derivatives were analysed periodically between dialysate samples to ensure the detector response remained reproducible over the course of the study.

#### 5.3.2.3 Voltammetric Analysis

A typical electropherogram of a derivatised brain dialysate obtained by in vivo microdialysis sampling is shown in Figure 5.12A. In addition to co-migration, the identity/purity of the amino acids was confirmed by voltammetric characterisation. The current ratios were calculated by measurement of the responses in the region where the current is most dependent on potential (+450 and +650 mV) and ratioed to the response where the current is no longer dependent on potential, i.e. the mass transport limited value (+800 mV). The current ratios recorded are given in Table 5.2. The ratios for standards of alanine, glutamate and aspartate agreed well with those of the dialysate components eluting at the same time, confirming peak identification and purity. However, the voltammetric behaviour of peak a, tentatively identified as GABA based on its migration time, differed significantly from the voltammetric behaviour of the GABA standard.



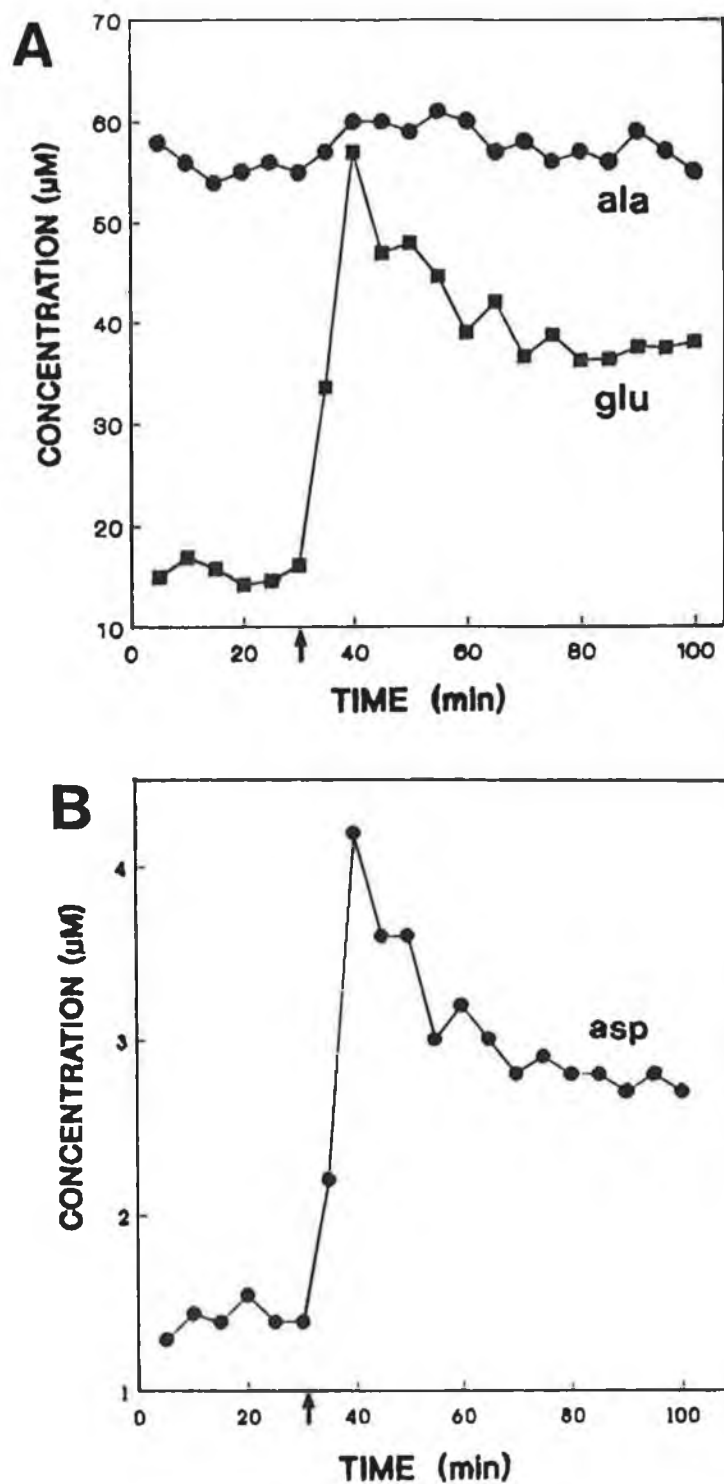
**Figure 5.12:** Derivatised brain dialysate samples obtained by perfusion with (A) normal Ringers solution; (B) high  $K^+$ -Ringers solution. Peak identification: (a) unknown, (b) alanine, (c) internal standard, (d) glutamate, and (e) aspartate. Separation conditions as outlined in Figure 5.10.

Table 5.2: Voltammetric Characterisation

Component	Retention time (min)	Current Ratios	
		500 mV/800 mV	650 mV/800 mV
Peak a	15.9	0.21	0.72
GABA	15.7	0.12	0.65
Peak b	16.2	0.12	0.64
Alanine	16.0	0.10	0.62
Peak d	24.4	0.04	0.55
Glutamate	24.1	0.03	0.55
Peak e	25.7	0.03	0.54
Aspartate	25.9	0.04	0.56

#### 5.3.2.4 Potassium-Evoked Amino Acid Overflow Analysis

High  $K^+$  stimulus of brain tissue is known to increase the overflow of several amino acids [25,26]. An electropherogram obtained from a typical NDA-labelled brain dialysate sample using 'normal' Ringers solution is illustrated in Figure 5.12A. Upon increasing the level of KCl from 4.0 mM to 100 mM (while still retaining the correct osmolality) the electropherogram (Figure 5.12B) showed a substantial increase in peak a,



**Figure 5.13:** Concentration-time curves of (A) alanine and glutamate and (B) aspartate in rat brain. Arrow indicates application of potassium stimulation.



glutamate (peak d) and aspartate (peak e). These increased levels are indicative of their roles as neurotransmitters. The levels of alanine (peak b) remained unaffected by the  $K^+$  stimulus, which was expected as it is thought only to have a role in metabolic functions. These results are in agreement with the findings of Tossman and co-workers [25]. The concentration-time curves obtained for alanine, glutamate and aspartate are illustrated in Figure 5.13. After 30 minutes of collecting dialysate samples of the basal amino acid concentration levels, the  $K^+$  stimulus was applied. For both glutamate and aspartate, a maximum increase over the basal concentration levels of nearly four-fold was observed. After an initial sharp increase, the levels of both amino acids decreased to a steady state level approximately 30 minutes after the stimulus was introduced. The curve obtained for alanine fluctuated between  $5.5 \times 10^{-5}$  M and  $6.2 \times 10^{-5}$  M, and did not show any response to the  $K^+$  stimulus. Previous studies of  $K^+$ -evoked overflow of amino acids in the brain [25,26] did not present a concentration-time curve; they reported only two concentration levels, i.e. a basal level and the level obtained after a 10 minute stimulation.

#### 5.4 CONCLUSION

The main purpose of both studies presented in this chapter was to demonstrate the application of in vivo microdialysis sampling coupled to CE with electrochemical detection. This coupling has been shown to be a promising analytical tool. Using CE as the analysis method offers advantages relative to the more commonly employed LC technique because of the respective sample volume requirements. The small sample volumes characteristically obtained by microdialysis sampling are quite amenable to analysis by CE. Although 3  $\mu$ L samples were collected in this

study, only 8.0 nL was injected onto the column. Much smaller dialysis sample volumes could easily be used to provide greater temporal resolution. The increased sampling rate capability will enable more intricate studies, and should make it possible to correlate findings obtained from other techniques, such as for example, electrophysiological studies. Additionally, because such small volumes are used with CE, multiple analyses could be performed on a single sample.

Another feature of these studies was to demonstrate the low limits of detection obtainable using electrochemical detection for CE. Mass detection limits of 234 amol for L-dopa, and sub-fmol levels for the derivatised amino acids were achieved. Furthermore, in the latter case, the capability of CE/electrochemical detection for analysing a wider range of analytes, using derivatising reagents was demonstrated.

## 5.5 REFERENCES

1. T.M. Olefirowicz and A.G. Ewing, Anal. Chem., 62 (1990) 1872.
2. C.E. Lunte, D.O. Scott and P.T. Kissinger, Anal. Chem., 63 (1991) 773A.
3. U. Ungerstedt, U.S. Patent 4,694,832, 1987.
4. U. Tossman, LC-GC, 3 (1989) 40.
5. U. Ungerstedt and C.H. Pycck, Bull. Schweiz. Akad. Med. Wiss., 30 (1974) 44.
6. K.M. Kendrik, Methods in Enzymol., 168 (1988) 182.
7. D.O. Scott, L.R. Sorenson and C.E. Lunte, J. Chromatogr., 506 (1990) 41.
8. D.O. Scott, K.L. Steel, L.R. Sorenson and C.E. Lunte, J. Pharm. Res., 8 (1991) 389.
9. K.L. Steel, D.O. Scott and C.E. Lunte, Anal. Chim. Acta, 246 (1991) 181.
10. D.O. Scott, M.A. Bell and C.E. Lunte, J. Pharm. Biomed. Anal., 7 (1989) 1249.
11. J.G. Nutt, W.R. Woodward, J.P. Hammerstadt, J.H. Carter and J.L. Anderson, N. Engl. J. Med., 310 (1984) 483.
12. D.Deleu, S. Sarre, P. Herregodts, G. Eblinger and Y. Michote, J. Pharm. Biomed. Anal., 9 (1991) 159.
13. M.Telting-Diaz, D.O. Scott and C.E. Lunte, Anal. Chem., (in press).
14. A.M. Herrera, D.O. Scott and C.E. Lunte, Pharm. Res., 7 (1990) 1077.
15. T.A. Last, Anal. Chim. Acta, 155 (1983) 287.
16. M.F. Beers, M. Stern, H. Hurtig, G. Melvin and A. Scarpa, J. Chromatogr., 336 (1984) 380.
17. P.S. Leppert, M. Cortese and J.A. Fix, Pharm. Res., 5 (1988) 587.

18. R.A. Wallingford and A.G. Ewing, Anal. Chem., 61 (1989) 98.
9. D.B. Caln, New Engl. J. Med., 310 (1984) 523.
20. D.B. Caln, J.L. Reid and S.D. Vakil, Clin. Pharmacol. Ther. 14 (1972) 386.
21. M.D. Oates and J.W. Jorgenson, Anal. Chem., 61 (1989) 432.
22. G. Gaxinos and C. Watson, The Rat Brain in Stereotaxic Coordinates, Academic Press, New York, 1982.
23. M. Nussbaum and S.M. Lunte, (submitted to Anal. Chem.).
24. S.M. Lunte and O.S. Wong, Current Separations, 10 (1990) 19.
25. U. Tossman, G. Jonsson and U. Ungerstedt, Acta Physiol. Scand., 127 (1986) 533.
26. U. Tossman, J. Segovia and U. Ungerstedt, Acta Physiol Scand., 127 (1986) 547.

## CHAPTER 6

### CONCLUSIONS

This thesis has described the development and application of some electrochemical detection systems based on modified electrodes and microelectrodes.

Modification of solid electrode surfaces is known to improve a means of improving the selectivity and sensitivity of many electroanalytical procedures. One promising approach for minimising overpotential effects is the use of chemically modified electrodes containing specifically selected redox mediators immobilised on conventional electrode materials. In this thesis it was demonstrated that the incorporation of such a mediator, a redox-active ruthenium polymer, into a carbon paste electrode provided a more stable environment than previously reported studies involving ruthenium polymers chemisorbed on the surface of glassy carbon electrodes. This is of important analytical consequence, especially if the CME is to be used under vigorous hydrodynamic conditions that prevail in flow systems. A natural follow on from this research would be the utilisation of the CME as a detection system for nitrite, following ion chromatographic separation. Additionally, the identification of the rate-controlling factors, and their interplay, would provide an insight into the mechanism of operation of mediators immobilised in a carbon paste matrix.

The remainder of the thesis dealt with the use of carbon fibre microelectrodes as detection systems. As characteristic of all solid electrodes, the surface of the electrode changes with time, and invariably a pretreatment procedure must be employed in order to obtain reproducible behaviour. An electrochemical pretreatment regime was developed which provides a sound rationale for the development of a pretreatment for the activation of carbon fibre microelectrodes. Its advantages lie

in its improved voltammetric response and its simplicity, requiring no additional instrumentation besides those already available for electrochemical measurements. It must be emphasised that the conclusions of this study will apply generally to most carbon fibre microelectrodes, however, differences will exist because of the diversity of composition and manufacturing mode of various commercially available carbon fibres. Therefore, an electrochemical pretreatment regime, using the protocol described in this thesis, should be developed for dissimilar carbon fibres.

The final section of the thesis involved the use of carbon fibre microelectrodes as an electrochemical detection system for capillary electrophoresis. The detection system described permitted detection limits at the  $1 \times 10^{-8}$  M level for several electroactive compounds, and demonstrated the feasibility of performing 'off-column' detection with CE without compromising the high efficiency inherent in this separation technique. The prospects for using the Nafion joint, designed in this thesis, to interface CE with other end-column detection systems such as mass spectrometry, flame ionisation and thermionic emission are very promising. The ability to couple such detection systems should increase the versatility and usefulness of CE.

The small sample volumes typically collected from microdialysis sampling were demonstrated to be easily analysed by CE and permitted greater temporal resolution to be obtained than that acquired from the more commonly employed LC analysis. This, in addition to the low limits of detection obtainable with this coupled technique, should prove a very powerful analytical tool, particularly for pharmacokinetic and neurological studies.

In conclusion this thesis has demonstrated the use of carbon fibre microelectrodes and modified electrodes to improve the

selectivity, sensitivity, stability and scope of electrochemical detection systems. The sophistication currently available for the modification of electrode surfaces has, as yet, not been widely utilised for microelectrodes. Because of the advantages that would accrue, it is expected that this combination of CME methodology will play an increasing role in the fabrication of microelectrodes in future electrochemical detection systems.



## APPENDIX I: PUBLICATIONS

1. Electrochemical Pretreatment of Carbon Fibre Microelectrodes for the Determination of Folic Acid, T.J. O'Shea, A. Costa Garcia, P. Tunon Blanco and M.R. Smyth, J. Electroanal. Chem., 307 (1991) 63.
2. Determination of Nitrite Based on the Mediated Oxidation at a Carbon Paste Electrode Modified with a Ruthenium Polymer, T.J. O'Shea, D. Leech, M.R. Smyth and J.G. Vos, Talanta, (1992), in press.
3. Capillary Electrophoresis with Electrochemical Detection Employing an On-column Nafion Joint, T.J. O'Shea, R.D. Greenhagen, S.M. Lunte, C.E. Lunte, M.R. Smyth, D.M. Radzik and N. Watanabe, J. Chromatogr., (1992), in press.
4. Determination of Amino Acids in Rat Brain by Capillary Electrophoresis, P. Weber, T.J. O'Shea, S.M. Lunte and M.R. Smyth, J. Pharm. Biomed. Anal., submitted.
5. Capillary Electrophoresis - Electrochemistry of Microdialysis Samples for Pharmacokinetic Studies, T.J. O'Shea, M.R. Smyth, M. Telting-Diaz, S.M. Lunte and C.E. Lunte, Electroanalysis, (1992), in press.
6. In vivo Microdialysis with Capillary Electrophoresis - Electrochemical Detection of Stimulated Amino Acid Release in Rat Brain, T.J. O'Shea, P. Weber, B. Bammel, S.M. Lunte, C.E. Lunte and M.R. Smyth, Anal. Chem., submitted.

7. T.J. O'Shea, Electrochemical Detection for Capillary Electrophoresis in "Applications of Capillary Zone Electrophoresis to Pharmaceutical and Biomedical Analysis", S.M. Lunte and D.M. Radzik, (Eds.), Pergamon Press, New York, manuscript in preparation.
8. Ion-Permeable Polymer Joint for use in Capillary Electrophoresis, T.J. O'Shea, U.S. Patent Application, submitted.